

UC Berkeley

UC Berkeley Electronic Theses and Dissertations

Title

The role of actin rearrangement inducing factor-1 in Autographa californica multiple nucleopolyhedrovirus infection

Permalink

<https://escholarship.org/uc/item/8022n35s>

Author

Lauko, Domokos

Publication Date

2020

Supplemental Material

<https://escholarship.org/uc/item/8022n35s#supplemental>

Peer reviewed|Thesis/dissertation

The role of actin rearrangement inducing factor-1 in *Autographa californica* multiple
nucleopolyhedrovirus infection

By

Domokos I Lauko

A dissertation submitted in partial satisfaction of the
requirements for the degree of
Doctor of Philosophy
in
Microbiology
in the
Graduate Division
of the
University of California, Berkeley

Committee in charge:

Professor Matthew D. Welch, Chair
Professor Britt Glaunsinger
Professor Arash Komeili
Professor David G. Drubin

Summer 2020

Copyright © 2020

Domokos I Lauko

Abstract

The role of actin rearranging inducing factor-1 in *Autographa californica* multiple nucleopolyhedrovirus infection

by

Domokos I Lauko

Doctor of Philosophy in Microbiology

University of California, Berkeley

Professor Matthew D. Welch, Chair

Viral pathogens are reliant on their hosts for replication. Thus, viruses have evolved many strategies to hijack and re-configure host cell processes for viral replication, transport, and dissemination. This dissertation focuses on baculoviruses, which are large DNA viruses that infect insects. The baculovirus *Autographa californica* multiple nucleopolyhedrovirus (AcMNPV) infects lepidopteran insects and has a striking dependence on the host cell actin cytoskeleton, a system of filaments that function in cell shape, movement, and intracellular transport. AcMNPV hijacks the actin cytoskeleton at almost every stage of infection, utilizing it for movement and cell-cell spread. During the delayed-early stage of AcMNPV infection, cells accumulate filamentous actin at their periphery. The AcMNPV protein actin rearrangement inducing factor-1 (ARIF-1) was previously shown to be necessary and sufficient for assembly of this peripheral actin. Furthermore, baculoviruses lacking functional ARIF-1 were shown to experience a significant delay in the infection of insect organ systems and host insect death, indicating that ARIF-1 accelerates the spread of viral infection. However, the mechanisms by which ARIF-1 induces actin accumulation and accelerates viral spread remain unknown.

My dissertation research has provided insights into the molecular mechanism of ARIF-1-induced peripheral actin assembly, as well as how it might accelerate systemic viral spread in the host insect. I found that ARIF-1 induces the formation of actin structures that behave like, and have a similar composition to podosomes and invadopodia (collectively known as ‘invadosomes’) in mammalian cells. Invadosomes are protrusive structures that direct degradation of the extracellular matrix (ECM) in conjunction with cell motility. By imaging cultured insect cells expressing GFP-tagged actin, I observed that beginning at 3 h post infection and persisting for hours thereafter, invadosome-like structures form in infected cells and are arranged into clusters or rings that dynamically change shape. Furthermore, I found that actin, ARIF-1, and the invadosome-associated proteins cortactin and the Arp2/3 complex localize to these invadosome-like structures. Finally, invadosome-like structure formation requires Arp2/3 complex activity. This indicates that invadosome-like structures in infected insect cells resemble mammalian invadosomes in their dynamics and composition. I speculate that in infected insects, ARIF-1-induced invadosome-like structures may degrade barriers to infection such as the midgut basal lamina (BL), a layer of ECM that sequesters the midgut. Degradation of the BL would allow AcMNPV to escape the midgut and spread through the insect body.

To determine how ARIF-1 induces changes in the actin cytoskeleton, I identified regions and sequences within ARIF-1 that are required for the formation of invadosome-like structures. ARIF-1 contains an N-terminal region with three transmembrane domains and a C-terminal cytoplasmic region. By constructing N-terminal and C-terminal truncations of ARIF-1, I found that the ARIF-1 C-terminal cytoplasmic region is required for formation of clusters of invadosome-like structures. Moreover, the N-terminal domain is dispensable, and the ARIF-1 C-terminal region (ARIF-1(303-417)), anchored to the plasma membrane by a heterologous transmembrane domain, is sufficient for formation of clusters of invadosome-like structures. Additionally, I mapped the residues required for ARIF-1 function by mutating seven individual tyrosine residues and eleven individual proline residues in the ARIF-1 C-terminal cytoplasmic region. I found that ARIF-1 residues Y332 and P335 play a role in forming clusters of invadosome-like structures. I speculate that Y332 is phosphorylated, and both Y332 and P335 serve as binding sites for host proteins that regulate actin assembly. Recruitment of these host proteins to ARIF-1 likely culminates in activation of the Arp2/3 complex and invadosome assembly/clustering. Future research will reveal the details of ARIF-1 induced invadosome-like structure formation, as well as if these structures function as invadosomes in the context of insect infection.

Table of contents

Abstract	1
Table of contents.....	i
List of figures and tables	ii
Acknowledgements.....	iii
Chapter 1: Introduction	1
Baculoviruses	2
Barriers to baculovirus infection.....	3
Actin dynamics	5
AcMNPV hijacks the actin cytoskeleton during infection	6
Baculovirus protein ARIF-1	7
Induction of invadosomes by viruses and growth factors	8
Overall hypothesis to be addressed	10
Chapter 2: Baculovirus actin rearrangement inducing factor-1 induces the formation of dynamic clusters of invadosome-like structures	12
Introduction.....	13
Results	14
Discussion.....	28
Materials and methods.....	31
Chapter 3: Future directions	37
What is the molecular mechanism through which ARIF-1 induces the formation of invadosome-like structures?	38
What is the function of ARIF-1-induced invadosome-like structures?.....	40
Summary.....	42
References	43
Appendix	57

List of figures and tables

Figure 1.1 – ARIF-1 may direct invadosome formation, facilitating basal lamina degradation ..	11
Figure 2.1 – Dynamic clusters of invadosome-like structures form in Sf21 insect cells during early AcMNPV infection.....	16
Figure 2.2 – Latrunculin A induces dissipation of clusters of invadosome-like structures.	17
Figure 2.3 – ARIF-1 is necessary and sufficient for formation of clusters of invadosome-like structures.....	19
Figure 2.4 – ARIF-1 expression corresponds with formation of clusters of invadosome-like structures.....	20
Figure 2.5 – ARIF-1 co-localizes with clusters of invadosome-like structures.....	21
Figure 2.6 – ARIF-1 residues 303 – 371 are necessary for formation of clusters of invadosome-like structures	23
Figure 2.7 – Cells expressing the ARIF-1 C-terminal cytoplasmic region form clusters of invadosome-like structures.....	24
Figure 2.8 – ARIF-1 residues Y332F and P335A are important for formation of clusters of invadosome-like structures.....	25
Figure 2.9 – Invadosome-like structures form in cells expressing ARIF-1 tyrosine and proline residue mutations	26
Figure 2.10 – ARIF-1 is expressed in cells transiently expressing ARIF-1 proline and tyrosine point mutants	27
Figure 2.11 – Cortactin and the Arp2/3 complex play a role in maintenance of clusters of invadosome-like structures.....	29

Acknowledgements

Many people have made critical academic, scientific, and personal contributions to my success in graduate school. First, I would like to thank Taro Ohkawa for his guidance, training, and mentorship. I would further like to thank Taro for his direct work on this project, including construction of the *AcΔARIF-1* virus, and providing me with numerous plasmids and protocols. I would also like to thank Susan Hepp, a former graduate student in the Welch lab, for scientific support and solidarity as a fellow graduate student and AcMNPV researcher.

Other current and past members of the Welch lab have also provided technical assistance and intellectual guidance in my research. I'd like to thank Vida Ahyong, Anna Albisetti, Gina Borgo, Thomas Burke, Lee Douglas, Patrik Engström, Joseph Graham, Bisco Hill, Natasha Kafai, Nora Kostow, Julie Choe, Becky Lamason, Curtis Sera, and Joseph Tran for all their help and for making the lab a pleasant and stimulating place to work.

Of course, one of the greatest thank you's goes to my PI, Matthew Welch, for the academic and personal support he has provided me over the past 6 years. Matt's intelligence, professionalism, patience, and work ethic has inspired me at every step of my PhD. His dedication to mentorship makes him a shining example of how PIs should treat their students, and I feel very lucky to have had such an amazing PI. My additional thesis committee members, Britt Glaunsinger, Arash Komeili, and David G. Drubin provided valuable feedback and suggestions, and have been a great inspiration throughout my time at Berkeley.

Many others also contributed to my work. I would like to thank Loy Volkman for her encouragement during hard times and motivating enthusiasm for all things baculovirus. Mary West and Christopher Noel from the QB3 High-Throughput Screening Facility assisted me in the use of the Opera Phenix microscope and image analysis software, which was used in Figure 2.3. Bisco Hill assisted me in mammalian cell transfections. Rebecca Heald, Nicole King, Abby Dernburg, and Gary Karpen and their respective labs have given me valuable comments and suggestions. I also want to thank Sergio Mares for his work on BmNPV ARIF-1 and Neil Fischer for proofreading help.

The current and former members of the PMB office staff provided me and all graduate students in PMB with a tremendous amount of support. Rocio Sanchez, Dana Janz, Lyn Riviera, and Rachel Kallet have worked tirelessly to give great advice, organize departmental events, and untangle the web of bureaucracy to make the department a uniquely supportive place.

I would also like to thank past mentors, including Sarah Boyer, Mike Anderson, Mary Montgomery, and Steve Sundby for introducing me to the joys of scientific research and encouraging me to continue my education in this field.

I also must thank my graduate student friends Brittney Nyugen, Eric Lee, Han-Teng Wong, and Margot White for their friendship and comradery inside and outside of the lab. I'd also like to thank Jake Beckert, Elsa Bruno, Will Demet, Casey Frensz, Andrew Groble, Travis Reynolds, and Dylan Shiltz for their ever-present friendship and encouragement.

I thank my family, and especially my parents, Gabriella Pinter and Istvan Lauko for always encouraging me to pursue my interests and supporting me throughout my life. Their dedication to their family, students, and work inspires me every day.

Finally, I thank my partner Alienor Baskevitch, for being here to celebrate my successes, encourage me in times of doubt, and always bringing me joy and laughter. I could not have made it through graduate school without her.

Chapter 1

Introduction

Baculoviruses

Viruses are ubiquitous in the environment and have adapted to parasitize almost all forms of life. This dissertation focuses on a diverse family of viruses, the *Baculoviridae*, which infect invertebrates. The roughly 84 species of baculoviruses (Harrison et al., 2018) are divided into four genera (Jehle et al., 2006). Alpha and betabaculoviruses infect lepidopteran insects while gammabaculoviruses and deltabaculoviruses infect hymenopteran and dipteran insects, respectively (Jehle et al., 2006; Rohrmann, 2019). Baculoviruses, particularly those that infect lepidopteran insects, have been well studied since these insects have been utilized for silk production for at least 5000 years (Vainker, 2004). Of the lepidoptera-infecting baculoviruses, alphabaculoviruses fall into the category of nucleopolyhedroviruses (NPVs) due to the formation of crystalline occlusion bodies in the nucleus of infected cells (Xeros, 1952), and betabaculoviruses are categorized as granuloviruses (GV) due to the formation of small, granular occlusion bodies (Jehle et al., 2006). The genus *Alphabaculovirus* is further split into two groups based on their fusion protein, with group I expressing the fusion protein gp64, and group II lacking gp64 but expressing the F fusion protein (de A. Zanotto et al., 1993; Pearson and Rohrmann, 2002; Rohrmann, 2019).

The *Alphabaculovirus* type species, *Autographa californica* multiple nucleopolyhedrovirus (AcMNPV), has a circular supercoiled DNA genome 133 kb in size and replicates in the nuclei of host cells (Ayres et al., 1994; Jehle et al., 2006; Rohrmann, 2019). AcMNPV exists in two forms: budded virus (BV) and occlusion derived virus (ODV) (Rohrmann, 2019). BV consist of a single nucleocapsid with an envelope derived from the host cell plasma membrane (Granados and Lawler, 1981), and disseminate viral infection to organs and tissues throughout the insect body (Rohrmann, 2019). In contrast, ODV are larger particles consisting of multiple nucleocapsids packaged together in an envelope derived from the nucleus (Rohrmann, 2019). Multiple ODV are encased in a matrix of polyhedrin protein to form large occlusion bodies (OB) (Rohrmann, 2019). These particles are responsible for transmitting viral infection from insect-to-insect, and OBs are thought to stabilize and preserve ODV and nucleocapsids under adverse environmental conditions until they come in contact with a suitable host (Rohrmann, 2019).

AcMNPV infection is initiated when the host orally ingests OBs. OBs then dissolve in the alkaline environment of the midgut, releasing ODVs, which pass through the peritrophic membrane and infect the epithelial cells lining the midgut (Granados and Lawler, 1981; Keddie et al., 1989). Oral infection is facilitated by viral per os infectivity factors (PIFs) present in ODV but not BV (Boogaard et al., 2018; Peng et al., 2010). Following viral replication in midgut epithelial cells, BV disseminate infection systemically through the host body, infecting all major organ systems (Rohrmann, 2019). In cells throughout the insect body, newly formed nucleocapsids are retained in the nucleus after BV dissemination and assembled into ODV and OBs (Rohrmann, 2019). At this stage of infection, infected insects undergo a period of increased locomotion (Goulson, 1997), after which their bodies disintegrate and liquefy (Ishimwe et al., 2015). Liquefaction is facilitated by expression of viral cathepsin proteases and chitinases, and releases newly formed OBs from cells into the environment (Hawtin et al., 1997; Ishimwe et al., 2015).

The different stages of viral infection are driven by successive transcription of groups of viral genes, allowing the virus to produce the gene products required in subsequent stages of

infection. The approximately 150 AcMNPV genes can be divided into early and late stage genes, with viral genome replication serving as the delineating point between these stages (Berretta et al., 2013; Rohrmann, 2019). The early and late genes and stages of infection are further subdivided into immediate early, delayed-early, late, and very late stages (Berretta et al., 2013). Upon entry into the cell nucleus, AcMNPV expresses early genes, whose products function in evasion of host immune processes, viral genome replication, and activation of late and very late stage gene expression (Berretta et al., 2013). Immediate early gene products generally activate transcription of delayed-early and late stage viral genes (Rohrmann, 2019). The product of the immediate early 1 (*ie-1*) gene in particular is a crucial transcriptional trans-activator of promoters of delayed-early and late genes (Guarino and Summers, 1986). While early genes are transcribed by the host RNA polymerase, late and very late genes are transcribed using a viral RNA polymerase (Fuchs et al., 1983). Late genes are expressed upon viral genome replication at around 6-24 hours post infection (hpi) and mediate the production and assembly of nucleocapsids, some of which then leave the host cell as BV (Rohrmann, 2019). Very late gene expression occurs from around 18-72 hpi and coincides with ODV assembly, polyhedrin production, and OB assembly.

Several very late promoters are extremely strong, driving robust transcription of genes. This aspect has made AcMNPV very useful for industrial and biotechnology applications. Recombinant AcMNPV is used as a vector for large-scale expression of eukaryotic proteins because of the strong late-stage promoters and because expression of proteins in insect cells preserves glycosylation and other posttranslational modifications that may be necessary for protein function (Altmann et al., 1999; Hassan and Roy, 1999). Additionally, baculoviruses are able to transduce a variety of cell types, including human cells (Carbonell and Miller, 1987; Volkman and Goldsmith, 1983), making them ideal for applications requiring mammalian cell transduction. These traits have also led to utilization of baculoviruses as vaccine vectors (Lu et al., 2012; van Oers, 2006). Lastly, baculoviruses have been used as biopesticides in an attempt to prevent lepidopteran pests from damaging crops (Wood and Granados, 1991). To accelerate the death of insects infected with a baculovirus-based biopesticide, strategies have been pursued to allow the virus to more rapidly overcome or bypass major barriers to infection within the host.

Barriers to baculovirus infection

One barrier to systemic baculovirus infection is the host insect basal lamina (BL), a layer of extracellular matrix (ECM) that is approximately 120 nm thick and secreted by epithelial cells at their basal surface (Passarelli, 2011). Composed of laminin, type IV collagen, and heparin sulfate proteoglycans, the BL functions to support cell layers, serves as a scaffold for epithelial cell regeneration, and prevents movement of cells across different tissues (Passarelli, 2011). Nearly all insect organs, including the midgut, are surrounded by basal laminae (Ashhurst, 1968; Engelhard et al., 1994).

The insect midgut BL forms a barrier to the spread of AcMNPV infection from the midgut epithelial cells to the rest of the host body (Clem and Passarelli, 2013; Passarelli, 2011). This arises from the fact that the pores in the BL are smaller than AcMNPV BV and thus do not permit viral passage (Hess and Falcon, 1987; Reddy and Locke, 1990). Because host insects slough off midgut epithelial cells upon infection (Engelhard et al., 1994; Keddie et al., 1989; Washburn et al., 1995), the virus must rapidly cross the midgut BL and establish secondary infection in other tissues to avoid being cleared (Keddie et al., 1989). Indeed, AcMNPV has been

detected in the insect hemocoel as soon as 30 min after oral infection (Granados and Lawler, 1981), indicating that the virus possesses robust methods for crossing the midgut BL and other basal laminae.

Two main hypotheses exist to explain how AcMNPV crosses the lepidopteran midgut BL. The first hypothesis is that AcMNPV bypasses the BL through infection of the insect respiratory system (Engelhard et al., 1994; Passarelli, 2011). The respiratory system is composed of a branched network of hollow chitinous tubes called tracheae, which conduct gas exchange in insect tissues (Hayashi and Kondo, 2018). The interior of tracheae are lined with tracheal epithelial cells, and terminal single-cell projections of the tracheal system called tracheoblasts may penetrate the midgut BL to provide gas exchange for midgut epithelial cells (Romoser et al., 2005, 2004). Concurrent with infection of midgut epithelial cells, AcMNPV has been observed infecting tracheoblasts and tracheal epithelial cells, suggesting that the virus could establish secondary infection in the tracheal system (Engelhard et al., 1994). Thus, AcMNPV may bypass the midgut BL barrier by infecting the tracheal system and utilizing it to disseminate and establish systemic infection (Engelhard et al., 1994; Passarelli, 2011). However, tracheoblasts and tracheal epithelial cells also maintain a BL, and it remains unexplained how AcMNPV preferentially penetrates the tracheoblast BL over the midgut epithelial BL, as well as how the virus escapes the tracheal system to establish systemic infection (Passarelli, 2011).

A second hypothesis for how AcMNPV bypasses the midgut BL is through inducing cellular growth-factor signaling pathways that lead to BL turnover and degradation (Passarelli, 2011). Fibroblast growth factors (FGFs) are a family of signaling proteins that have numerous roles in development in multicellular organisms (Ornitz and Itoh, 2015). FGFs bind to heparin sulfate proteoglycans, and this complex binds and activates FGF receptors, leading to dimerization, tyrosine phosphorylation, and initiation of a signaling cascade which leads to cell motility and proliferation (Ornitz and Itoh, 2015). In *Drosophila*, the FGF homologue, Branchless, mediates development and branching of the insect tracheal system (Reichman-Fried et al., 1994; Sutherland et al., 1996). Oxygen-deprived cells secrete Branchless, which acts as a mitogen, binding to the tracheoblast receptor Breathless, and stimulating tracheoblasts to migrate and expand toward hypoxic tissues and mediate branching of the terminal tracheal system (Jarecki et al., 1999; Sato and Kornberg, 2002; Sutherland et al., 1996). The tracheoblast response to Branchless is rapid and can extend over two cell layers (Sato and Kornberg, 2002; Sutherland et al., 1996), and over the course of this response the tracheoblast BL is locally degraded (Passarelli, 2011).

Intriguingly, baculoviruses encode an FGF homologue that causes many of the same effects as Branchless. The baculovirus gene *viral fibroblast growth factor* (*vfgf*) is conserved in baculoviruses that escape the midgut to establish systemic infection (Detvisitsakun et al., 2005). *vfgf* is expressed during early infection at around 3-6 hpi, and vFGF is secreted from infected cells (Detvisitsakun et al., 2005; Katsuma et al., 2004; Lehiy et al., 2009). Interestingly, vFGF also binds to heparin sulfate proteoglycans (Detvisitsakun et al., 2005) and to a lepidopteran Breathless homologue (Katsuma et al., 2006a), inducing motility in cultured lepidopteran cells and hemocytes (Detvisitsakun et al., 2005; Katsuma et al., 2004). The parallels between the effects of baculovirus vFGF and *Drosophila* Branchless have led to the hypothesis that baculoviruses exploit FGF signaling pathways in insects to bypass the midgut BL barrier. While vFGF does not have an effect on AcMNPV infection in cell culture (Detvisitsakun et al., 2006),

oral infection with AcMNPV lacking *vfgf* results in a significant delay in host death, showing that vFGF functions in baculovirus dissemination in the host (Detvisitsakun et al., 2007; Katsuma et al., 2006b). During infection of midgut epithelial cells, vFGF is thought to diffuse across the midgut BL and act as a mitogen, inducing tracheoblast motility, and causing them to degrade the tracheal and midgut BL through expression and secretion of matrix metalloproteases and cathepsin proteases (Means and Passarelli, 2010; Passarelli, 2011). Such migration disrupts the integrity of the midgut and/or tracheal BL, allowing viral transit into the host body or the tracheal system (Passarelli, 2011). Indeed, inhibition of matrix metalloprotease or caspase activity prevents AcMNPV escape from the insect midgut (Means and Passarelli, 2010). While this hypothesis is intriguing, we speculate that there may be additional viral pathways that mediate how the virus crosses the midgut BL. We propose that one such a pathway involves baculovirus hijacking of the actin cytoskeleton, as outlined below.

Actin dynamics

The actin cytoskeleton has myriad roles in the cell and is regulated by intricate machinery. One of the most abundant proteins in eukaryotic cells, actin, is a globular protein of 42 kDa that is the major component of the actin cytoskeleton (Pollard, 2016). It exists as free-floating monomers (G-actin) that can spontaneously polymerize into filaments (F-actin) (Pollard, 2016). F-actin has polarity with a fast growing plus (or barbed) end and a slower growing minus (or pointed) end (Pollard, 2016). Actin filaments are utilized by the cell to provide structural support that is resilient, dynamic, and rapidly alterable (Rottner et al., 2017). Actin polymerization can also exert force on surfaces, such as the plasma membrane, and actin forms the core of cellular structures such as filopodia and lamellipodia (Buracco et al., 2019; Rottner et al., 2017; Schaks et al., 2019; Svitkina, 2018). This function makes the actin cytoskeleton critical to cellular processes such as cell migration, clathrin-mediated endocytosis, and intracellular trafficking (Buracco et al., 2019; Lu et al., 2016; Rottner et al., 2017; Schaks et al., 2019; Svitkina, 2018). However, in order to carry out its many functions, actin polymerization must be finely regulated.

One level of control of actin polymerization is achieved by proteins that function to nucleate actin filaments (Pollard, 2016). Actin nucleating proteins regulate actin polymerization so that it occurs in the correct context, space, and time (Campellone and Welch, 2010; Rottner et al., 2017). One class of actin nucleating proteins, the Arp2/3 complex, is composed of five protein subunits together with two actin related proteins, Arp2 and Arp3, which facilitate actin nucleation (Buracco et al., 2019; Campellone and Welch, 2010; Pollard, 2016; Rottner et al., 2017). Activated Arp2/3 complex binds to the side of actin filaments (called mother filaments), and induces polymerization of a new (daughter) filament at a 70-degree angle, creating a branching, Y-shaped structure (Campellone and Welch, 2010; Pollard, 2016; Svitkina, 2018). Thus, Arp2/3 complex activity induces formation of highly branched actin networks (Svitkina, 2018). In motile cells, the leading edges of lamellipodia are pushed forward by Arp2/3 complex-mediated actin polymerization of a highly branched cortical actin network (Schaks et al., 2019; Svitkina, 2018). The activity of the Arp2/3 complex is regulated by proteins called nucleation promoting factors (NPFs) (Pollard, 2016). One NPF is Neural Wiskott-Aldrich Syndrome protein (N-WASP), which binds and activates the Arp2/3 complex, facilitating actin polymerization (Rottner et al., 2017; Schaks et al., 2019; Svitkina, 2018). N-WASP activity is itself regulated by phosphorylation, the small Rho GTPase Cdc42, as well as PIP2 (Campellone and Welch, 2010).

While actin polymerization in cells is regulated at multiple levels to ensure it takes place at the right place and time, pathogens that hijack the actin cytoskeleton mimic proteins involved in this regulation to induce host actin polymerization to their benefit (Lamason and Welch, 2017; Stradal and Schelhaas, 2018).

AcMNPV hijacks the actin cytoskeleton during infection

Viral pathogens are masters of cell biology, re-programming the host cell and hijacking host cell processes to aid in viral replication and spread. The cytoskeleton, and particularly microtubules, are commonly utilized by viruses for intracellular movement (Leite and Way, 2015; Pietrantonio et al., 2020; Simpson and Yamauchi, 2020; Walsh and Naghavi, 2019). For example, vaccinia virus intracellular enveloped virions (IEV) recruit kinesin-1 (Ward and Moss, 2004) and are transported from perinuclear assembly sites to the cell periphery along microtubules (Hollinshead et al., 2001; Leite and Way, 2015; Rietdorf et al., 2001; Ward and Moss, 2004, 2001).

Viruses also utilize the actin cytoskeleton for intracellular transport and dissemination. HIV manipulates cell signaling by activating the Rho GTPases Rac1 and CDC42, initiating downstream Arp2/3 complex activity which is vital for viral entry and egress from cells (Alberto Ospina Stella and Stuart Turville, 2018; Swaine and Dittmar, 2015). Vaccinia virus directly utilizes the actin cytoskeleton for virus dissemination. Intracellular enveloped virions (IEVs) transit to the cell periphery where they fuse with the plasma membrane, but remain attached to the cell as cell-associated virus (CEV) (Leite and Way, 2015). Vaccinia virus transmembrane protein A36, localized at the plasma membrane beneath CEV (Smith et al., 2002; van Eijl et al., 2000), is phosphorylated by Src and Abl tyrosine kinases (Frischknecht et al., 1999; Newsome et al., 2004, 2006), recruiting Nck-1 (Frischknecht et al., 1999; Scaplehorn et al., 2002). Nck-1 recruits WASP-interacting protein (WIP), N-WASP, and the Arp2/3 complex to the site underneath the CEV (Donnelly et al., 2013; Moreau et al., 2000; Snapper et al., 2001; Weisswange et al., 2009; Zettl and Way, 2002). Arp2/3 complex activation induces the formation of a branched actin network and growth of an actin tail, forming cell membrane protrusions with CEV at the tip (Cudmore et al., 1996, 1995). These protrusions extend to surrounding cells, allowing CEV to potentially access uninfected cells (Cudmore et al., 1996). Additionally, already infected cells can propel superinfecting CEV onward to potentially uninfected cells, enabling efficient dissemination of the virus (Doceul et al., 2010). Finally, Ebolavirus nucleocapsid transit from viral inclusions to the host cell plasma membrane is dependent on actin polymerization and Arp2/3 complex activity (Schudt et al., 2015). Moreover, fluorescent labeling of F-actin shows that ebolavirus nucleocapsids appear to form actin comet tails (Schudt et al., 2015).

While actin cytoskeleton manipulation is undertaken by many viruses, baculoviruses are unique in the extent that they depend on the actin cytoskeleton. In fact, baculoviruses such as AcMNPV do not require microtubules for intracellular transport (Ohkawa and Welch, 2018; Volkman and Zaal, 1990), and instead utilize the host actin cytoskeleton in almost every stage of infection (Charlton and Volkman, 1993, 1991; Volkman et al., 1992, 1987; Volkman and Kasman, 2000). AcMNPV BV enter insect cells through absorptive endocytosis (Volkman et al., 1984), and decreasing pH in the endocytic vesicle triggers the viral protein gp64 to initiate fusion of the viral envelope and vesicle membrane, releasing the nucleocapsid into the host cell cytoplasm (Blissard and Wenz, 1992; Monsma et al., 1996). Nucleocapsids then undergo actin-

based motility through the cytoplasm, forming actin comet tails consisting of Y-branched filaments, facilitating transit to the nucleus (Mueller et al., 2014; Ohkawa et al., 2010). Actin assembly is initiated by nucleocapsid protein p78/83, which acts as a viral NPF, recruiting and activating the host Arp2/3 complex (Goley et al., 2006). After the expression of viral early genes, F-actin either accumulates at the cell periphery or at the basal plasma membrane into ‘ventral aggregates’ (Charlton and Volkman, 1991; Roncarati and Knebel-Mörsdorf, 1997). The function of these aggregates was previously uncharacterized, and this dissertation will explore hypotheses concerning their formation and role in AcMNPV infection.

As infection progresses, G-actin is imported into the nucleus due to the activity a set of viral nuclear-localization of actin (NLA) genes (Gandhi et al., 2012; Ohkawa et al., 2002). Actin then polymerizes around viral replication centers during the late stage of infection (Charlton and Volkman, 1993, 1991; Goley et al., 2006; Hepp et al., 2018; Ohkawa et al., 2002; Ohkawa and Volkman, 1999; Volkman et al., 1992). Importantly, nuclear actin polymerization is required for productive viral infection and may play a role in viral nucleocapsid assembly (Goley et al., 2006; Ohkawa and Volkman, 1999; Volkman, 1988; Volkman and Kasman, 2000).

Following viral replication, a population of newly assembled nucleocapsids again undergo p78/83-mediated actin-based motility in the nucleus, using it to escape to the cytoplasm and transit to the cell membrane where they bud out to form BV (Ohkawa and Welch, 2018). Thus, control of the actin cytoskeleton is crucial for AcMNPV to achieve productive infection.

Baculovirus protein ARIF-1

Another AcMNPV protein that impacts the actin cytoskeleton is the actin rearrangement inducing factor-1 (ARIF-1) (Roncarati and Knebel-Mörsdorf, 1997). ARIF-1 was identified in a screen for AcMNPV genes that regulate actin cytoskeleton rearrangements, and expression of *arif-1* in cultured TN368 and BmN cell lines is sufficient to induce the accumulation of F-actin at the cell periphery during the early stage of AcMNPV infection (Katsuma et al., 2015; Roncarati and Knebel-Mörsdorf, 1997).

ARIF-1 is expressed as a delayed-early gene during AcMNPV infection and localizes to the cell plasma membrane (Dreschers et al., 2001). Structurally, ARIF-1 is predicted to have three transmembrane domains, along with a 200 amino acid cytoplasmic C-terminal domain that is rich in proline residues (Dreschers et al., 2001). Additionally, ARIF-1 is known to be tyrosine phosphorylated during infection on its N-terminal 255 residues, though it is unknown which exact residues are phosphorylated. ARIF-1 seems to acquire additional tyrosine phosphorylation as infection progresses, and this is thought to be linked to disappearance of the peripheral actin accumulation during late infection (Dreschers et al., 2001). ARIF-1 is conserved in alphabaculoviruses, though it does not have homology with any other known proteins (Rohrmann, 2019). In addition to being sufficient to induce actin cytoskeleton rearrangement when expressed in insect cells, ARIF-1 is required for actin rearrangement during infection, since deletion of the C-terminal 163 amino acids or the insertion of *LacZ* into the middle of *arif-1* prevents the accumulation of actin at the periphery of infected TN368 cells (Dreschers et al., 2001). However, deletion of *arif-1* does not impact progeny virus production in infected cell cultures (Dreschers et al., 2001; Katsuma et al., 2015). While ARIF-1 is necessary and sufficient for the accumulation of actin at the plasma membrane of lepidopteran cells, the mechanism by which it does so remains unclear.

In addition to actin rearrangement, ARIF-1 has a role in the progression of viral infection in live insect hosts (Katsuma et al., 2015). When orally infected with BmNPV (a close relative of AcMNPV) carrying a deletion of the *arif-1* gene, infection of major organ systems, progeny virus production, and death is significantly delayed in live insects (Katsuma et al., 2015). As observed for AcMNPV lacking *arif-1*, the deletion of *arif-1* does not impact BmNPV BV titres in cell culture, but does prevent early stage actin rearrangement (Katsuma et al., 2015). Together, these data indicate that ARIF-1 plays a role in accelerating baculovirus systemic infection in insect hosts.

Consistent with a role in viral escape from the insect midgut, a study of the expression level of AcMNPV genes in host insect midguts found that expression of *arif-1* and *vfgf* is significantly higher in midgut cells than in cell culture (Shrestha et al., 2018). ARIF-1 is expressed at 4 hpi, consistent with the timing of actin rearrangement, and remains detectable at the plasma membrane until 24 hpi (Dreschers et al., 2001). However, the mechanisms by which ARIF-1 accelerates systemic viral infection and induces early stage actin rearrangement, and whether these two effects are linked, remain unknown. The goal of my dissertation project has been to understand the role that ARIF-1 plays in these processes.

Induction of invadosomes by viruses and growth factors

Nearly 30 years ago, Charlton & Volkman described the formation of aggregates of F-actin at the basal side of infected Sf21 cells (Charlton and Volkman, 1991). Based on my work, described in Chapter 2, we now know that ARIF-1 is responsible for formation of these structures, but their function remains unknown. We suggest that ARIF-1-induced delayed-early actin structures behave and function as podosomes or invadopodia (collectively known as ‘invadosomes’), which are protrusive structures that direct ECM degradation in conjunction with cell motility (Paterson and Courtneidge, 2018).

Invadosomes were first observed in Rous sarcoma virus (RSV) transformed fibroblasts, where proteins associated with ECM contact sites, vinculin and alpha-actinin, cluster into rosette-like structures (David-Pfeuty and Singer, 1980). This discovery was refined by Tarone *et al.*, who showed that vinculin and alpha-actinin rosettes in RSV transformed fibroblasts contain actin, and are associated with cellular protrusions that contact the ECM, and coined these structures ‘podosomes’, meaning cellular feet (Tarone et al., 1985). It was further shown in RSV-transformed fibroblasts that the viral Src (v-Src) tyrosine kinase localized to cell protrusions, and these protrusions are associated with degradation of underlying ECM (Chen et al., 1985). The observation of ECM degradation led to the re-coining of rosettes and podosomes as ‘invadopodia’ (Chen, 1989). The term ‘podosome’ is used to describe structures that appear in normal cells, whereas ‘invadopodia’ describes similar structures in cancer cells. Nonetheless, podosomes and invadopodia are similar in both composition and function, and it is possible that their differences can be explained by cell-type and experimental conditions (Paterson and Courtneidge, 2018). We will use the collective term ‘invadosomes’ to describe these structures. Invadosomes are defined as dot-like protrusive structures 0.5-2 microns in diameter with a core of dynamic F-actin and other proteins, surrounded by a ring of adhesion proteins (Murphy and Courtneidge, 2011; Paterson and Courtneidge, 2018).

Further research into invadosomes has generated a nuanced understanding of their composition and the processes of their assembly. Invadosomes form in response to both internal

and external cell signaling (Paterson and Courtneidge, 2018). In particular, signaling by growth factors such as vascular endothelial growth factor (VEGF)(Seano et al., 2014; Spuul et al., 2016), epidermal growth factor (EGF) (Díaz et al., 2013; Hwang et al., 2012; Yamaguchi et al., 2005), platelet-derived growth factor (PDGF) (Hanna et al., 2013), and transforming growth factor- β (TGF- β) (Rottiers et al., 2009; Varon et al., 2006) are known to stimulate invadosome formation.

First, binding of growth factors to cellular receptors stimulates cellular Src (c-Src) tyrosine kinase activity, which phosphorylates substrates tyrosine kinase with five SH3 domains (Tks5) (Burger et al., 2014, 2011; Lock, 1998; Seals et al., 2005) and cortactin (Ayala et al., 2008; Kanner et al., 1990; Seals et al., 2005). Though Src-family kinases are usually required for invadosome formation, reports of these structures in cells despite the presence of Src inhibitors (Burger et al., 2011; Di Martino et al., 2014; Mader et al., 2011; Seals et al., 2005; Seiler et al., 2012) suggest that other cytoplasmic tyrosine kinases such as ABL-family may contribute to invadosome formation (Mader et al., 2011). In contrast, Tks5 is required for invadosome formation and activity, and is a marker of invadosomes because it is not present in other cellular structures such as focal adhesions or filipodia (Di Martino et al., 2014; Paterson and Courtneidge, 2018). Additionally, overexpression of Tks5 may be sufficient to initiate invadopodia formation (Burger et al., 2014; Ferrari et al., 2019; Li et al., 2013; Seals et al., 2005).

Second, phosphorylated Tks5 localizes to phosphatidylinositol lipids at the basal cell membrane (Abram et al., 2003; Murphy and Courtneidge, 2011; Paterson and Courtneidge, 2018). Tks5 serves as a scaffold, recruiting cortactin (Hiura et al., 1995; Oser et al., 2009), the adaptor proteins noncatalytic regions of tyrosine kinase 1 and 2 (Nck1, Nck2) (Stylli et al., 2009), and growth factor receptor-bound protein 2 (Grb2) (Oikawa et al., 2008; Stylli et al., 2009), the small Rho GTPase Cdc42 (Di Martino et al., 2014; Yamaguchi et al., 2005), WASP-interacting protein (WIP) (Bañón-Rodríguez et al., 2011; Chou et al., 2006; Donnelly et al., 2013; García et al., 2012; Tsuboi, 2007), and the NPFs WASP and N-WASP (Linder et al., 1999; Mizutani et al., 2002; Oikawa et al., 2008). Cortactin and WASP/N-WASP recruit the Arp2/3 complex (Burns et al., 2001; Linder et al., 2000; Oser et al., 2009), which binds to existing actin filaments and initiates the formation of a branched F-actin core whose polymerization drives protrusion in the cell membrane (Ferrari et al., 2019, p. 1).

Third, invadosomes enter the ‘mature’ phase. Proteases, including serine proteases (Monsky et al., 1994; Mueller et al., 1999), cathepsin cysteine proteases (Tu et al., 2008), and zinc-regulated matrix metalloproteases (Castro-Castro et al., 2016; Nakahara et al., 1997; Sato, 1997) are secreted or directed to invadosomes (El Azzouzi et al., 2016). In particular, membrane type 1 matrix metalloprotease (MT1-MMP) is recruited to the membrane protrusions, enabling degradation of the underlying ECM (Ferrari et al., 2019; Murphy and Courtneidge, 2011; Nakahara et al., 1997; Poincloux et al., 2009). While the key proteins involved in invadosome formation and maturation are known, many of the interactions between the components of these structures and how they are regulated are still being uncovered.

Invadosome clusters form in a variety of cell types, including osteoclasts (Destaing et al., 2003; Kanehisa et al., 1990; Miyachi et al., 1990; Zambonin-Zallone et al., 2009), monocyte-derived cells (Murphy and Courtneidge, 2011; Paterson and Courtneidge, 2018), smooth muscle cells (Kaverina et al., 2003; Webb et al., 2005; Zhou et al., 2006), and endothelial cells (Moreau

et al., 2003; Varon et al., 2006). In osteoclasts, individual invadosomes gather into clumps surrounded by an actin cloud and gradually form a ring around the periphery of the cell (Destaing et al., 2008).

Invadosome formation and ECM degradation are thought to be linked to cell motility (Albiges-Rizo et al., 2009; Collin et al., 2008; Murphy and Courtneidge, 2011). Indeed, invadosomes are common in motile cells such as macrophages that transit to sites of infection (Burger et al., 2011; Labernadie et al., 2014; Paterson and Courtneidge, 2018), and their formation is associated with metastatic, aggressive cancers (Eddy et al., 2017; Paz et al., 2014; Williams et al., 2019; Yamaguchi, 2012). The ability of these structures to degrade the extracellular matrix through the localization of proteases make them an interesting candidate for structures that may be utilized by viruses for remodeling barriers to viral infection.

Overall hypothesis to be addressed

As discussed above, baculoviruses may utilize multiple pathways to escape the insect midgut. In Chapter 2 of this dissertation, I document the observation that ARIF-1 is necessary and sufficient for the formation of invadosome-like structures in cultured insect cells *in vitro*. This suggests that ARIF-1 induces the formation of invadosome-like structures in infected insects *in vivo*, including in midgut epithelial cells. In turn, invadosome-like structures degrade the underlying BL, opening a path for systemic viral infection of the host (**Fig 1A**). This proposed process may act in conjunction with other mechanisms by which AcMNPV escapes the midgut. While vFGF diffuses across the BL and induces tracheoblast migration across the BL towards the midgut epithelium, simultaneous degradation of the BL by invadosome-like structures in gut epithelial cells may occur (**Fig 1B**). The additive effects of these two strategies could result in breaks or disruption of the midgut BL, allowing the virus to cross the BL, and/or infect exposed tracheoblasts and enter the insect tracheal system. Thus, utilizing multiple strategies for BL degradation may enable AcMNPV to ensure midgut escape, limiting the danger of clearance from the host body.

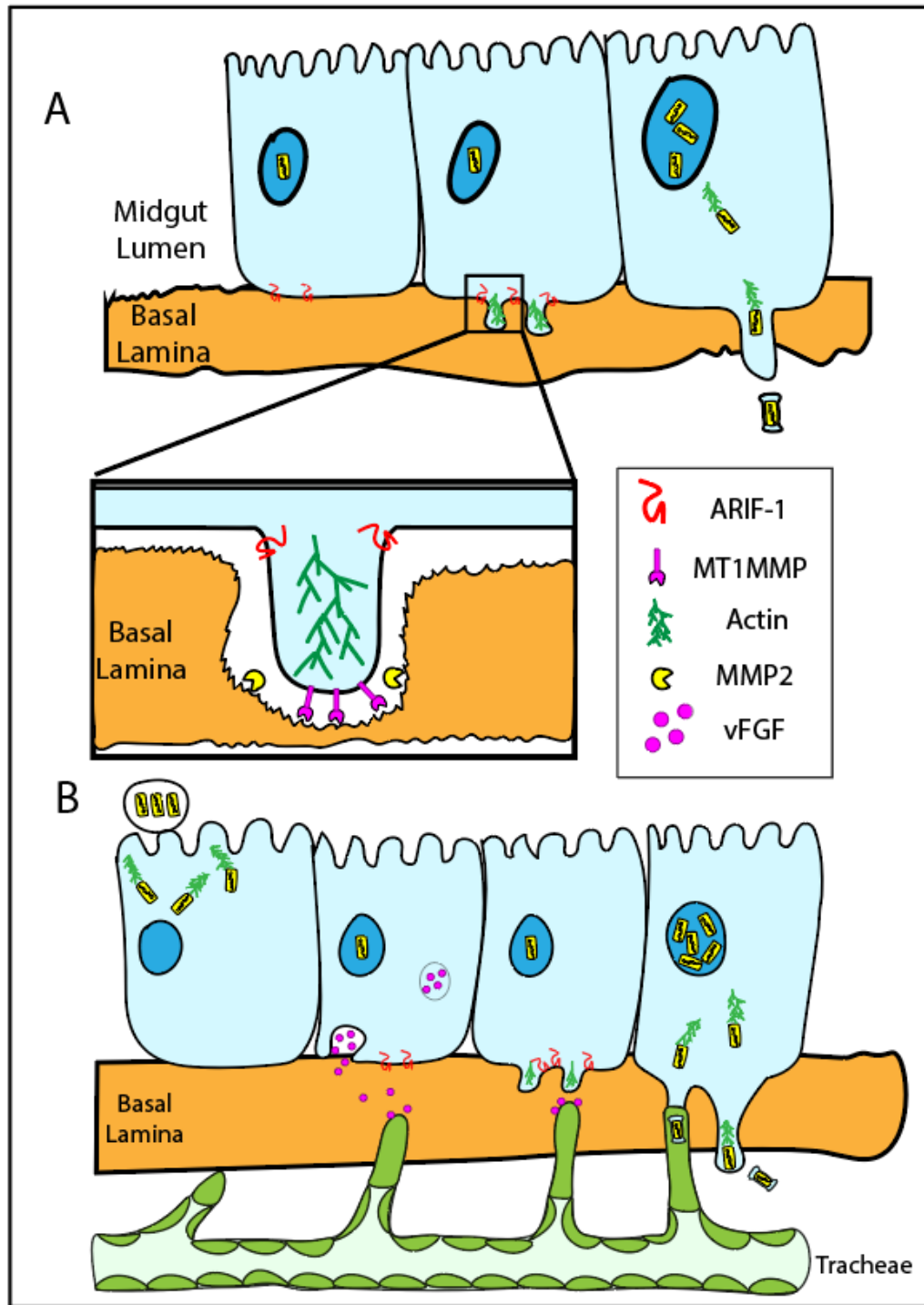


Figure 1.1: ARIF-1 may direct invadosome formation, facilitating basal lamina degradation. (A) ARIF-1 expression during delayed-early AcMNPV infection may induce invadosome formation in lepidopteran midgut epithelial cells. Invadosomes direct degradation of the basal lamina through matrix metalloprotease secretion. Invadosome BL degradation may enable viral nucleocapsids to transit across the basal lamina and into deeper insect tissues. (B) ARIF-1 mediated invadosome formation may act in conjunction with vFGF signaling to bypass the basal lamina. vFGF-induced tracheoblast growth may coincide with ARIF-1-mediated invadosome formation. Together, they may degrade or invade the basal lamina from opposite sides, facilitating basal lamina disruption and/or infection of tracheal epithelial cells.

Chapter 2

Baculovirus actin rearrangement inducing factor-1 induces the formation of dynamic clusters of invadosome-like structures

Introduction

Intracellular microbial pathogens are master manipulators of host cell biology and have evolved myriad strategies to hijack host cell machinery and repurpose host processes to facilitate infection. One such strategy is to hijack the host actin cytoskeleton, which can facilitate pathogen invasion, intracellular movement, and/or cell-cell spread. The baculovirus *Autographa californica* multiple nucleopolyhedrovirus (AcMNPV), an enveloped DNA virus that orally infects larval lepidopteran insects (caterpillars), is notable for manipulating the host actin cytoskeleton extensively throughout infection. Upon entry into the host cell cytoplasm, AcMNPV nucleocapsids undergo actin-based motility, using the viral p78/83 protein to activate host Arp2/3 complex to polymerize actin filaments (Goley et al., 2006; Ohkawa et al., 2010). Upon expression of early viral genes, actin filaments accumulate at the plasma membrane of infected cells (Charlton and Volkman, 1991; Dreschers et al., 2001; Roncarati and Knebel-Mörsdorf, 1997). This accumulation dissipates during late viral gene expression as monomeric actin is imported into and polymerizes within the nucleus (Charlton and Volkman, 1993, 1991; Hepp et al., 2018; Ohkawa et al., 2002; Ohkawa and Volkman, 1999; Volkman et al., 1992). Newly assembled viral nucleocapsids also harness p78/83 and Arp2/3 complex to polymerize actin and are propelled to the nuclear periphery to facilitate nuclear egress (Ohkawa and Welch, 2018). As both actin polymerization in the nucleus and viral actin-based motility are required for successful viral infection (Goley et al., 2006; Hess et al., 1989, 1989; Ohkawa and Volkman, 1999; Volkman, 1988; Volkman et al., 1987; Volkman and Kasman, 2000), the ability of AcMNPV to hijack the host actin cytoskeleton is of critical importance.

A second AcMNPV protein that impacts the actin cytoskeleton is the actin rearrangement inducing factor-1 (ARIF-1) (Roncarati and Knebel-Mörsdorf, 1997). ARIF-1 is a delayed-early viral protein that was identified in a screen for AcMNPV genes that cause alterations in the actin cytoskeleton when expressed in insect cells, and was shown to be necessary and sufficient to induce the accumulation of actin filaments at the plasma membrane during early infection (Roncarati and Knebel-Mörsdorf, 1997). ARIF-1 is conserved in alphabaculoviruses (Roncarati and Knebel-Mörsdorf, 1997) and contains three predicted transmembrane domains and a C-terminal proline-rich cytoplasmic domain (Dreschers et al., 2001). While ARIF-1 localizes to the plasma membrane in infected cells and is phosphorylated on tyrosine residues (Dreschers et al., 2001), the mechanism by which it induces actin polymerization is unknown. Interestingly, ARIF-1 is not important for viral replication in cultured cells (Dreschers et al., 2001; Katsuma et al., 2015; Taka et al., 2013). However, insects infected with an *arif-1* mutant *Bombyx mori* NPV (BmNPV; closely related to AcMNPV) experienced delays in infection of major organ systems and death, indicating that ARIF-1 accelerates systemic infection (Katsuma et al., 2015). Nevertheless, the mechanisms by which ARIF-1 functions in rearrangement of the host actin cytoskeleton in cells, and systemic infection in caterpillars, are still unknown.

During infection in caterpillars, AcMNPV must bypass barriers to systemic infection. AcMNPV infects through the oral route and establishes initial infection in midgut epithelial cells (Rohrmann, 2019). After replication, the virus spreads from the midgut to most major organ systems (Rohrmann, 2019). However, the basal lamina (BL), a layer of extracellular matrix (ECM) that surrounds the midgut and other major organ systems, represents a barrier to virus spread (Clem and Passarelli, 2013; Passarelli, 2011), as gaps or pores in the BL are thought to be too small for viral particles to cross (Hess and Falcon, 1987; Reddy and Locke, 1990). Because

AcMNPV is found in the caterpillar circulatory system only 30 min post-infection (Granados and Lawler, 1981), the virus must possess mechanisms to rapidly bypass the BL.

An unexplored mechanism for BL penetration is that of BL breakdown using actin-rich invadosomes. Podosomes and invadopodia (collectively known as invadosomes) are dot-like structures of 0.5 to 1 μm in diameter, characterized by a dynamic actin core surrounded by a ring of adhesion proteins (Murphy and Courtneidge, 2011). Proteins associated with these structures in mammalian cells include the actin-associated proteins cortactin (Hiura et al., 1995; Kanner et al., 1990; Oser et al., 2009) and the Arp2/3 complex (Burns et al., 2001; Linder et al., 2000; Oser et al., 2009), as well as the scaffold protein Tks5 (Seals et al., 2005). Invadosomes are sites of directed ECM degradation by matrix metalloproteases (Murphy and Courtneidge, 2011), and are common in cells that remodel the ECM, such as osteoclasts (Marchisio et al., 1984), or those that penetrate the ECM during migration, such as monocyte-derived cells (Marchisio, 1987), though they also occur in smooth muscle cells (Kaverina et al., 2003; Webb et al., 2005; Zhou et al., 2006) and endothelial cells (Moreau et al., 2003; Varon et al., 2006). Many individual invadosomes may be organized into clusters shaped as rings or rosettes (Murphy and Courtneidge, 2011). Formation of invadosomes is also associated with aggressive cancer cell lines and enables them to remodel the ECM and undergo metastasis (Murphy and Courtneidge, 2011). Viral infection can also induce invadosome formation. For example, transformation of fibroblasts with Rous sarcoma virus leads to expression of viral v-Src, a tyrosine kinase that can induce invadosome formation through activation of Tks5 (Chen, 1989; David-Pfeuty and Singer, 1980; Seals et al., 2005; Tarone et al., 1985). Thus, vertebrate tumor viruses can alter cell signaling mechanisms to induce invadosome formation.

To better understand the role of ARIF-1 in AcMNPV infection, we investigated ARIF-1-induced actin rearrangements. We found that ARIF-1 is necessary and sufficient for formation of dynamic actin-containing structures in lepidopteran cells whose appearance and dynamics are similar to invadosome clusters in mammalian cells. In addition, we found that the plasma membrane anchored ARIF-1 C-terminal cytoplasmic region is sufficient and that individual tyrosine and proline residues are necessary for formation of clusters of invadosome-like structures. Finally, we observed that clusters of invadosome-like structures co-localize with ARIF-1, cortactin, and the Arp2/3 complex, and Arp2/3 complex activity is required for their formation and maintenance. Together, our findings suggest that ARIF-1 induces the formation of invadosome-like structures that may play a role in accelerating viral infection in hosts.

Results

AcMNPV infection induces the formation of invadosome-like structures

To investigate actin cytoskeleton rearrangements induced by AcMNPV during the early stage of infection, we transiently transfected lepidopteran Sf21 cells with a plasmid expressing GFP-tagged actin (GFP-actin) and infected them with AcMNPV. As soon as 3 hours post infection (hpi), infected cells formed striking actin structures that appeared as small round clusters, circular rosettes, or elongated belts, ranging between 3 and 20 μm in size (**Fig 2.1A**). TIRF microscopy revealed that these structures were basally located on the substrate-facing cell surface (**Fig 2.1A**). We then quantified the percentage of cells with these actin structures over the

course of viral infection. We found that actin structures began to form in cells at 3 to 4 hpi, were most prevalent between 4 and 8 hpi, and could be found at times as late as 32 hpi (**Fig 2.1B**).

To further investigate the dynamics of these structures, we imaged live, infected Sf21 cells from 0 to 8 hpi. We found that the actin structures were highly dynamic in shape and position, could persist for more than 4.5 h, and could undergo fusion or fission events (**Fig 2.1C**, **Video S1**). Interestingly, the larger actin structures were comprised of many smaller $\sim 0.5 \mu\text{m}$ dot-like actin puncta (**Fig 2.1C**, **Video S2**). Individual actin puncta remained stationary relative to the substrate, and the shape of the cluster changed through appearance or disappearance of individual actin puncta (**Fig 2.1C**, **Video S2**). The appearance and behavior of the actin structures in AcMNPV-infected Sf21 cells were markedly similar to podosome rings and rosettes found in some mammalian cell types, prompting us to designate them as clusters of invadosome-like structures.

To investigate the kinetics of actin polymerization-depolymerization in invadosome-like structures, we added $4 \mu\text{M}$ latrunculin A (latA) to live infected cells and measured their persistence. Addition of latA caused GFP-actin signal in clusters of invadosome-like structures to rapidly fade with a half-life of ~ 7 -8 min, so that none of the structures remain ~ 15 min after drug addition (**Video S3**, **Fig 2.2**). The rapid disappearance of invadosome-like structures indicates that actin disassembly in these structures is relatively rapid, and that continuous actin polymerization is needed for their assembly and maintenance. We next set out to define the requirements for formation of AcMNPV-induced invadosome-like structures and to investigate their similarities with podosomes formed in mammalian cells.

ARIF-1 is necessary and sufficient for formation of invadosome-like structures

The AcMNPV *arif-1* gene is necessary and sufficient to induce accumulation of actin filaments at the cell periphery in TN368 insect cells (Roncarati and Knebel-Mörsdorf, 1997), suggesting that it may be responsible for inducing the formation of invadosome-like structures in Sf21 cells. To determine whether ARIF-1 plays a role in the formation of these structures, we constructed an *Ac Δ arif-1* virus in the AcMNPV WOBpos background that contains a deletion of 70% of the *arif-1* coding region (WOBpos is derived from the E2 strain of AcMNPV and its genome can be propagated as a bacmid in *Escherichia coli*). We also constructed an *Ac Δ arif-1 rescue* virus in which the *arif-1* gene and 500 bp flanking regions were inserted at the nearby *polyhedrin* locus in the *Ac Δ arif-1* viral genome. Sf21 cells infected with *Ac Δ arif-1* completely lacked clusters of invadosome-like structures (**Fig 2.3A, B**). Formation of clusters of invadosome-like structures was fully restored in cells infected with the *Ac Δ arif-1 rescue* virus (**Fig 2.3A, B**). This demonstrates that ARIF-1 is necessary for invadosome-like structure formation in infected Sf21 cells.

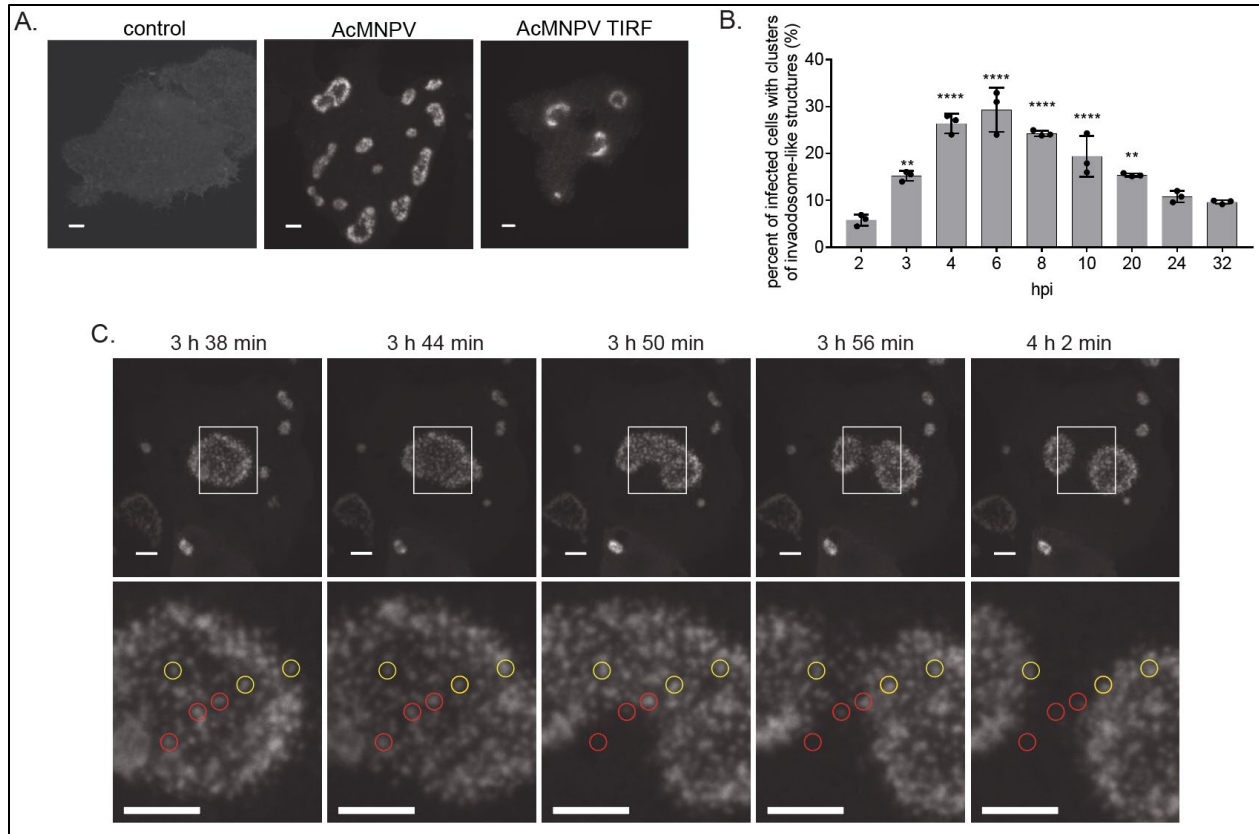


Figure 2.1: Dynamic clusters of invadosome-like structures form in Sf21 insect cells during early AcMNPV infection. (A) Confocal and TIRF images of Sf21 insect cells transiently transfected with GFP-actin and mock infected or infected with AcMNPV. Images were taken 4 to 7 hours post infection. Scale bars are 5 μ m. (B) Clusters of invadosome-like actin structures in AcMNPV infected Sf21 cells were quantified from 2 to 32 hpi. Data are mean \pm SD of three biological replicates. Asterisks show significance relative to 2 hpi timepoint. (C) Confocal time-lapse images of Sf21 insect cells transiently transfected with GFP-actin and infected with AcMNPV. Inset images on the bottom row show yellow and red circles enclosing stationary actin puncta that are maintained or disappear respectively. Scale bars are 5 μ m. Time post infection is indicated.

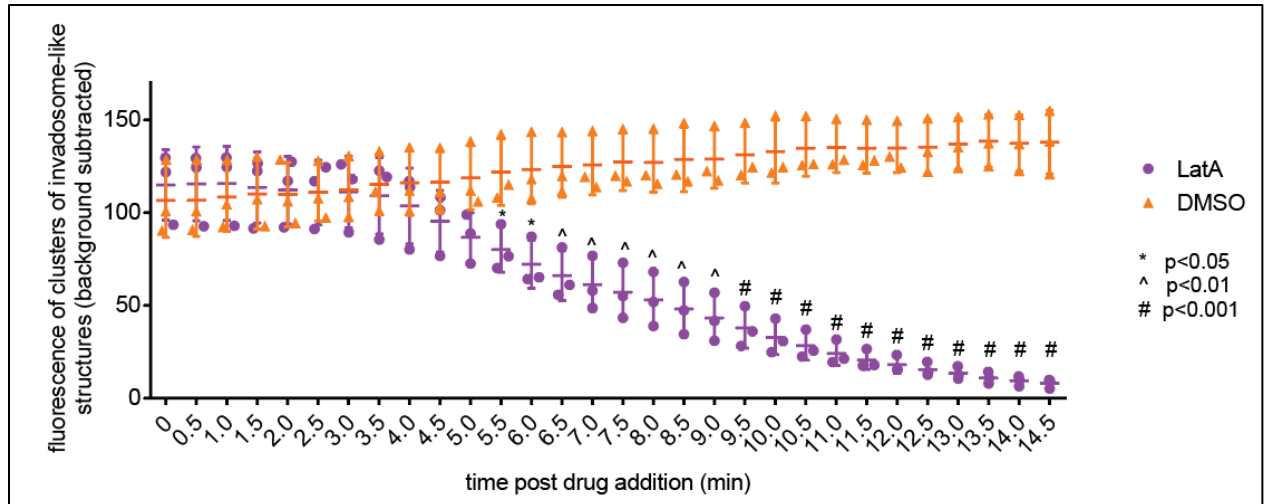


Figure 2.2: Latrunculin A induces dissipation of clusters of invadosome-like structures.

Individual clusters of invadosome-like structures were identified in live Sf21 cells transiently expressing GFP-actin and infected with AcMNPV 2 days post transfection. 4 μ M Latrunculin A was added to cells, and fluorescence of clusters of invadosome-like structures was measured from 0 to 14.5 min post drug addition. Data are mean \pm SD of three biological replicates. Symbols indicate significance from 0 min post drug addition timepoint.

To determine if ARIF-1 is sufficient for invadosome-like structure formation, we transiently transfected Sf21 cells with plasmid pACT-*arif-1*, which included *arif-1* under the control of the *B. mori* actin promoter. Transfected Sf21 cells formed clusters of invadosome-like structures (**Fig 2.3C, D**) that maintained a similar variety of shapes (small and round, circular rosettes, or elongated belts). The dynamic behavior of these structures was also similar to that in infected cells (**Video S4**). Overall, these data indicate that expression of *arif-1* alone is sufficient for the formation of clusters of invadosome-like structures in Sf21 cells.

To verify that the timing of ARIF-1 expression is consistent with that of invadosome-like structure formation, we raised a polyclonal ARIF-1 antibody and probed lysates of cells infected with AcMNPV, *AcΔarif-1*, and *AcΔarif-1 rescue* viruses over a time course of infection (**Fig 2.4**). ARIF-1 was expressed in cells infected with wild-type and *AcΔarif-1 rescue* viruses, but absent from cells infected with *AcΔarif-1*. Furthermore, the timing of ARIF-1 expression was consistent with the timing of invadosome-like structure formation and disappearance (**Fig 2.1B, Fig 2.4**). This confirms that invadosome-like structure formation is correlated with ARIF-1 expression.

ARIF-1 is localized to clusters of invadosome-like structures

ARIF-1 was previously reported to exhibit general localization to the plasma membrane in TN368 cells (Dreschers et al., 2001). To determine if ARIF-1 concentrates in invadosome-like structures, we investigated the localization of ARIF-1 in Sf21 cells. In cells transiently transfected with GFP-tagged ARIF-1 (GFP-ARIF-1), GFP-ARIF-1 localized to the plasma membrane, with a concentration at clusters of invadosome-like structures (**Fig 2.5**). In some instances, the localization appeared uniform throughout the cluster, and in others it appeared to be more prominent at the periphery of the cluster (**Fig 2.5**). Thus, ARIF-1 is enriched at clusters of invadosome-like structures.

The ARIF-1 C-terminal region is necessary and sufficient for formation of clusters of invadosome-like structures

Prior structural predictions and our own analyses suggested that ARIF-1 contains three N-terminal transmembrane domains and a ~200 aa C-terminal region that extends into the cytoplasm (Dreschers et al., 2001) (**Fig. 2.6A**). We first sought to determine which parts of the ARIF-1 C-terminal region are necessary for formation of clusters of invadosome-like structures. We constructed a series of C-terminal truncations of ARIF-1 (**Fig 2.6B**) and quantified formation of clusters of invadosome-like structures in transiently transfected Sf21 cells (**Fig 2.6B, Fig 2.7A**). Although expression of ARIF-1(1-401) (containing C-terminal residues up through amino-acid 401), ARIF-1(1-398), ARIF-1(1-378), and ARIF-1(1-371) caused a reduced percentage of cells with clusters of invadosome-like structures when compared with expression of the full-length protein ARIF-1(1-417), these clusters still formed. However, no such structures formed in cells transfected with ARIF-1(1-274). This indicates that the ARIF-1 C-terminus between residues 274-371 is necessary for formation of clusters of invadosome-like structures.

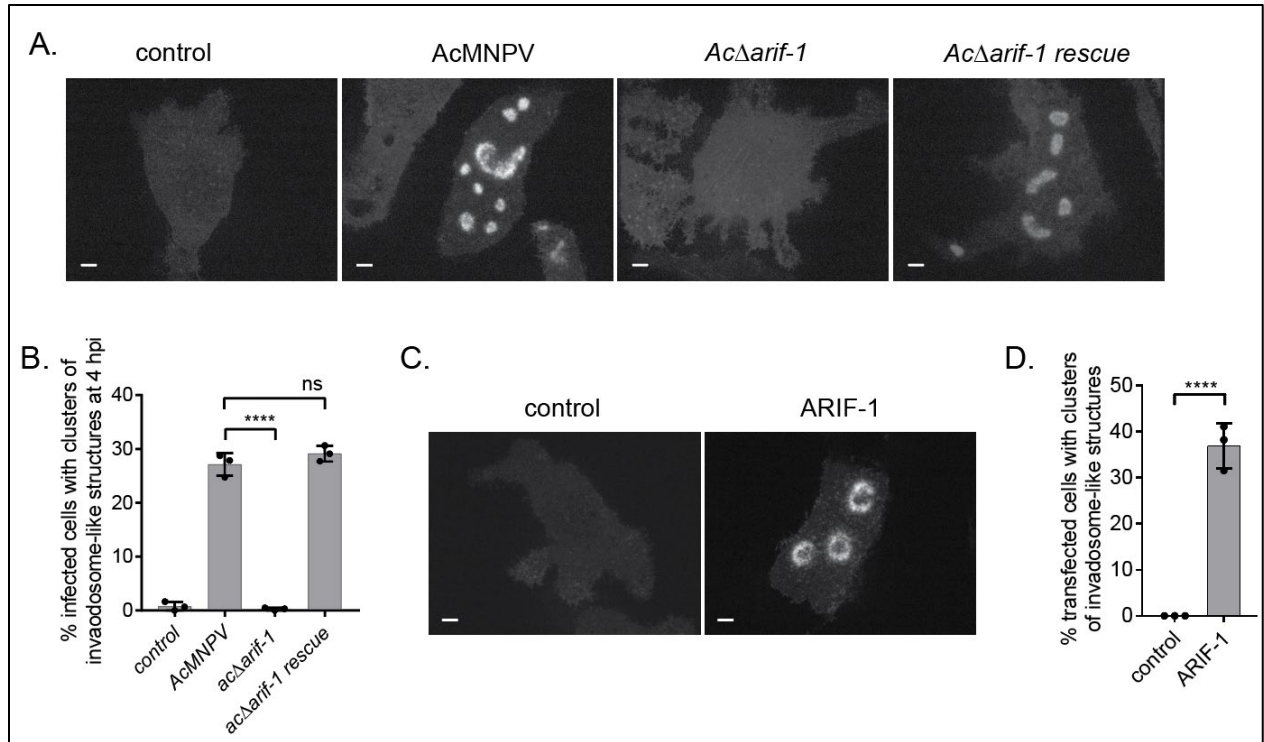


Figure 2.3: ARIF-1 is necessary and sufficient for formation of clusters of invadosome-like structures. (A) Confocal images of Sf21 cells transiently transfected with GFP-actin and infected with MOI = 10 of the indicated virus. Images were taken 4 hpi and are representative of three biological replicates. Scale bars are 5 μ m. **(B)** Clusters of invadosome-like structures in infected cells were quantified at 4 hpi. Data are mean \pm SD of three biological replicates. **(C)** Confocal images of Sf21 cells transiently expressing GFP-actin and ARIF-1. Images were taken 2 days post transfection and are representative of three biological replicates. Scale bars are 5 μ m. **(D)** Quantification of clusters of invadosome-like structures in cells transfected with GFP-actin and ARIF-1. Structures were quantified by eye 2 days post transfection. Data are mean \pm SD of three biological replicates.

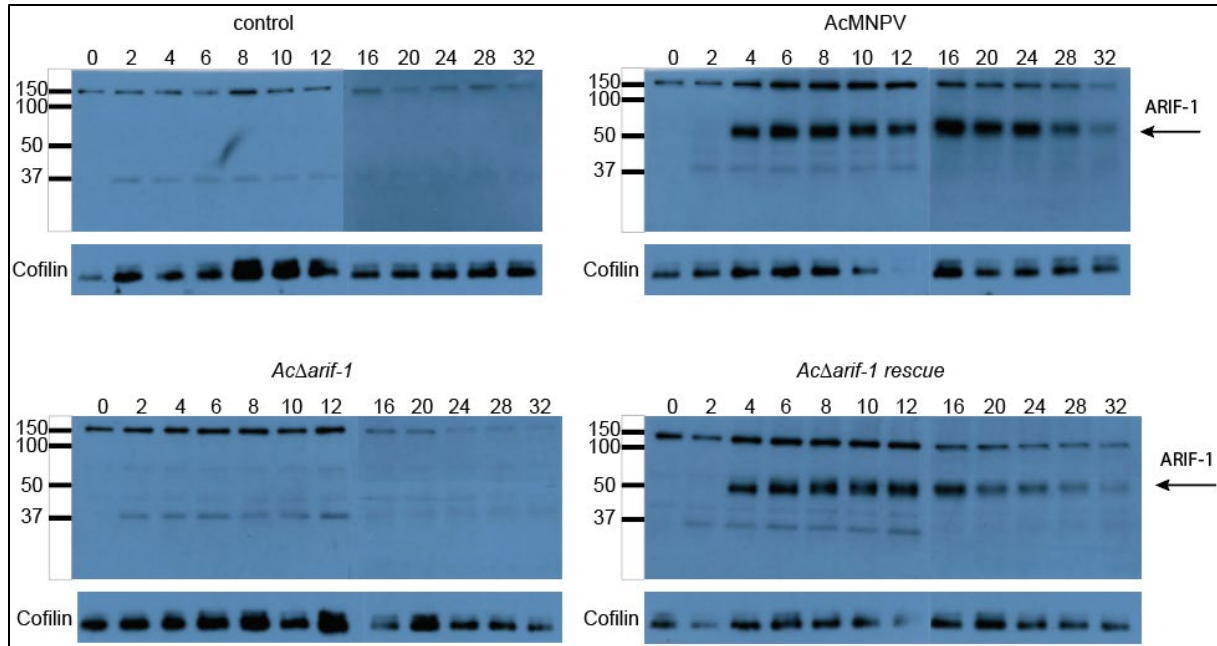


Figure 2.4: ARIF-1 expression corresponds with formation of clusters of invadosome-like structures. Western blots of lysates of Sf21 cells infected with the indicated virus harvested at 0 to 32 hpi. Lysates were probed with an anti-rabbit ARIF-1 antibody. Cofilin is shown as a loading control.

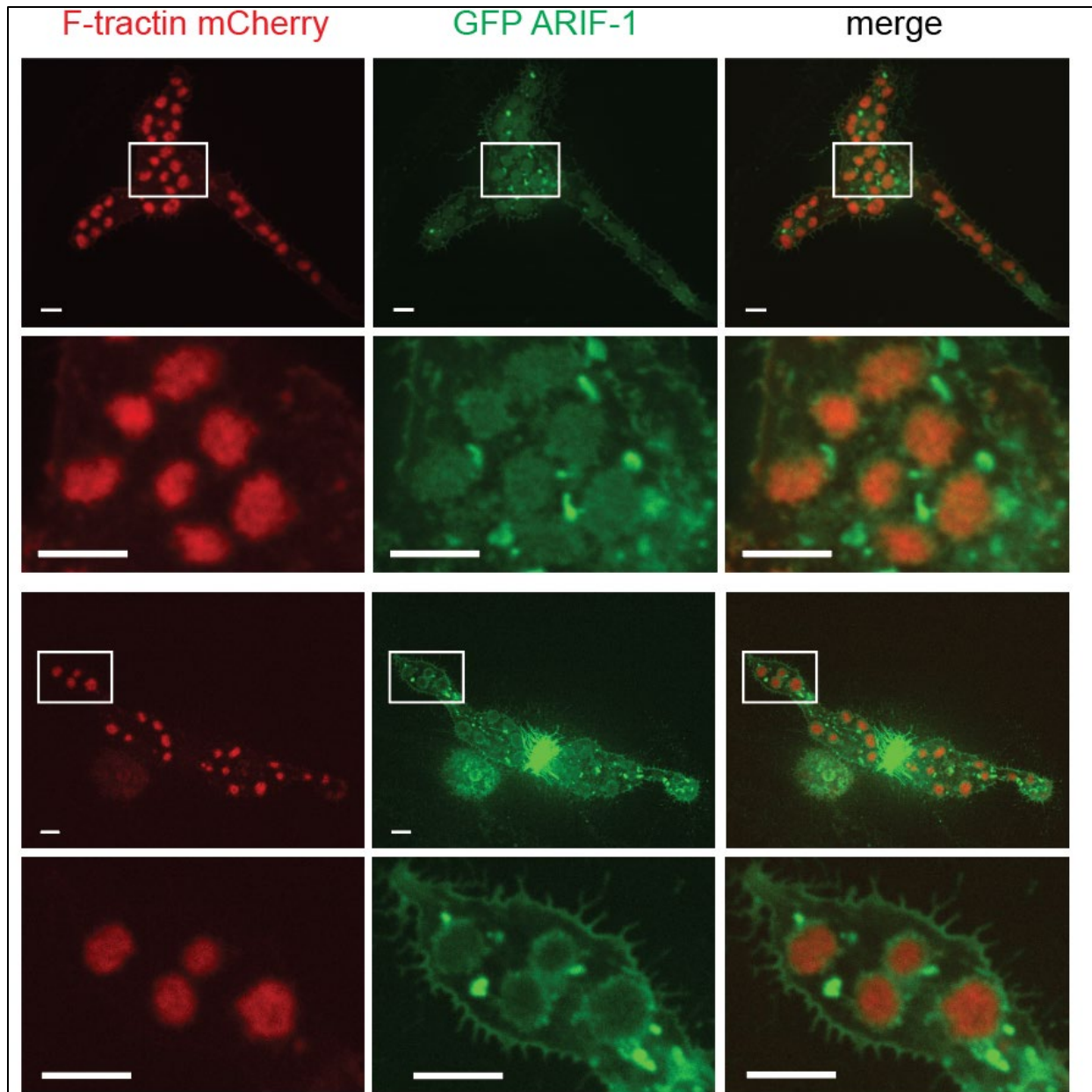


Figure 2.5: ARIF-1 co-localizes with clusters of invadosome-like structures. Confocal images of Sf21 cells transiently expressing Lifeact mCherry and GFP-tagged ARIF-1. Images were taken 2 days post transfection and are representative of three biological replicates. Scale bars are 5 μm .

To determine the contributions of the ARIF-1 N-terminal and transmembrane regions, we transfected cells with a plasmid that expressed ARIF-1(219-417) missing N-terminal amino acids 1-218 that encode for the predicted transmembrane domains and cytoplasmic loop (**Fig 2.6C**). Sf21 cells transiently transfected with ARIF-1(219-417) did not form invadosome-like structures (**Fig 2.6C**), indicating that the transmembrane domains are required for ARIF-1 function. Next, to test whether membrane targeting of the C-terminus is sufficient for formation of clusters of invadosome-like structures, we expressed a variant of ARIF-1 in which the ARIF-1 C-terminus was fused to the unrelated AcMNPV transmembrane protein gp64 (**Fig 2.6A, right**). Surprisingly, a similar percentage of cells expressing gp64::ARIF-1(219-417) formed clusters of invadosome-like structures compared with cells expressing full-length ARIF-1(1-417) (**Fig 2.6C, Fig 2.7B, Video S5**). This indicates that the membrane targeted ARIF-1 C-terminus from residues 219-417 is sufficient for formation of clusters of invadosome-like structures, and the ARIF-1 N-terminal cytoplasmic loop and transmembrane regions function to anchor the ARIF-1 C-terminal region to the plasma membrane.

To further narrow down which regions of the ARIF-1 C-terminus are necessary for formation of clusters of invadosome-like structures, we constructed a series of N-terminal truncations to gp64::ARIF-1(219-417) and quantified invadosome-like structure formation in transiently transfected Sf21 cells (**Figure 2.6C**). Cells expressing gp64::ARIF-1(274-417) and gp64::ARIF-1(303-417) had clusters of invadosome-like structures, whereas these structures were completely absent in cells expressing gp64::Arif-1(320-417). Altogether, the data from expression of truncation derivatives indicates that the ARIF-1 C-terminus between residues 303-371 is necessary for formation of clusters of invadosome-like structures.

ARIF-1 residues Y332F and P335A are important for formation of clusters of invadosome-like structures

We next sought to identify individual residues in the ARIF-1 C-terminal region that may be important for the formation of clusters of invadosome-like structures. ARIF-1 is tyrosine-phosphorylated during infection, though which tyrosine residues are phosphorylated is unknown (Dreschers et al., 2001). The ARIF-1 C-terminus also contains several stretches rich in proline residues (**Fig 2.8A, left**). We sought to assess the importance of individual tyrosine and proline residues by mutating tyrosine to phenylalanine and proline to alanine (**Fig 2.8A, Fig 2.9**). We then quantified clusters of invadosome-like structures in Sf21 cells transiently expressing ARIF-1 mutants (**Fig 2.8 B, C**). While most mutations did not significantly affect the formation of clusters of invadosome-like structures, cells transiently transfected with ARIF-1(Y332F) and ARIF-1(P335F) mutations had no clusters, but form invadosome-like structures uniformly dispersed across the basal cell surface (**Fig 2.8D, Fig 2.9 A, B, Video S6, S7**). To verify that differences in formation of clusters of invadosome-like structures in ARIF-1 tyrosine and proline point mutants were not due to differences in expression levels of the ARIF-1 point mutant, we probed cell lysates using the ARIF-1 antibody (**Fig 2.10**). ARIF-1 was detected in cells transfected with ARIF-1 Y332F and P335A mutations, demonstrating that the lack of clusters of invadosome-like structures was not due to decreased ARIF-1 expression. Our results are consistent with truncation analyses, which pointed to key residues between 303-371, and suggest that adjacent residues Y332 and P335 facilitate the formation of clusters of invadosome-like structures.

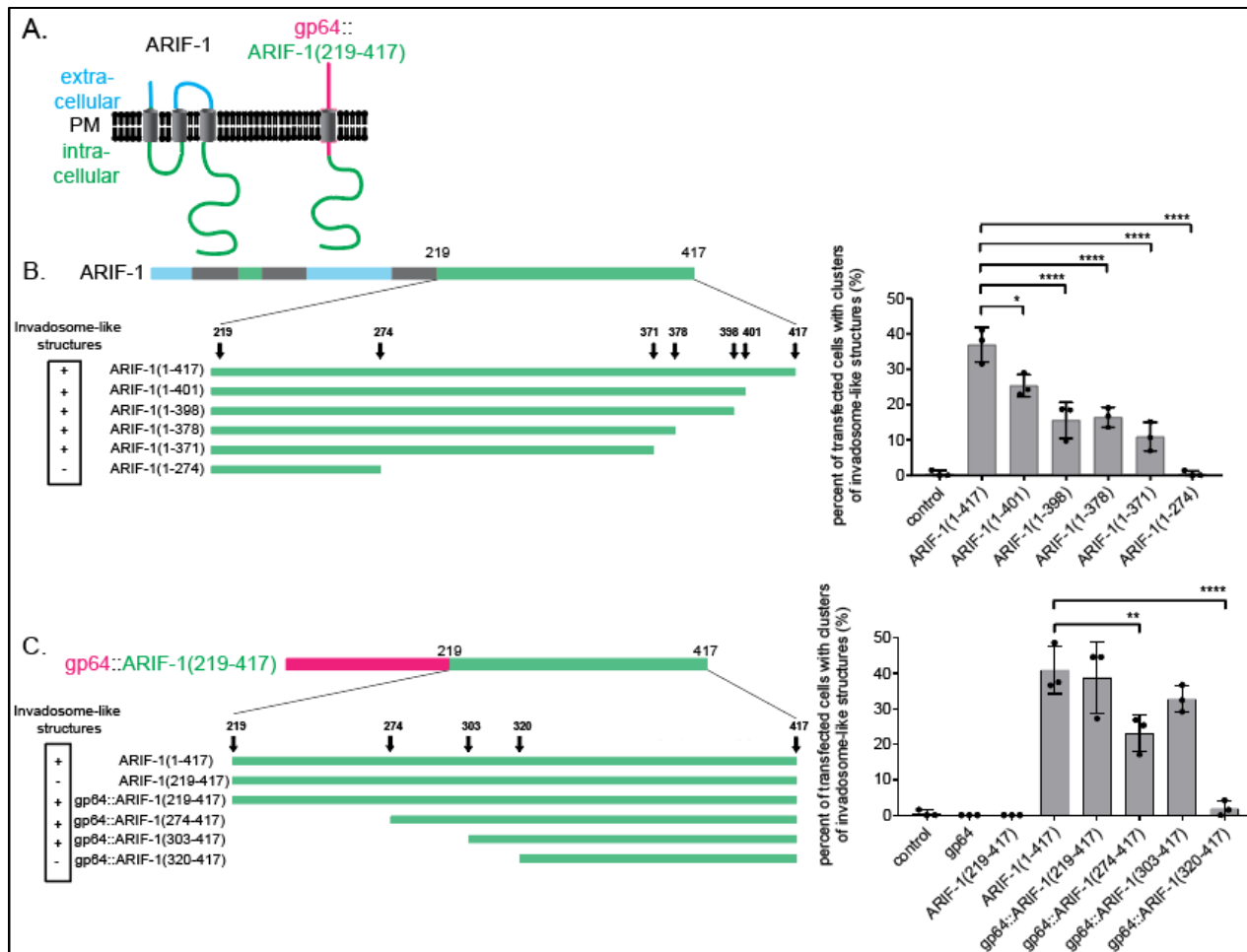


Figure 2.6: ARIF-1 residues 303-371 are necessary for formation of clusters of invadosome-like structures. (A) Left: predicted ARIF-1 structure with three transmembrane domains and a cytoplasmic C-terminal region (amino acids 219-417). Right: AcMNPV transmembrane protein gp64 (red) fusion to ARIF-1 C-terminal region. (B) Left: visual representation of ARIF-1 C-terminal truncations. Right: quantification of clusters of invadosome-like structures in Sf21 cells transiently expressing GFP-actin and truncated ARIF-1 2 days post transfection. Data are mean +/- SD of three biological replicates. Asterisks indicate significance relative to ARIF-1(1-417). (C) Left: visual representation of AcMNPV transmembrane protein gp64 (red) fused to ARIF-1(219-417) and N-terminal truncations. Right: quantification of clusters of invadosome-like structures in Sf21 cells transiently expressing GFP-actin and the indicated construct 2 days post transfection. Data are mean +/- SD of three biological replicates. Asterisks indicate significance relative to ARIF-1(1-417).

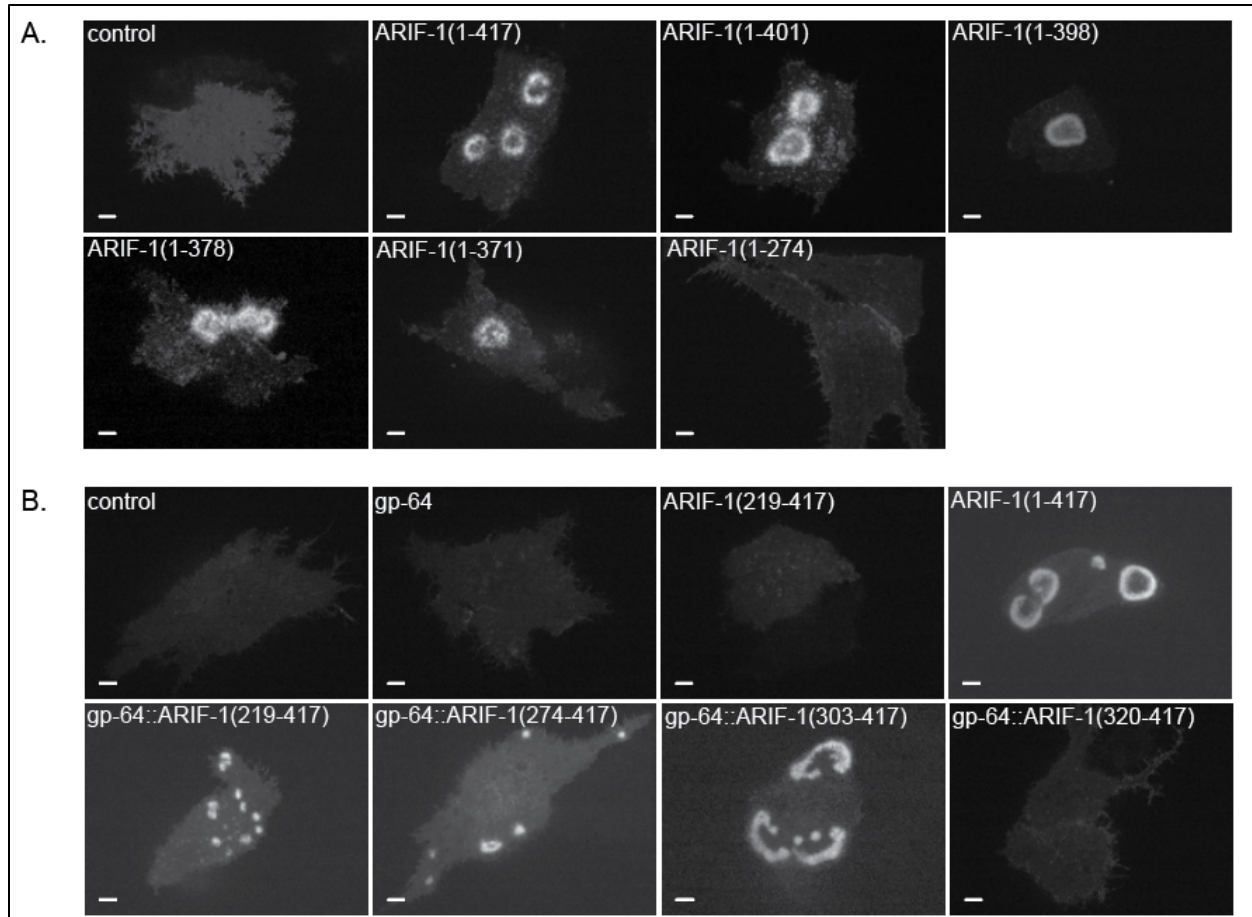


Figure 2.7: Cells expressing the ARIF-1 C-terminal cytoplasmic region form clusters of invadopodia-like structures. (A) Confocal images of Sf21 cells transiently expressing GFP-actin and ARIF-1 C-terminal truncations. Images were taken two days post transfection and are representative of three biological replicates. Scale bars are 5 μm . **(B)** Confocal images of Sf21 cells transiently expressing GFP-actin and ARIF-1 N-terminal truncations and gp64 fused ARIF-1 truncations. Images were taken two days post transfection and are representative of three biological replicates. Scale bars are 5 μm .

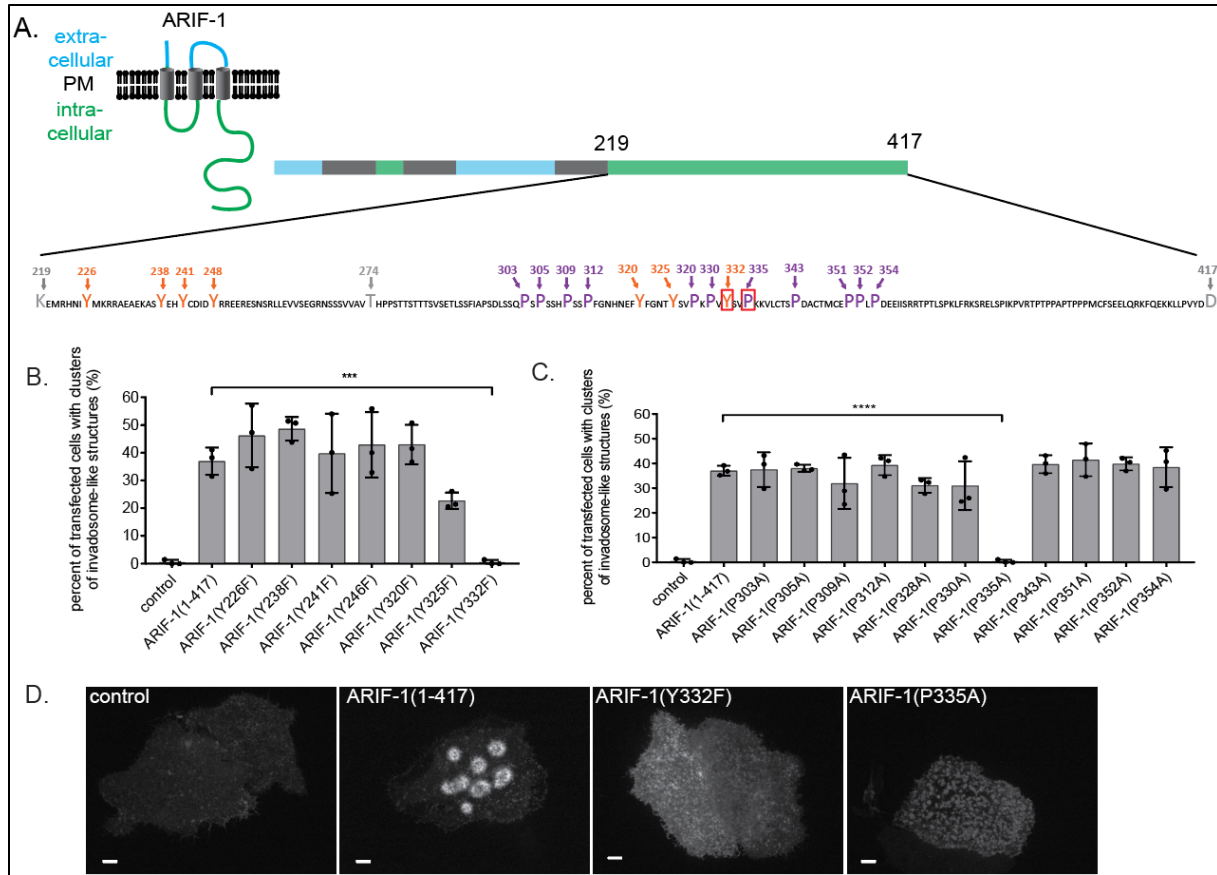


Figure 2.8: ARIF-1 residues Y332F and P335A are important for formation of clusters of invadosome-like structures. (A) Tyrosine (orange) and proline (purple) residues are indicated on the C-terminal region of ARIF-1. Amino acid identification is shown. (B) Clusters of invadosome-like structures in cells transiently transfected with GFP-actin and the indicated tyrosine to phenylalanine point mutations were quantified 2 days post transfection. Data are mean \pm SD of three biological replicates. Asterisks indicate significance relative to ARIF-1(1-417). (C) Clusters of invadosome-like structures in cells transiently transfected with GFP-actin and the indicated proline to alanine point mutations were quantified 2 days post transfection. Data are mean \pm SD of three biological replicates. Asterisks indicate significance relative to ARIF-1(1-417). (D) Confocal images of Sf21 cells transiently expressing GFP-actin and the indicated ARIF-1 mutation. Images are representative of three biological replicates. Scale bars are 5 μ m.

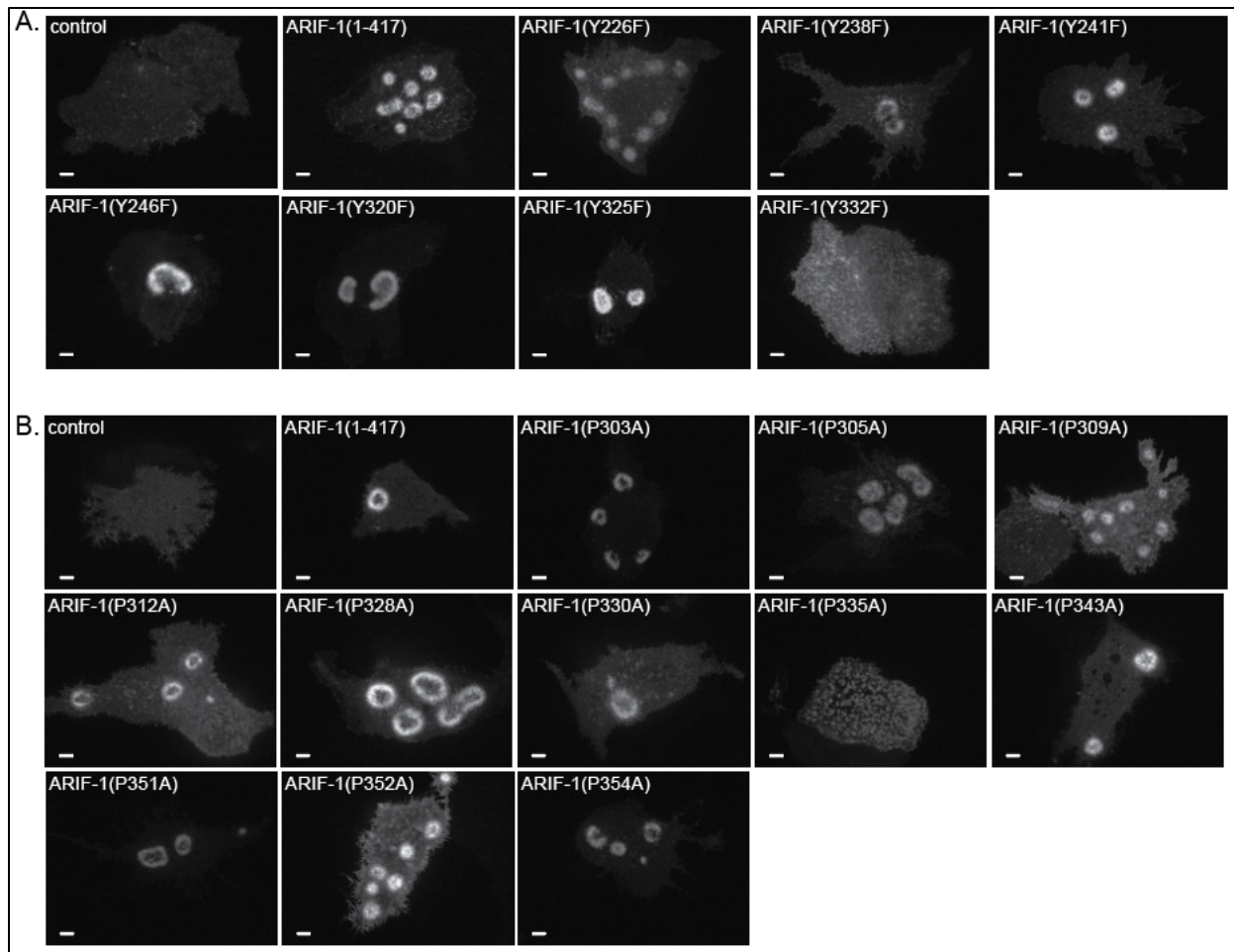


Figure 2.9: Invadosome-like structures form in cells expressing ARIF-1 tyrosine and proline residue mutations. (A) Confocal images of Sf21 cells transiently expressing GFP-actin and ARIF-1 tyrosine point mutations. Images were taken two days post transfection and are representative of three biological replicates. Scale bars are 5 μm. (B) Confocal images of Sf21 cells transiently expressing GFP-actin and ARIF-1 proline point mutations. Images were taken two days post transfection and are representative of three biological replicates. Scale bars are 5 μm.

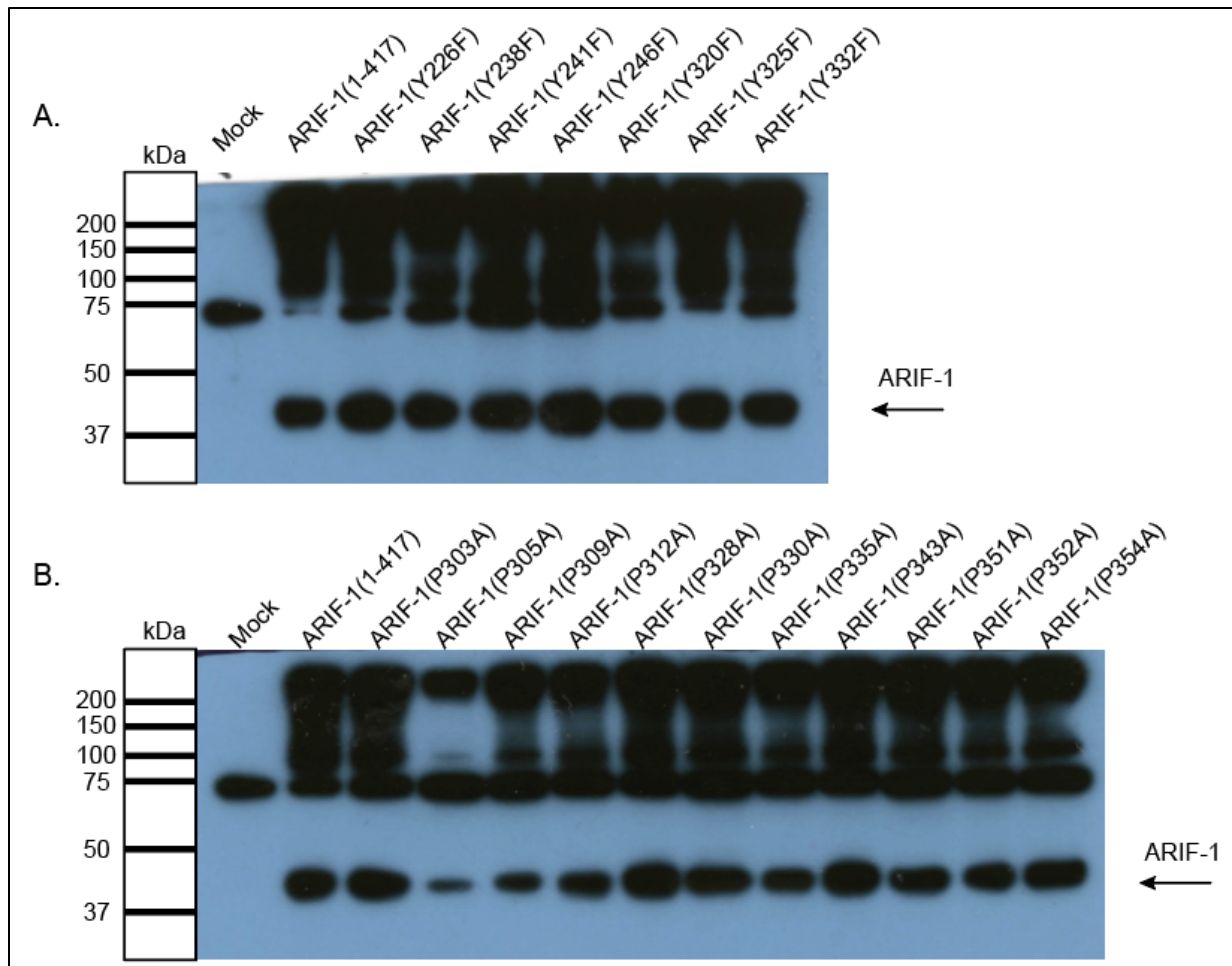


Figure 2.10: ARIF-1 is expressed in cells transiently expressing ARIF-1 proline and tyrosine point mutants. (A) Western blot of lysates of Sf21 cells transiently transfected with ARIF-1 tyrosine point mutants. Blots were probed with ARIF-1 antibody. (B) Western blot of lysates of Sf21 cells transiently transfected with ARIF-1 proline point mutants. Blots were probed with ARIF-1 antibody.

Cortactin and the Arp2/3 complex play a role in the formation and maintenance of invadosome-like structures.

The actin core of podosomes in mammalian cells includes cortactin (Hiura et al., 1995; Pfaff and Jurdic, 2001) and the Arp2/3 complex (Linder et al., 2000) (Hiura et al., 1995; Mizutani et al., 2002). To determine if invadosome-like structures in lepidopteran cells have a similar protein composition, we investigated whether cortactin and the Arp2/3 complex colocalize with these structures. GFP-tagged *S. frugiperda* cortactin (GFP-cortactin) was expressed in Sf21 cells by transient transfection, which were subsequently infected with AcMNPV WOBpos and imaged at 4 hpi. GFP-cortactin co-localized with actin in invadosome-like structures (**Fig 2.11C**). To determine if the Arp2/3 complex localizes to clusters of invadosome-like structures, we expressed GFP-tagged Arp2/3 complex subunit ARPC3 (GFP-ARPC3) in Sf21 cells by transient transfection and infected these cells with AcMNPV. At 4hpi, GFP-ARPC3 also co-localized with clusters of invadosome-like structures (**Fig 2.11B**). Thus, both cortactin and the Arp2/3 complex are present at these areas of dynamic actin polymerization.

To determine if the host Arp2/3 complex plays a role in formation and maintenance of invadosome-like structures, we treated infected cells with Arp2/3 complex inhibitor CK666, or with the inactive control drug CK869. Clusters of invadosome-like structures were virtually eliminated 1 h post treatment with Arp2/3 inhibitor CK666, but no significant effect was observed upon treatment with the inactive control drug CK869 (**Fig 2.11A, Video S7, S8, S9**). Thus, host Arp2/3 complex function is required for formation and maintenance of these structures.

Discussion

Here, we describe the formation of dynamic actin structures in AcMNPV-infected lepidopteran insect cells that coalesce into clusters, rosettes, and rings, resembling podosome clusters in mammalian cells. We further show that the AcMNPV protein ARIF-1 is necessary and sufficient for formation of these invadosome-like structures. We identify regions of ARIF-1 and individual proline and tyrosine residues critical for their formation. Lastly, we verify that ARIF-1, cortactin, and the Arp2/3 complex localize with clusters of invadosome-like structures, and that Arp2/3 complex function is important for their maintenance. Our results suggest that ARIF-1 induces the formation of invadosome-like structures in lepidopteran cells, and that these structures may facilitate systemic AcMNPV spread in hosts.

Our results add to previous observations by describing the formation of AcMNPV-induced and ARIF-1-dependent invadosome-like structures. Previously, it was noted that during early stage AcMNPV infection, actin accumulated evenly around the periphery of TN368 and BmN cells (Katsuma et al., 2015; Roncarati and Knebel-Mörsdorf, 1997), and in Sf21 cells accumulated in “ventral aggregates” on the basal cell surface (Charlton and Volkman, 1991). However, the finer organization and dynamics of this peripheral actin was not described. Using live cell imaging, we observed that ARIF-1 induces formation of actin puncta that cluster together into dynamic clumps, rosettes, or belts, and that these can persist for hours and change shape and position. Though we have not observed clusters of invadosome-like structures in TN368 cells, they are present in Sf9 (Taro Ohkawa, personal communication), Sf21

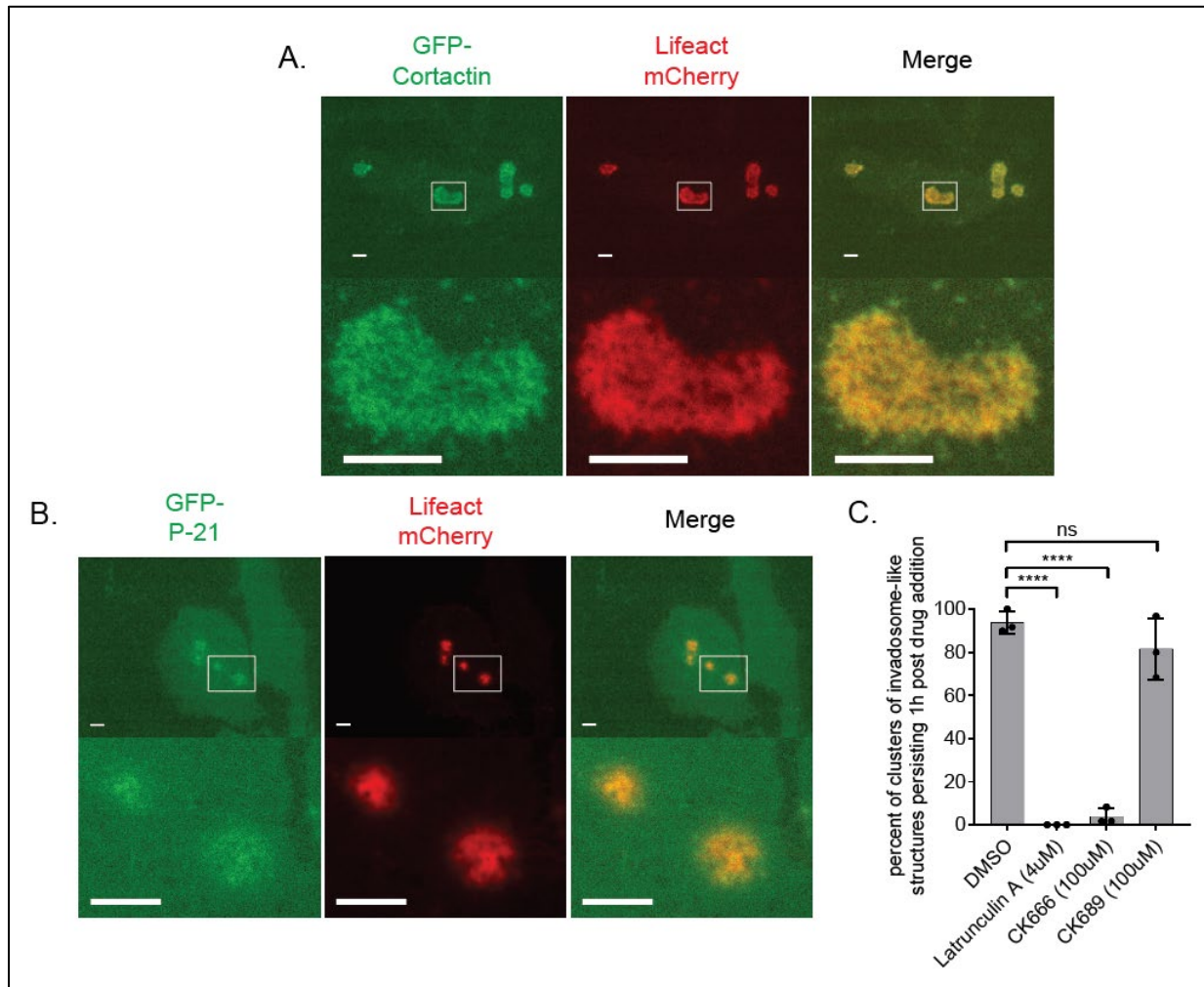


Figure 2.11: Cortactin and the Arp2/3 complex play a role in maintenance of clusters of invadosome-like structures. (A) Confocal images of Sf21 cells transiently expressing Lifeact mCherry and GFP-tagged *S.frugiperda* cortactin. Images were taken 2 days post transfection and are representative of three biological replicates. Scale bars are 5 μ m. (B) Confocal images of Sf21 cells transiently expressing Lifeact mCherry and GFP-tagged Arp2/3 complex subunit P21. Images were taken 2 days post transfection and are representative of three biological replicates. Scale bars = 5 μ m. (C) Clusters of invadosome-like structures were quantified 1 hour after cytoskeleton-affecting drugs were added to Sf21 cells infected with AcMNPV 4hpi. Data are mean \pm SD of three biological replicates of 40 invadosome-like structures. Scale bars are 5 μ m.

(Charlton and Volkman, 1991), and BmN (data not shown) cell lines, indicating that they are not restricted to a single cell line or even species.

ARIF-1 induced actin structures in Sf21 cells are similar to podosomes and invadopodia in appearance and dynamics. In mammalian osteoclasts, many stationary dot-like podosomes organize into clusters that merge to form one large ring around the cell periphery (Destaing et al., 2003; Luxenburg et al., 2007). The shape of these ring structures is determined by selective activation and inactivation of stationary podosomes, much like how individual pixels on a screen turn on and off to create a moving image (Destaing et al., 2003). We have observed a similar phenomenon in clusters of invadosome-like structures in AcMNPV-infected or *arif-1*-transfected Sf21 cells. However, instead of full podosome rings as seen in osteoclasts, these structures more closely resemble invadopodia rosettes in *src*-transformed fibroblast cells (Kuo et al., 2018). Intriguingly, invadopodia rosettes have also been described as dynamically changing shape, fusing together, or splitting in two to form new invadopodia rosettes (Kuo et al., 2018), all of which we observed in clusters of invadosome-like structures in lepidopteran cells. Individual osteoclast podosomes persist for 2 min on average, with actin turnover on the order of 1 min (Destaing et al., 2003). Meanwhile, podosome clusters in these cells persist for several hours (Destaing et al., 2003). In lepidopteran cells, actin in invadosome-like structures has a half-life of approximately 7 min and clusters persist for hours.

ARIF-1 induced actin structures also have similar protein composition to podosomes and invadopodia. We confirmed that ARIF-1 localizes to the plasma membrane, concentrating around the clusters of invadosome-like structures. Furthermore, actin, cortactin, and the Arp 2/3 complex localize to invadosome-like structures themselves. These are also critical components of mammalian podosomes and invadopodia (Linder, 2007; Murphy and Courtneidge, 2011), implying a parallel between those structures and ARIF-1-induced invadosome-like structures. Interestingly, the scaffolding protein tyrosine kinase with five SH3 domains (Tks5), which is a distinct marker of podosomes and invadopodia in mammalian cell types (Murphy and Courtneidge, 2011; Seals et al., 2005), lacks a clear ortholog in *S. frugiperda*. This suggests the possibility that ARIF-1 itself may be acting as a scaffolding protein, playing a similar role to mammalian Tks5 in podosome assembly.

We have identified a stretch of the ARIF-1 C-terminal region as well as specific residues of ARIF-1 that are required for forming clusters of invadosome-like structures. While the ARIF-1 C-terminal region 303-371 is required for formation of invadosome-like structures, the residues Y332 and P335 are required for cluster formation. In cells expressing ARIF-1 with Y332F and P335A point mutations, invadosome-like structures were distributed across the entire basal plasma membrane rather than in defined clusters. That a phosphoablative tyrosine to phenylalanine mutation at residue 332 causes this phenotype suggests that Y332 is phosphorylated. Phosphorylated tyrosine residues are key components of binding sites for Src homology 3 (SH3) domains, which are common in proteins such as Tks5, Grb-2, and Nck-1 that regulate actin cytoskeleton activity. A truncated ARIF-1 (ARIF-1(1-255)) is tyrosine-phosphorylated during infection (Dreschers et al., 2001), and previous reports speculated that increased ARIF-1 phosphorylation as infection progresses is correlated with disappearance of the ARIF-1 induced peripheral actin in TN368 cells (Dreschers et al., 2001). Thus, ARIF-1 tyrosine phosphorylation at Y332 may play a role during early AcMNPV infection, possibly by

generating a binding site for cellular or viral proteins that induce or regulate actin polymerization in invadosome-like structures, leading to formation of organized clusters. However, we have not definitively shown that ARIF-1 Y332 is phosphorylated, or how phosphorylation of ARIF-1 may influence interactions with other cellular or viral proteins.

Our findings describe an ARIF-1-induced invadosome-like structure in insect cells. At the level of the host caterpillar, ARIF-1 has also been shown to play a role in viral spread. One explanation that could link the cellular- and organismal-level functions of ARIF-1 is that ARIF-1-induced podosome or invadopodia-like structures might mediate degradation of the underlying ECM and degrade barriers to viral infection, such as the insect BL. While we have not confirmed that ECM degradation underneath clusters of invadosome-like structures occurs, this hypothesis may inform current models of how other viruses, including human arbovirus pathogens, cross the BL in their insect hosts. For example, Eastern equine encephalitis virus disrupts the midgut BL of infected mosquitos (Weaver, 1988), though the mechanism of this disruption is unknown. While podosome formation has not previously been described in lepidopteran cell lines, invadosome-like structures have been described playing a role in myoblast fusion in *Drosophila*, though these structures were not organized into larger clusters (Duan et al., 2012; Sens et al., 2010). Such insect invadosome-like structures may hint at the existence of an ancestral podosome or invadopodium activation pathway retained by both mammalian and invertebrate animals that may be taken advantage of by viral pathogens. Thus, further understanding of the molecular mechanisms of podosome and invadopodia formation in both mammalian and insect cell models may uncover conserved roles in infection and other diseases.

Materials and Methods

Cell lines and viruses

Spodoptera frugiperda ovarian-derived Sf9 cells were maintained in suspension culture in ESF 921 media (Expression Systems, Davis, CA) and in adherent culture in Grace's media (Gemini Bio-Products, West Sacramento, CA) with 10% fetal bovine serum (FBS; Gemini Bio-Products) on T-25 tissue culture flasks at 28°C. *S. frugiperda* ovarian-derived Sf21 cells were maintained in suspension culture in Grace's media (Gemini Bio-Products) with 10% FBS (Gemini Bio-Products) and 0.1% Pluronic F-68 (Gibco from Thermo Fisher Scientific, Waltham, MA) at 28°C, and in adherent culture on T-25 tissue culture flasks in Grace's media (Gemini Bio-Products; Expression systems) with 10% FBS (Gemini Bio-Products) at 28°C. *Bombyx mori* ovarian-derived BmN cells were a generous gift from Kostas Iatrou (Institute of Biosciences & Applications, National Centre for Scientific Research, Greece), through Don Jarvis (University of Wyoming). These cells were maintained in adherent culture on T-25 tissue culture flasks in TC-100 media (Gibco from Thermo Fisher Scientific) with 10% FBS (Gemini Bio-Products) at 28°C. MDA-MB-231 human breast adenocarcinoma cells were maintained in adherent culture on T-75 tissue culture flasks in Dubelco's modified eagle medium (Gibco from Thermo Fisher Scientific) supplemented with 10% FBS (Atlas Biologicals, Fort Collins, CO) that was heat-inactivated at 65°C for 20 min. AcMNPV WOBpos virus (Goley et al., 2006), derived from AcMNPV E2, was used as the wild-type virus.

Generation of recombinant viruses

To generate AcMNPV lacking a functional *arif-1* gene (*AcΔarif-1*), we constructed a transfer vector by subcloning a Sall/XhoI fragment of AcMNPV viral genomic fragment EcoRI A which contains *arif-1* into the XhoI site of pBluescript II SK+ (Addgene, Watertown, MA) to create the plasmid pEcoRI_ASAlxh.pBSKS.rev. This plasmid was digested with MluI (New England Biolabs, Ipswich, MA), removing 74% of the *arif-1* coding region, which was replaced with a subcloned 5.4 kb fragment of MluI digested pBlue-Tet, containing *lacZ* and tetracycline-resistance (*tetR*) genes (Goley et al., 2006; Ohkawa et al., 2005) to help in the selection of recombinant bacmids. The transfer vector was linearized by digestion with SmaI and ApaI (New England Biolabs) and purified by agarose gel electrophoresis. 30 fmol of DNA was co-electroporated with 0.2 μg of WOBpos bacmid DNA (containing the kanamycin-resistance (*kanR*) gene) into BW251143/pKD46 *E.coli* (Datsenko and Wanner, 2000), which expresses an arabinose-inducible recombinase on a plasmid with temperature-sensitive replication (Goley et al., 2006). Recombinant bacmids were selected by plating on Luria-Bertani (LB) agar plates with 50 μg/ml kanamycin (Gibco from Thermo Fisher Scientific) and 10 μg/ml tetracycline (MilliporeSigma, St. Louis, MO).

To generate an *AcΔarif-1* rescue virus (*AcΔarif-1 rescue*), we introduced the *arif-1* gene into the polyhedrin locus of the *AcΔarif-1* bacmid. To do this, we generated the transfer plasmid pARIF-1-Rescue-2 by PCR, amplifying a 2.2 kb fragment including *arif-1* and 500 bp 5' and 3' flanking sequences from pEcoRI_ASAlxh.pBSKS.rev (Table 1), and inserted it using Gibson assembly (New England Biolabs; Gibson et al., 2009) into pWOBCAT (Ohkawa et al., 2010) (Table 1) amplified and linearized by PCR, inserting it upstream of a chloramphenicol resistance (*cat*) gene to help in the selection of recombinant bacmids. The resulting plasmid was digested with NotI and KasI (New England Biolabs) to remove a truncated *kanR* gene upstream of *arif-1*, which was replaced by ligating (Takara Bio USA) a 2 kb PCR-amplified fragment from pWOBpos2 (Goley et al., 2006) (Table 1) including the AcMNPV mini-F replicon and a full *kanR* gene in place of the truncated *kanR* gene. This plasmid transfer vector, pARIF-1-Rescue-2, was linearized through KpnI digestion (New England Biolabs) and purified by agarose gel electrophoresis. 30 fmol of DNA was electroporated with 0.2 μg of *AcΔarif-1* bacmid DNA into BW251143/pKD46 *E.coli* as described above, and bacteria were plated on LB agar plates with 25 μg/ml chloramphenicol and 10 μg/ml tetracycline (MilliporeSigma).

In all cases, positive colonies were grown in 2x YT media (MilliporeSigma) with 25 μg/ml kanamycin (Gibco from Thermo Fisher Scientific) for 18 hours at 37°C. Bacmid DNA was extracted and transfected into Sf9 cells using TransIT-Insect Transfection reagent (Mirus Bio, Madison, WI). Resulting virus was amplified by passaging in Sf9 cells, and correct homologous recombination verified through restriction enzyme digestion of viral DNA. PCR and sequencing of viral DNA was also used to confirm the presence of each desired genome modification.

Plasmid construction for expression of wild type and mutant ARIF-1

To express full-length ARIF-1 and ARIF-1 C-terminal truncations, we used PCR to amplify the following AcMNPV *arif-1* regions from pEcoRI_ASAlxh.pBSKS.rev (listed as amino acid numbers): ARIF-1(1-417), ARIF-1(1-219), ARIF-1(1-274), ARIF-1(1-371), ARIF-

1(1-378), ARIF-1(1-398), and ARIF-1(1-401) along with C-terminal TAG stop codons (Table 1). Fragments were purified by agarose gel electrophoresis and individually subcloned into BamHI/NotI digested pBluescript II KS+ (Addgene). Colonies positive for the plasmid were selected on LB agar with 100 µg/ml ampicillin (Gibco from Thermo Fisher Scientific), 100 µM 5-bromo-4-chloro-3-indolyl-β-D-galactopyranoside (X-Gal) and 100 µM Isopropyl β- d-1-thiogalactopyranoside (IPTG). Next, these plasmids were digested with BamHI and NotI (New England Biolabs) and subcloned into BamHI/NotI digested pACT (Ohkawa et al., 2002). The resulting plasmids have a *B. mori* actin promoter driving expression of each ARIF-1 truncation.

To generate ARIF-1 C-terminally tagged with eGFP-FLAG as well as GlyGlyGlyGlySer-eGFP-FLAG (with a N-terminal linker), we amplified two DNA fragments with PCR and used Gibson assembly to subclone these into the BamHI site of pBluescript II KS+ (Addgene). The first fragment, containing *arif-1*, was amplified from pEcoRI_ASAlxh.pBSKS.rev with reverse primers incorporating or not incorporating a C-terminal GlyGlyGlyGlySer linker (Table 1). The second fragment, containing *eGFP*, was amplified from pEGFPN1 (Takara Bio USA) with the reverse primer incorporating a FLAG tag (Table 1). Colonies positive for the assembled plasmid were selected on LB agar with 100 µg/ml ampicillin and 0.1mM X-Gal and IPTG. We then PCR-amplified the ARIF-1-eGFP-FLAG or ARIF-1-GlyGlyGlyGlySer-eGFP-FLAG sequence and used Gibson assembly to subclone it into the NotI site of pACT (Table 1).

To generate fusions of ARIF-1 and its N-terminal truncations to AcMNPV gp64, we PCR-amplified 2 fragments and assembled them into the NotI site of pACT. The first fragment was *gp64* from the 14 kb viral fragment XhoI G (Table 1). The second fragment was amplified from pEcoRI_ASAlxh.pBSKS.rev and encoded one of the following regions of *arif-1* (listed as amino acid numbers): K219-D417, T274-D417, P303-D417, or Y320-D417 (Table 1). The resulting plasmids encode ARIF-1 and its truncations fused to the C-terminus of gp64.

To express ARIF-1 with point mutations of proline and tyrosine residues, PCR site-directed mutagenesis was done by amplification of pACT ARIF-1 M1-D417 (full length) using primers to incorporate the desired mutation. Overlapping primers were used to generate proline to alanine mutations at ARIF-1 amino acids P303, P305, P309, P312, P328, P330, P335, P343, P351, P352, and P354 (Table 1), as well as tyrosine to phenylalanine mutations in ARIF-1 at amino acids Y226, Y238, Y241, Y246, Y320, Y325, and Y332 (Table 1). In all cases, the PCR product was purified by agarose gel electrophoresis, digested with DpnI (New England Biolabs) to remove template DNA, transformed into XL-1 Blue *E.coli* (University of California BerkeleyQB3 Macro Lab) and plated on LB agar plates with 100 µg/ml ampicillin (Gibco from Thermo Fisher Scientific). Plasmid DNA from resulting colonies was sequence verified to ensure the desired changes had been made.

In all cases, to generate DNA ready for transfection, plasmids were transformed into JM109 *E.coli* and cultures grown in 150 ml 2x YT media (MilliporeSigma) overnight at 37°C. A Genelute endotoxin-free Maxiprep kit (MilliporeSigma) was used to purify the DNA.

Plasmid construction for expression of GFP-tagged cortactin and Arp2/3 complex

To amplify the *S. frugiperda* cortactin gene, total mRNA was isolated from Sf21 cells using an RNeasy kit (Qiagen, Hilden, Germany), and reverse transcribed to cDNA using a

Protoscript II First Strand DNA Synthesis kit (New England Biolabs) using random hexamers as primers. *S. frugiperda* cortactin-specific primers (Table 1) were used to PCR amplify a 1.9 kb fragment from cDNA that was then used as a template for PCR amplification with a second primer set (Table 1). Next, we constructed a plasmid vector for an N-terminal GFP-tagged *S. frugiperda* cortactin. *eGFP* was PCR-amplified from pEGFPN1 (Takara Bio USA) and inserted using Gibson assembly into a NotI/BamHI-digested pACT (Table 1). The amplified cortactin fragment was then subcloned into the NotI site of the resulting plasmid using Gibson assembly (Table 1). The resulting plasmid expresses GFP fused to the N-terminus of *S. frugiperda* cortactin (GFP-cortactin).

To express a fusion of EGFP to the C-terminus of the p21 (ARPC3) subunit of the Arp2/3 complex (p21-EGFP), the *Trichoplusia ni arpc3* gene from pIZ-p21-EYFP (Goley et al., 2006) was PCR-amplified and subcloned using Gibson assembly, along with *eGFP* PCR-amplified from pEGFP-N1 (Takara Bio USA), into the BamHI site of pACT (Table 1).

In all cases, to generate DNA ready for transfection, plasmids were transformed into JM109 *E. coli* and cultures grown in 150 ml 2x YT media (MilliporeSigma) overnight at 37°C. A GenElute endotoxin-free Maxiprep kit (MilliporeSigma) was used to purify the DNA.

ARIF-1 purification, anti-ARIF-1 antibody generation, and western blotting

To express recombinant ARIF-1 protein in *E. coli*, the portion of the *arif-1* gene encoding the cytoplasmic C-terminal region (base pairs 654-1254, encoding the C-terminal 199 amino acids) was amplified by PCR from pEcoRI_ASAlxh.pBSKS.rev and subcloned into the SspI site of pET-1M (University of California Berkeley QB3 Macro Lab) using Gibson Cloning. This generated the plasmid pET-M1 ARIF-1 219 (Table 1) encoding a fusion protein of the predicted *arif-1* C-terminal cytoplasmic region with an N-terminal 6xHis tag, maltose binding protein (MBP), and tobacco-etch virus (TEV) protease cleavage site (6xHi-MBP-TEV-ARIF-1-219-417). This plasmid was transformed into *E. coli* strain BL21(DE3) (New England Biolabs), the bacteria were grown at 37°C to an OD₆₀₀ of 0.5, and expression was induced with 250 μM IPTG for 2 h. Bacteria were harvested by centrifugation at 4000 rpm for 25 min at 4°C in a Beckman J6M clinical centrifuge (Beckman Coulter Diagnostics; Brea, California), and re-suspended on ice in lysis buffer (50 mM Tris pH 7.5, 200 mM KCl, 1 mM EDTA, 1 μg/mL each leupeptin, pepstatin, and chymostatin (LPC, MilliporeSigma), 1 μg/mL aprotinin (MP Biomedicals LLC, Irvine, CA), and 1 mM phenylmethylsulfonyl fluoride (PMSF, MilliporeSigma)). Lysozyme (MilliporeSigma) was added to the cells at 1 mg/ml; the bacteria were sonicated on ice at 30% power for 4x 15 sec in a Branson 450 Digital sonifier and centrifuged at 20,000 x g for 25 min using an SS34 rotor in a Sorvall RC 6+ centrifuge. The supernatant was dripped twice through a 10 ml packed volume of amylose resin (New England Biolabs), washed with 5 column volumes of column buffer (20 mM Tris, pH 7.0, 200 mM NaCl), and eluted with column buffer containing 10 mM maltose. Fractions containing protein were pooled, and protein concentration was determined by Bradford protein assay (Bio-Rad Laboratories, Hercules, CA).

Purified 6xHi-MBP-TEV-ARIF-1-219-417 was used to immunize rabbits (Pocono Rabbit Farm and Laboratory, Canadensis PA) using a 91-day protocol. Before affinity-purifying anti-ARIF-1 antibody, serum was first depleted of anti-MBP antibodies. Buffer exchange was carried out on 10 mg 6xHi-MBP-TEV, purified as described above using an Amicon Ultracell 10 kDa spin concentrator (MilliporeSigma) to concentrate the protein to 20 mg/ml in coupling buffer

(0.2M NaHCO₃, 500 mM NaCl, pH 8.0). This protein was coupled to a 1 ml packed column volume of NHS-activated Sepharose 4 Fast Flow resin (GE Healthcare Life Sciences, Marlborough, MA). 10 ml of serum was diluted 1:1 in binding buffer (20mM Tris, pH 8.0), passed through a 0.22 µm filter, passed over the MBP affinity resin six times at room temperature, and the flow-through was collected. Buffer exchange was carried out as described above to concentrate 10 mg of purified 6xHi-MBP-TEV-ARIF-1-219-417 to 10 mg/mL in coupling buffer. This protein was coupled to another 1 ml packed column volume of NHS-activated Sepharose 4 fastflow resin, and 10 ml of MBP antibody-depleted serum was passed over the 6xHi-MBP-TEV-ARIF-1-219-417 affinity resin. Antibodies were eluted with 100 mM glycine, pH 2.5, and immediately brought to pH 7.5 by addition of 1 M Tris, pH 8.8. Purified antibody was stored at -20°C.

To observe ARIF-1 expression over the course of early viral infection, Sf21 cells were infected with AcMNPV WOBpos, *AcΔarif-1*, and *AcΔarif-1* rescue viruses at an MOI of 10 and harvested at 0, 2, 4, 6, 8, 10, 12, 16, 20, 24, 28, and 36 hpi. Cells were lysed in protein sample buffer (50 mM Tris, pH 6.8, 10 mM SDS, 370 µM bromophenol blue, 5% glycerol, 1 µg/ml LPC (MilliporeSigma), 1 µg/ml aprotinin (MP Biomedicals LLC), 1 mM PMSF (MilliporeSigma)), and boiled for 5 min. Cell lysates were subjected to SDS-PAGE, transferred to PVDF membrane (Immobilon from MilliporeSigma, Burlington, MA), and probed by Western blotting with rabbit anti-ARIF-1 and rabbit anti-cofilin loading control (provided by Kris Gunsalus; NYU-AD and Michael Goldberg; Cornell).

To observe expression of ARIF-1 and its truncated and mutated derivatives, adherent Sf21 cells were transfected with plasmids expressing ARIF-1 using TransIT-Insect transfection reagent (Mirus Bio, Madison, WI). At 3 d post transfection, cells were collected, lysed in protein sample buffer (0.2M Tris HCl, 0.4 M DTT, 277 mM SDS, 6mM Bromophenol Blue, 4.3M glycerol), and boiled and subjected to SDS-PAGE and Western blotting as described above.

Fluorescence microscopy

To image actin structures in live infected cells, Sf21 cells were plated onto 3 cm No 1.5 glass coverslip dishes (MatTek, Ashland, MA) and incubated overnight at 28°C in Grace's with 10% FBS (Gemini Bio-Products). Cells were transfected with 5 µg of pACT-GFP-actin using TransIT-Insect transfection reagent (Mirus Bio) and incubated for 2 d at 28°C in Grace's media with 10% FBS and antibiotics (100 µg/ml penicillin/streptomycin and 0.25 µg/ml Amphotericin B). Cells were infected with an MOI = 10, and after 1 h adsorption at 28°C, they were washed with Grace's media with 10% FBS (this point is defined as 0 hpi), and were incubated at 28°C in Grace's media with 10% FBS until imaging.

To image actin structures in live cells, Sf21 cells were plated as described above and co-transfected with 5 µg of pACT-ARIF-1 or its truncated or mutated derivatives, pACT-GFP-ARIF-1 (Goley et al., 2006), pACT-GFP-P21, or pACT-GFP-Cortactin. Cells were incubated for 2 d at 28°C in Grace's media with 10% FBS and antibiotics/antimycotics and imaged.

To quantify formation of clusters of invadosome-like structures in Sf21 cells transfected with pACT-ARIF-1, without or with truncations and mutations, cells were transfected as described above. At 2 d post transfection, 60 random cells per condition expressing visible GFP-actin were imaged in triplicate at one Z plane at the basal side of the cell. The number of cells

with invadosome-like structures, number of invadosome-like structures in each cell, and the shape of the invadosome-like structures were recorded. The data is a result of three biological replicates.

Imaging was performed using a Nikon/Andor confocal microscope with a Yokogawa CSU-XI spinning disc, 100X VC objective, a Clara Interline CCD camera (Oxford Instruments Inc, Pleasanton, CA), and MetaMorph software (Molecular Devices LLC, San Jose, CA) using a 100X VC objective at 488 nm.

TIRF imaging was performed on a Leica DMi8 S Infinity TIRF HP system with a 100X/1.47 TIRF oil immersion objective, a 488 nm excitation laser, and detected with a Hamamatsu Flash V.4.0 sCMOS camera. Images were processed using ImageJ software.

To quantify invadosome-like structure formation in infected cells over a time course, Sf21 cells were plated onto µclear CELLSTAR black-walled 96-well plates (Greiner Bio-One, Kremsmunster, Austria) and infected in triplicate at an MOI of 10 with WOBpos, *AcΔarif-1*, or *AcΔarif-1 rescue* virus as described above. Cells were fixed with 4% paraformaldehyde in PHEM buffer (60 mM PIPES, pH6.9, 25 mM HEPES, 10 mM EGTA, 2 mM MgCl₂), quenched with 0.1 M glycine in PHEM buffer, permeabilized in 0.15% Triton X-100 in PHEM buffer, and blocked with 5% normal goat serum (MP Biomedicals, Irvine, CA) and 1% bovine serum albumin in PHEM. Cells were stained with anti-gp64 B12D5 primary antibody (a gift from Dr. Loy Volkman) at a 1:200 dilution in PHEM buffer, and with a secondary Goat anti-mouse AlexaFluor 488 conjugated antibody (Invitrogen from Thermo Fisher Scientific) at a 1:400 dilution, both in PHEM buffer. F-actin was visualized with Alexa Fluor 568 Phalloidin (Invitrogen from Thermo Fisher Scientific) diluted 1:200 in PHEM buffer, and DNA was visualized with 5 µg/ml Hoechst (MilliporeSigma) in PHEM buffer. Cells were imaged with an Opera Phenix high-content image screening system (PerkinElmer, Waltham, MA) using a 40x water immersion objective (PerkinElmer). Images were analyzed on Harmony image analysis software (PerkinElmer) using maximum intensity projections, and the number of cells, number of cells with gp64 signal, and number of cells with clusters of invadosome-like structures, and the number of clusters of invadosome-like structures in each cell were recorded. The data is a result of three biological replicates.

For Arp2/3 complex drug inhibition experiments, Sf21 cells were plated and transfected with pACT GFP-actin as described above. Cells were infected with WOBpos virus as described above, and at 4 hpi we added drugs latrunculin A to a concentration of 4 µM in DMSO, or CK666, or CK689 to concentration of 100 µM in DMSO. Imaging was begun immediately, with 8 cells imaged every 30 s. Images were processed in image J, and the percent of invadosome-like actin structures remaining was recorded. Data is a result of three biological replicates.

Chapter 3

Future Directions

My dissertation focuses on the AcMNPV protein ARIF-1 and the previously uncharacterized structures that its expression induces in insect cells. We discovered that ARIF-1 is necessary and sufficient for the formation of structures that are similar to invadosomes in mammalian cells in terms of dynamics and composition. These results raise interesting questions to examine in future research. First, the molecular mechanism through which ARIF-1 induces invadosome-like structure formation remains unknown. ARIF-1 may be tyrosine phosphorylated at Y332 and at other residues (Dreschers et al., 2001), and phosphorylation at these sites could facilitate interactions between ARIF-1 and host proteins. Second, the function of ARIF-1 induced invadosome-like structures is unclear. Invadosome-like structures may direct targeted degradation of the underlying ECM, though whether these structures form in live insects and can degrade the insect BL is unknown. We speculate that ARIF-1 induces the formation of invadosome-like structures in midgut epithelial cells, which can degrade the midgut BL, accelerating viral escape of the midgut and systemic infection of the insect body. Here, I will discuss each of these possibilities, outlining future directions that would be interesting to pursue.

What is the molecular mechanism through which ARIF-1 induces the formation of invadosome-like structures?

It is likely that cytoplasmic tyrosine kinase signaling plays a role in ARIF-1 induced invadosome-like structure formation. Cytoplasmic tyrosine kinases are one of two major classes of tyrosine kinase that convert external and internal signals into cellular responses (Shah et al., 2018). Many cytoplasmic tyrosine kinases have Src homology 2 (SH2) and Src homology 3 (SH3) domains, both of which serve as sites for protein-protein interactions (Mayer et al., 1988; Sadowski et al., 1986; Shah et al., 2018). Regions of proteins that interact with SH2 domains are marked by phosphorylated tyrosine residues (Sadowski et al., 1986; Shah et al., 2018), while regions that interact with SH3 domains are characterized by proline-rich sequences (Mayer et al., 1988; Shah et al., 2018). The proteins Nck1 and Grb2 also have SH2 and SH3 domains and are involved in coupling phosphotyrosine signaling to actin dynamics (Buday et al., 2002; Li et al., 2001). For example, during formation of vaccinia virus-induced actin pedestals, vaccinia virus protein A36 is phosphorylated at Y112 and Y132, which act as binding sites for the SH2 domains of Nck1 and Grb2, respectively (Frischknecht et al., 1999; Leite and Way, 2015; Scaplehorn et al., 2002). Nck1, along with WIP and N-WASP, are recruited to phosphorylated A36 Y112, and together they mediate Arp2/3 complex recruitment and activation (Frischknecht et al., 1999; Leite and Way, 2015; Moreau et al., 2000; Scaplehorn et al., 2002; Snapper et al., 2001).

Invadosome formation is similarly mediated by protein-protein interactions through SH2 and SH3 domains. Phosphorylation of Tks5 at tyrosine 557 mediates binding to the SH2 domains of Nck1 and Nck2, which may play a role in N-WASP recruitment (Stylli et al., 2009). Furthermore, SH3 domains of Tks5 bind to N-WASP proline-rich sequences (Oikawa et al., 2008), and mutation of several of the five SH3 domains in Tks5 prevents the formation of invadopodia (Daly et al., 2020). Thus, protein-protein interactions involving SH2 and SH3 domains are crucial for viral hijacking of the actin cytoskeleton as well as for invadosome formation.

Although ARIF-1 is tyrosine phosphorylated, the mechanism of how tyrosine phosphorylation directs invadosome-like structure organization is unclear. It was previously

reported that ARIF-1 is tyrosine phosphorylated within its first 255 residues by 4 hpi and is further phosphorylated as infection progresses, becoming hyperphosphorylated between 12 hpi and 48 hpi (Dreschers et al., 2001). Since hyperphosphorylation is correlated with disappearance of F-actin from the cell periphery, previous studies postulated that hyperphosphorylation inhibits ARIF-1 function (Dreschers et al., 2001).

In Chapter 2 of this dissertation, we showed that a phosphoablative mutation of ARIF-1 residue Y332 prevents the organization of invadosome-like structures into clusters. To investigate if Y332 is phosphorylated during early infection, future studies could purify ARIF-1 from infected insect cells, and mass spectrometry could be used to determine if Y332 and other tyrosine residues are phosphorylated. Furthermore, such studies could determine if residues other than tyrosine, such as serine or threonine, are phosphorylated, or if there are other post-translational modifications. These may mark sites of protein-protein interactions, as discussed below, or they may otherwise regulate ARIF-1 function or stability. To follow up these studies, mutations of individual or multiple residues could be made, and ARIF-1 expression and invadosome-like structure formation could be assessed. Additionally, future studies could also determine the identity of the kinase that phosphorylates ARIF-1

While it seems likely that ARIF-1 Y332 is phosphorylated, it is unclear if this marks a binding site for host or viral proteins, or how mutation of this residue influences the clustering of invadosome-like structures. If ARIF-1 functions as a scaffold protein for invadosome-like structure formation in a manner analogous to Tks5 or A36, we would expect SH2 domain-containing proteins Nck-1 or Grb-2 to bind to ARIF-1 phosphotyrosine residues, activating a pathway that leads to Arp2/3 complex recruitment and formation of invadosome-like structures. However, a phosphoablative Y332F mutation does not prevent actin polymerization in invadosome-like structures, as it does for actin pedestal formation in phosphoablative mutations of vaccinia virus A36 Y112 (Frischknecht et al., 1999). Rather, the Y332F mutation causes invadosome-like structures to form throughout the entire cell rather than in clusters.

The presence of another ARIF-1 phosphotyrosine residue may thus be required for invadosome formation. However, of the six other individual phosphoablative mutations we constructed in ARIF-1, none had a significant effect on formation of invadosome-like structures by themselves. These results suggest a possible redundancy in phosphotyrosine residues required for invadosome formation, and future studies could involve constructing multiple ARIF-1 phosphoablative mutations at once. Mass spectrometry data indicating which of the residues are phosphorylated could inform the decision of which combinations of residues to mutate.

Similar to the phenotype caused by the Y332F mutation, we found that mutation of ARIF-1 residue P335 prevents the organization of invadosome-like structures into clusters. Furthermore, we showed that while a large portion of the AcMNPV ARIF-1 C-terminal proline-rich region (371-417) enhances the frequency of clusters of invadosome-like structures, it is not required for them to form. These results are not incongruous with previous studies that found that the ARIF-1 C-terminal region is required for actin rearrangement, because the C-terminal truncations in those studies also included P335 (Dreschers et al., 2001; Katsuma et al., 2015). Thus, our work refines our understanding of the regions of ARIF-1 that are required for its function. These proline-rich regions warrant future investigation as they could serve as binding

sites for proteins with SH3 domains. While P335 does not appear to reside in a canonical SH3 binding domain – which generally consist of the core motif PXXP (Ren et al., 1993) – it is possible that the host insect has alternative SH3 binding motifs that have not yet been identified. Thus, it is important for future studies to determine how various ARIF-1 proline-rich regions enhance invadosome-like structure formation. Future studies could construct mutations of additional proline residues to determine the sites of protein-protein interactions at this region, specifically concentrating on potential SH3 domain binding sites.

Another approach to interrogating proline-rich domains would be to consider sequence conservation between ARIF-1 orthologs in other baculoviruses. For example, BmNPV ARIF-1 contains a 22 amino acid insertion at the C-terminus that is enriched in proline residues (Xu et al., 2010), and it is unknown what role this insertion plays in infection or invadosome-like structure formation. We found that mutations in BmNPV ARIF-1 that correspond to AcMNPV ARIF-1(Y332F) and ARIF-1(P335A) have the same effects on invadosome-like structure formation as they do for AcMNPV ARIF-1 (our unpublished data). This is perhaps not surprising, given that AcMNPV and BmNPV are both closely related Group I alphabaculoviruses (Jehle et al., 2006). However, it is possible that BmNPV ARIF-1 has additional protein-protein interaction sites at the C-terminal proline-rich region that may contribute to invadosome-like structure formation. Future studies investigating the role of ARIF-1 proline rich regions could construct recombinant AcMNPV containing ARIF-1 orthologs from an array of different baculoviruses, and determine how the presence of proline-rich regions affects invadosome-like structure formation.

To determine how ARIF-1 contributes to invadosome-like structure formation, future studies will also need to identify the proteins that interact with ARIF-1, especially at residues Y332 and P335. To do this, cells would be infected with recombinant AcMNPV with a tagged wild-type ARIF-1, ARIF-1(Y332F), or ARIF-1(P335A). Proteins interacting with ARIF-1 could be identified following pulldowns of ARIF-1 and subsequent mass spectrometry. Since ARIF-1 is sufficient for invadosome-like structure formation, we expect that these interacting proteins would be involved in the eventual recruitment and activation of the Arp2/3 complex.

The identification of proteins interacting with ARIF-1, especially at Y332 and P335 as described above, would provide candidates whose function could be explored by subsequent localization experiments to examine their presence in invadosome-like structures, and targeted knockdowns by RNAi to examine their functions. Other candidate proteins could be investigated based on the fact that they are commonly found in invadosomes in mammalian cells. These could include SH2/SH3 domain-containing proteins such as Nck1 and Grb2, as well as adhesion proteins vinculin and alpha-actinin, cytoskeleton proteins such as N-WASP, a Tks5 homologue, and matrix metalloproteases. Identifying the components of invadosome-like structures and how they interact with ARIF-1 would allow us to better understand the function of invadosome-like structures. Moreover, it could help uncover a unique pathway of virus-induced invadosome formation in insect cells.

What is the function of ARIF-1 induced invadosome-like structures?

The role of invadosome-like structures during baculovirus infection is also not understood. Specifically, it is not known if the role of ARIF-1 in the formation of invadosome-

like structures in cultured cells *in vitro* is connected to the delay of systemic infection during *in vivo* infection of insects (Katsuma et al., 2015). Our hypothesis, which attempts to connect these two functions of ARIF-1, is that invadosome-like structures mediate insect BL degradation. However, to make this connection, future studies will have to be conducted to first answer whether invadosome-like structures mediate ECM degradation, and second, if this occurs during infection of live insect hosts.

To verify that invadosome-like structures direct degradation of underlying ECM, we have attempted to use an ECM degradation assay (Chen, 1989; Chen et al., 1985). While preliminary data that suggests gelatin ECM degradation does occur underneath invadosome-like structures (our unpublished data), we have not yet been able to reliably reproduce these results. Thus, future studies would include attempting this assay with various cultured insect cell lines, as well as using a variety of different ECM compositions including gelatin, fibronectin, or laminin in order to approximate the physiological conditions present in the insect. Future studies could also attempt to utilize a fluorescently quenched matrix, which would fluoresce in areas where degradation has taken place (Jedieszko et al., 2008). Such a matrix could provide direct evidence of degradation, allowing detection of low-levels of ECM degradation, and could distinguish between a lack of ECM due to protrusive force from the invadosome-like structure and bona fide degradation.

The second task is to test whether matrix degradation takes place in the body of the insect host. This would involve, in part, implementation of an assay to track the progression of viral infection in caterpillars. One such assay involves infecting insects with AcMNPV expressing LacZ (Engelhard et al., 1994). After infection, the host midgut is extracted and treated with X-gal, allowing the areas infected with virus to produce a colored pigment (Engelhard et al., 1994). Future studies could utilize this assay to test if the size of infection foci is significantly smaller when insects are infected with *AcAarif-1*, and with recombinant AcMNPV with ARIF-1(Y332F) or ARIF-1 (P335A). To more directly test for BL degradation in insects, electron microscopy could be used to investigate if the integrity of midgut BL is significantly different (Means and Passarelli, 2010; Tang et al., 2007) in insects infected with wild-type AcMNPV versus mutants for which invadosome-like structure formation is inhibited.

Although we suspect that ARIF-1 plays a role in degradation of the midgut BL, an alternative hypothesis for the role of ARIF-1 in infection is that it facilitates the release of nucleocapsids from cells before viral replication. While AcMNPV ODV contain multiple nucleocapsids, other baculoviruses such as single nucleopolyhedroviruses (SNPVs) only have viral particles with single nucleocapsids (Ackermann and Smirnoff, 1983; Hughes and Addison, 1970; Summers and Volkman, 1976), raising the question of why multiple nucleocapsid packaging has evolved. Interestingly, oral infection of caterpillars with AcMNPV ODV containing multiple versus single nucleocapsids showed that ODV with multiple nucleocapsids were more efficient at establishing secondary infection in tracheal cells, and infected tracheal cells at a much higher rate (Washburn et al., 1999). These results confirm an earlier observation that following entry of multiple nucleocapsids from AcMNPV ODV into a midgut epithelial cell, some nucleocapsids transited to the basal plasma membrane and were able to bud out of the cell at 2 hpi (Granados and Lawler, 1981). Theoretically, such a transit would allow AcMNPV to accelerate systemic viral infection of the host by dispersing nucleocapsids to uninfected cells

more quickly than if they were released after viral replication. Additionally, this pre-replicative nucleocapsid escape strategy could prevent the virus from being cleared from the insect by the sloughing off of gut epithelial cells, since this strategy would allow the virus to escape the gut epithelium prior to the onset of sloughing (Washburn et al., 1999). Pre-replicative transit could be accomplished by expression of early viral gene products, including gp64 (Washburn et al., 1999), and as a delayed-early gene, ARIF-1 could play a role in this process by directing modifications of the cortical actin cytoskeleton, allowing nucleocapsids to transit to the cell membrane and bud out to form BV.

While pre-replicative nucleocapsid escape is an intriguing hypothesis, ARIF-1 likely has other, or additional roles in baculovirus infection. ARIF-1 orthologs are present in genomes of SNPV viruses, though such viruses could not undertake pre-replicative nucleocapsid escape by the mechanism described above. Indeed, while ARIF-1 is only present in alphabaculoviruses (Rohrmann, 2019), both SNPV and MNPV viruses are members of this family (Jehle et al., 2006) since SNPV and MNPV classification does not conform to virus phylogeny (de A. Zanotto et al., 1993). Furthermore, the number of nucleocapsids packaged into ODV is somewhat dependent on the context of infection. For example, the baculovirus BomaNPV S2 produces single nucleocapsid ODV when infecting cells derived from *Bombyx mori*, but produces multiple nucleocapsid ODV when infecting cell lines derived from *Trichoplusia ni* (Xu et al., 2012). Thus, ARIF-1 may play a role in pre-replicative nucleocapsid escape, though it is likely to have persisted in alphabaculoviruses for other reasons.

Summary

Since the discovery of the first oncovirus, Rous sarcoma virus (RSV) (Rous, 1910) and the observation of invadosomes in RSV-transformed fibroblasts, our understanding of how viruses hijack basic cellular pathways to promote their proliferation and spread has only expanded. The work presented in this dissertation is a step forward in uncovering the function of AcMNPV ARIF-1; however, this work also uncovers a previously undiscovered instance of virus-induced invadosomes. Indeed, to our knowledge, no previous work has shown virus-induced invadosomes in the lepidopteran lineage. The observation that invadosomes might form in insect cells suggests the presence of an evolutionarily conserved pathway that both vertebrate and invertebrate viruses have evolved to take advantage of. Further research on this topic could illuminate the molecular mechanisms of invadosome-like structure formation, as well as determine if these structures aid in virus dissemination. Overall, such work could uncover a unique mechanism that a viral pathogen uses to establish and spread infection.

References

- Abram, C.L., Seals, D.F., Pass, I., Salinsky, D., Maurer, L., Roth, T.M., Courtneidge, S.A., 2003. The adaptor protein fish associates with members of the ADAMs family and localizes to podosomes of Src-transformed cells. *J. Biol. Chem.* 278, 16844–16851. <https://doi.org/10.1074/jbc.M300267200>
- Ackermann, H.-W., Smirnov, W.A., 1983. A morphological investigation of 23 baculoviruses. *Journal of Invertebrate Pathology* 41, 269–280. [https://doi.org/10.1016/0022-2011\(83\)90244-6](https://doi.org/10.1016/0022-2011(83)90244-6)
- Alberto Ospina Stella, Stuart Turville, 2018. All-Round Manipulation of the Actin Cytoskeleton by HIV. *Viruses* 10, 63. <https://doi.org/10.3390/v10020063>
- Albiges-Rizo, C., Destaing, O., Fourcade, B., Planus, E., Block, M.R., 2009. Actin machinery and mechanosensitivity in invadopodia, podosomes and focal adhesions. *J. Cell. Sci.* 122, 3037–3049. <https://doi.org/10.1242/jcs.052704>
- Altmann, F., Staudacher, E., Wilson, I.B.H., März, L., 1999. Insect cells as hosts for the expression of recombinant glycoproteins, in: Berger, E.G., Clausen, H., Cummings, R.D. (Eds.), *Glycotechnology*. Springer US, Boston, MA, pp. 29–43. https://doi.org/10.1007/978-1-4615-5257-4_3
- Ashhurst, D.E., 1968. The Connective Tissues of Insects. *Annu. Rev. Entomol.* 13, 45–74. <https://doi.org/10.1146/annurev.en.13.010168.000401>
- Ayala, I., Baldassarre, M., Giacchetti, G., Caldieri, G., Tetè, S., Luini, A., Buccione, R., 2008. Multiple regulatory inputs converge on cortactin to control invadopodia biogenesis and extracellular matrix degradation. *J. Cell. Sci.* 121, 369–378. <https://doi.org/10.1242/jcs.008037>
- Ayres, M.D., Howard, S.C., Kuzio, J., Lopez-Ferber, M., Possee, R.D., 1994. The complete DNA sequence of *Autographa californica* nuclear polyhedrosis virus. *Virology* 202, 586–605. <https://doi.org/10.1006/viro.1994.1380>
- Bañón-Rodríguez, I., Monypenny, J., Ragazzini, C., Franco, A., Calle, Y., Jones, G.E., Antón, I.M., 2011. The cortactin-binding domain of WIP is essential for podosome formation and extracellular matrix degradation by murine dendritic cells. *European Journal of Cell Biology, Invadosomes* 90, 213–223. <https://doi.org/10.1016/j.ejcb.2010.09.001>
- Berretta, M.F., Ferrelli, M.L., Salvador, R., Sciocco, A., Romanowski, V., 2013. Baculovirus Gene Expression. *Current Issues in Molecular Virology - Viral Genetics and Biotechnological Applications*. <https://doi.org/10.5772/56955>
- Blissard, G.W., Wenz, J.R., 1992. Baculovirus gp64 envelope glycoprotein is sufficient to mediate pH-dependent membrane fusion. *Journal of Virology* 66, 6829–6835. <https://doi.org/10.1128/JVI.66.11.6829-6835.1992>
- Boogaard, B., van Oers, M.M., van Lent, J.W.M., 2018. An Advanced View on Baculovirus per Os Infectivity Factors. *Insects* 9. <https://doi.org/10.3390/insects9030084>
- Buday, L., Wunderlich, L., Tamás, P., 2002. The Nck family of adapter proteins: Regulators of actin cytoskeleton. *Cellular Signalling* 14, 723–731. [https://doi.org/10.1016/S0898-6568\(02\)00027-X](https://doi.org/10.1016/S0898-6568(02)00027-X)
- Buracco, S., Claydon, S., Insall, R., 2019. Control of actin dynamics during cell motility. *F1000Res* 8, 1977. <https://doi.org/10.12688/f1000research.18669.1>
- Burger, K.L., Davis, A.L., Isom, S., Mishra, N., Seals, D.F., 2011. The podosome marker protein Tks5 regulates macrophage invasive behavior. *Cytoskeleton* 68, 694–711. <https://doi.org/10.1002/cm.20545>

- Burger, K.L., Learman, B.S., Boucherle, A.K., Sirintrapun, S.J., Isom, S., Díaz, B., Courtneidge, S.A., Seals, D.F., 2014. Src-dependent Tks5 phosphorylation regulates invadopodia-associated invasion in prostate cancer cells: Tks5 Phosphorylation and Cell Invasion. *Prostate* 74, 134–148. <https://doi.org/10.1002/pros.22735>
- Burns, S., Thrasher, A.J., Blundell, M.P., Machesky, L., Jones, G.E., 2001. Configuration of human dendritic cell cytoskeleton by Rho GTPases, the WAS protein, and differentiation. *Blood* 98, 1142–1149. <https://doi.org/10.1182/blood.V98.4.1142>
- Campellone, K.G., Welch, M.D., 2010. A nucleator arms race: cellular control of actin assembly. *Nat Rev Mol Cell Biol* 11, 237–251. <https://doi.org/10.1038/nrm2867>
- Carbonell, L.F., Miller, L.K., 1987. Baculovirus interaction with nontarget organisms: a virus-borne reporter gene is not expressed in two mammalian cell lines. *Applied and Environmental Microbiology* 53, 1412–1417. <https://doi.org/10.1128/AEM.53.7.1412-1417.1987>
- Castro-Castro, A., Marchesin, V., Monteiro, P., Lodillinsky, C., Rossé, C., Chavrier, P., 2016. Cellular and Molecular Mechanisms of MT1-MMP-Dependent Cancer Cell Invasion. *Annu. Rev. Cell Dev. Biol.* 32, 555–576. <https://doi.org/10.1146/annurev-cellbio-111315-125227>
- Charlton, C.A., Volkman, L.E., 1993. Penetration of *Autographa californica* Nuclear Polyhedrosis Virus Nucleocapsids into IPLB Sf 21 Cells Induces Actin Cable Formation. *Virology* 197, 245–254. <https://doi.org/10.1006/viro.1993.1585>
- Charlton, C.A., Volkman, L.E., 1991. Sequential rearrangement and nuclear polymerization of actin in baculovirus-infected *Spodoptera frugiperda* cells. *Journal of Virology* 65, 1219–1227. <https://doi.org/10.1128/JVI.65.3.1219-1227.1991>
- Chen, W.-T., 1989. Proteolytic activity of specialized surface protrusions formed at rosette contact sites of transformed cells. *J. Exp. Zool.* 251, 167–185. <https://doi.org/10.1002/jez.1402510206>
- Chen, W.T., Chen, J.M., Parsons, S.J., Parsons, J.T., 1985. Local degradation of fibronectin at sites of expression of the transforming gene product pp60src. *Nature* 316, 156–158. <https://doi.org/10.1038/316156a0>
- Chou, H.-C., Antón, I.M., Holt, M.R., Curcio, C., Lanzardo, S., Worth, A., Burns, S., Thrasher, A.J., Jones, G.E., Calle, Y., 2006. WIP Regulates the Stability and Localization of WASP to Podosomes in Migrating Dendritic Cells. *Curr Biol* 16, 2337–2344. <https://doi.org/10.1016/j.cub.2006.10.037>
- Clem, R.J., Passarelli, A.L., 2013. Baculoviruses: Sophisticated Pathogens of Insects. *PLoS Pathog* 9, e1003729. <https://doi.org/10.1371/journal.ppat.1003729>
- Collin, O., Na, S., Chowdhury, F., Hong, M., Shin, M., Wang, F., Wang, N., 2008. Self-Organized Podosomes Are Dynamic Mechanosensors. *Current biology: CB* 18, 1288–94. <https://doi.org/10.1016/j.cub.2008.07.046>
- Cudmore, S., Cossart, P., Griffiths, G., Way, M., 1995. Actin-based motility of vaccinia virus. *Nature* 378, 636–638. <https://doi.org/10.1038/378636a0>
- Cudmore, S., Reckmann, I., Griffiths, G., Way, M., 1996. Vaccinia virus: a model system for actin-membrane interactions. *Journal of Cell Science* 109, 1739–1747.
- Daly, C., Logan, B., Breeyear, J., Whitaker, K., Ahmed, M., Seals, D.F., 2020. Tks5 SH3 domains exhibit differential effects on invadopodia development. *PLoS ONE* 15, e0227855. <https://doi.org/10.1371/journal.pone.0227855>

- Datsenko, K.A., Wanner, B.L., 2000. One-step inactivation of chromosomal genes in *Escherichia coli* K-12 using PCR products. *Proceedings of the National Academy of Sciences* 97, 6640–6645. <https://doi.org/10.1073/pnas.120163297>
- David-Pfeuty, Th., Singer, S.J., 1980. Altered distributions of the cytoskeletal proteins vinculin and α -actinin in cultured fibroblasts transformed by Rous sarcoma virus. *Proc. Natl. Acad. Sci. USA* 5.
- de A. Zanotto, P.M., Kessing, B.D., Maruniak, J.E., 1993. Phylogenetic Interrelationships among Baculoviruses: Evolutionary Rates and Host Associations. *Journal of Invertebrate Pathology* 62, 147–164. <https://doi.org/10.1006/jipa.1993.1090>
- Destaing, O., Saltel, F., Géminard, J.-C., Jurdic, P., Bard, F., 2003. Podosomes Display Actin Turnover and Dynamic Self-Organization in Osteoclasts Expressing Actin-Green Fluorescent Protein. *Molecular Biology of the Cell* 14, 407–416. <https://doi.org/10.1091/mbc.E02-07-0389>
- Destaing, O., Sanjay, A., Itzstein, C., Horne, W.C., Toomre, D., De Camilli, P., Baron, R., 2008. The Tyrosine Kinase Activity of c-Src Regulates Actin Dynamics and Organization of Podosomes in Osteoclasts. *Molecular Biology of the Cell* 19, 394–404. <https://doi.org/10.1091/mbc.e07-03-0227>
- Detvisitsakun, C., Berretta, M.F., Lehiy, C., Passarelli, A.L., 2005. Stimulation of cell motility by a viral fibroblast growth factor homolog: Proposal for a role in viral pathogenesis. *Virology* 336, 308–317. <https://doi.org/10.1016/j.virol.2005.03.013>
- Detvisitsakun, C., Cain, E.L., Passarelli, A.L., 2007. The *Autographa californica* M nucleopolyhedrovirus fibroblast growth factor accelerates host mortality. *Virology* 365, 70–78. <https://doi.org/10.1016/j.virol.2007.03.027>
- Detvisitsakun, C., Hutfless, E.L., Berretta, M.F., Passarelli, A.L., 2006. Analysis of a baculovirus lacking a functional viral fibroblast growth factor homolog. *Virology* 346, 258–265. <https://doi.org/10.1016/j.virol.2006.01.016>
- Di Martino, J., Paysan, L., Gest, C., Lagrée, V., Juin, A., Saltel, F., Moreau, V., 2014. Cdc42 and Tks5: A minimal and universal molecular signature for functional invadosomes. *Cell Adhesion & Migration* 8, 280–292. <https://doi.org/10.4161/cam.28833>
- Díaz, B., Yuen, A., Iizuka, S., Higashiyama, S., Courtneidge, S.A., 2013. Notch increases the shedding of HB-EGF by ADAM12 to potentiate invadopodia formation in hypoxia. *Journal of Cell Biology* 201, 279–292. <https://doi.org/10.1083/jcb.201209151>
- Doceul, V., Hollinshead, M., van der Linden, L., Smith, G.L., 2010. Repulsion of Superinfecting Virions: A Mechanism for Rapid Virus Spread. *Science* 327, 873–876. <https://doi.org/10.1126/science.1183173>
- Donnelly, S.K., Weisswange, I., Zettl, M., Way, M., 2013. WIP Provides an Essential Link between Nck and N-WASP during Arp2/3-Dependent Actin Polymerization. *Curr Biol* 23, 999–1006. <https://doi.org/10.1016/j.cub.2013.04.051>
- Dreschers, S., Roncarati, R., Knebel-Mörsdorf, D., 2001. Actin Rearrangement-Inducing Factor of Baculoviruses Is Tyrosine Phosphorylated and Colocalizes to F-Actin at the Plasma Membrane. *J. Virol.* 75, 3771–3778. <https://doi.org/10.1128/JVI.75.8.3771-3778.2001>
- Duan, R., Jin, P., Luo, F., Zhang, G., Anderson, N., Chen, E.H., 2012. Group I PAKs function downstream of Rac to promote podosome invasion during myoblast fusion *in vivo*. *Journal of Cell Biology* 199, 169–185. <https://doi.org/10.1083/jcb.201204065>

- Eddy, R.J., Weidmann, M.D., Sharma, V.P., Condeelis, J.S., 2017. Tumor Cell Invadopodia: Invasive Protrusions that Orchestrate Metastasis. *Trends in Cell Biology* 27, 595–607. <https://doi.org/10.1016/j.tcb.2017.03.003>
- El Azzouzi, K., Wiesner, C., Linder, S., 2016. Metalloproteinase MT1-MMP islets act as memory devices for podosome reemergence. *Journal of Cell Biology* 213, 109–125. <https://doi.org/10.1083/jcb.201510043>
- Engelhard, E.K., Kam-Morgan, L.N., Washburn, J.O., Volkman, L.E., 1994. The insect tracheal system: a conduit for the systemic spread of *Autographa californica* M nuclear polyhedrosis virus. *Proceedings of the National Academy of Sciences* 91, 3224–3227. <https://doi.org/10.1073/pnas.91.8.3224>
- Ferrari, R., Martin, G., Tagit, O., Guichard, A., Cambi, A., Voituriez, R., Vassilopoulos, S., Chavrier, P., 2019. MT1-MMP directs force-producing proteolytic contacts that drive tumor cell invasion. *Nat Commun* 10, 4886. <https://doi.org/10.1038/s41467-019-12930-y>
- Frischknecht, F., Moreau, V., Röttger, S., Gonfloni, S., Reckmann, I., Superti-Furga, G., Way, M., 1999. Actin-based motility of vaccinia virus mimics receptor tyrosine kinase signalling. *Nature* 401, 926–929. <https://doi.org/10.1038/44860>
- Fuchs, L.Y., Woods, M.S., Weaver, R.F., 1983. Viral Transcription During *Autographa californica* Nuclear Polyhedrosis Virus Infection: a Novel RNA Polymerase Induced in Infected *Spodoptera frugiperda* Cells. *Journal of Virology* 48, 641–646. <https://doi.org/10.1128/JVI.48.3.641-646.1983>
- Gandhi, K.M., Ohkawa, T., Welch, M.D., Volkman, L.E., 2012. Nuclear localization of actin requires AC102 in *Autographa californica* multiple nucleopolyhedrovirus-infected cells. *J Gen Virol* 93, 1795–1803. <https://doi.org/10.1099/vir.0.041848-0>
- García, E., Jones, G.E., Machesky, L.M., Antón, I.M., 2012. WIP: WASP-interacting proteins at invadopodia and podosomes. *European Journal of Cell Biology* 91, 869–877. <https://doi.org/10.1016/j.ejcb.2012.06.002>
- Goley, E.D., Ohkawa, T., Mancuso, J., Woodruff, J.B., D’Alessio, J.A., Cande, W.Z., Volkman, L.E., Welch, M.D., 2006. Dynamic Nuclear Actin Assembly by Arp2/3 Complex and a Baculovirus WASP-Like Protein. *Science* 314, 464–467. <https://doi.org/10.1126/science.1133348>
- Goulson, D., 1997. Wipfelkrankheit: modification of host behaviour during baculoviral infection. *Oecologia* 109, 219–228. <https://doi.org/10.1007/s004420050076>
- Granados, R.R., Lawler, K.A., 1981. *In vivo* pathway of *Autographa californica* baculovirus invasion and infection. *Virology* 108, 297–308. [https://doi.org/10.1016/0042-6822\(81\)90438-4](https://doi.org/10.1016/0042-6822(81)90438-4)
- Guarino, L.A., Summers, M.D., 1986. Functional mapping of a trans-activating gene required for expression of a baculovirus delayed-early gene. *Journal of Virology* 57, 563–571. <https://doi.org/10.1128/JVI.57.2.563-571.1986>
- Hanna, S.C., Krishnan, B., Bailey, S.T., Moschos, S.J., Kuan, P.-F., Shimamura, T., Osborne, L.D., Siegel, M.B., Duncan, L.M., O’Brien, E.T., Superfine, R., Miller, C.R., Simon, M.C., Wong, K.-K., Kim, W.Y., 2013. HIF1 α and HIF2 α independently activate SRC to promote melanoma metastases. *J. Clin. Invest.* 123, 2078–2093. <https://doi.org/10.1172/JCI66715>
- Harrison, R.L., Herniou, E.A., Jehle, J.A., Theilmann, D.A., Burand, J.P., Becnel, J.J., Krell, P.J., van Oers, M.M., Mowery, J.D., Bauchan, G.R., ICTV Report Consortium, 2018.

- ICTV Virus Taxonomy Profile: *Baculoviridae*. *Journal of General Virology* 99, 1185–1186. <https://doi.org/10.1099/jgv.0.001107>
- Hassan, S.S., Roy, P., 1999. Expression and Functional Characterization of Bluetongue Virus VP2 Protein: Role in Cell Entry. *J. Virol.* 73, 9832–9842. <https://doi.org/10.1128/JVI.73.12.9832-9842.1999>
- Hawtin, R.E., Zarkowska, T., Arnold, K., Thomas, C.J., Gooday, G.W., King, L.A., Kuzio, J.A., Possee, R.D., 1997. Liquefaction of *Autographa californica* nucleopolyhedrovirus-infected insects is dependent on the integrity of virus-encoded chitinase and cathepsin genes. *Virology* 238, 243–253. <https://doi.org/10.1006/viro.1997.8816>
- Hayashi, S., Kondo, T., 2018. Development and Function of the *Drosophila* Tracheal System. *Genetics* 209, 367–380. <https://doi.org/10.1534/genetics.117.300167>
- Hepp, S.E., Borgo, G.M., Tica, S., Ohkawa, T., Welch, M.D., 2018. Baculovirus AC102 Is a Nucleocapsid Protein That Is Crucial for Nuclear Actin Polymerization and Nucleocapsid Morphogenesis. *J Virol* 92, e00111-18, /jvi/92/11/e00111-18.atom. <https://doi.org/10.1128/JVI.00111-18>
- Hess, R.T., Falcon, L.A., 1987. Temporal events in the invasion of the codling moth, *Cydia pomonella*, by a granulosis virus: An electron microscope study. *Journal of Invertebrate Pathology* 50, 85–105. [https://doi.org/10.1016/0022-2011\(87\)90108-X](https://doi.org/10.1016/0022-2011(87)90108-X)
- Hess, R.T., Goldsmith, P.A., Volkman, L.E., 1989. Effect of cytochalasin D on cell morphology and AcMNPV replication in a *Spodoptera frugiperda* cell line. *Journal of Invertebrate Pathology* 53, 169–182. [https://doi.org/10.1016/0022-2011\(89\)90005-0](https://doi.org/10.1016/0022-2011(89)90005-0)
- Hiura, K., Lim, S.-S., Little, S.P., Lin, S., Sato, M., 1995. Differentiation dependent expression of tensin and cortactin in chicken osteoclasts. *Cell Motil. Cytoskeleton* 30, 272–284. <https://doi.org/10.1002/cm.970300405>
- Hollinshead, M., Rodger, G., Van Eijl, H., Law, M., Hollinshead, R., Vaux, D.J., Smith, G.L., 2001. Vaccinia virus utilizes microtubules for movement to the cell surface. *J. Cell Biol.* 154, 389–402. <https://doi.org/10.1083/jcb.200104124>
- Hughes, K.M., Addison, R.B., 1970. Two nuclear polyhedrosis viruses of the Douglas-fir tussock moth. *Journal of Invertebrate Pathology* 16, 196–204. [https://doi.org/10.1016/0022-2011\(70\)90060-1](https://doi.org/10.1016/0022-2011(70)90060-1)
- Hwang, Y.S., Park, K.-K., Chung, W.-Y., 2012. Invadopodia formation in oral squamous cell carcinoma: The role of epidermal growth factor receptor signalling. *Archives of Oral Biology* 57, 335–343. <https://doi.org/10.1016/j.archoralbio.2011.08.019>
- Ishimwe, E., Hodgson, J.J., Clem, R.J., Passarelli, A.L., 2015. Reaching the melting point: Degradative enzymes and protease inhibitors involved in baculovirus infection and dissemination. *Virology* 479–480, 637–649. <https://doi.org/10.1016/j.virol.2015.01.027>
- Jarecki, J., Johnson, E., Krasnow, M.A., 1999. Oxygen Regulation of Airway Branching in *Drosophila* Is Mediated by Branchless FGF. *Cell* 99, 211–220. [https://doi.org/10.1016/S0092-8674\(00\)81652-9](https://doi.org/10.1016/S0092-8674(00)81652-9)
- Jedezsko, C., Sameni, M., Olive, M., Moin, K., Sloane, B.F., 2008. Visualizing Protease Activity in Living Cells: From Two Dimensions to Four Dimensions. *Curr Protoc Cell Biol* 0 4, Unit-4.20. <https://doi.org/10.1002/0471143030.cb0420s39>
- Jehle, J.A., Blissard, G.W., Bonning, B.C., Cory, J.S., Herniou, E.A., Rohrmann, G.F., Theilmann, D.A., Thiem, S.M., Vlak, J.M., 2006. On the classification and nomenclature of baculoviruses: A proposal for revision. *Arch Virol* 151, 1257–1266. <https://doi.org/10.1007/s00705-006-0763-6>

- Kanehisa, J., Yamanaka, T., Doi, S., Turksen, K., Heersche, J.N.M., Aubin, J.E., Takeuchi, H., 1990. A band of F-actin containing podosomes is involved in bone resorption by osteoclasts. *Bone* 11, 287–293. [https://doi.org/10.1016/8756-3282\(90\)90082-A](https://doi.org/10.1016/8756-3282(90)90082-A)
- Kanner, S.B., Reynolds, A.B., Vines, R.R., Parsons, J.T., 1990. Monoclonal antibodies to individual tyrosine-phosphorylated protein substrates of oncogene-encoded tyrosine kinases. *Proceedings of the National Academy of Sciences* 87, 3328–3332. <https://doi.org/10.1073/pnas.87.9.3328>
- Katsuma, S., Daimon, T., Mita, K., Shimada, T., 2006a. Lepidopteran Ortholog of *Drosophila* Breathless Is a Receptor for the Baculovirus Fibroblast Growth Factor. *JVI* 80, 5474–5481. <https://doi.org/10.1128/JVI.00248-06>
- Katsuma, S., Horie, S., Daimon, T., Iwanaga, M., Shimada, T., 2006b. *In vivo* and *in vitro* analyses of a *Bombyx mori* nucleopolyhedrovirus mutant lacking functional vfgf. *Virology* 355, 62–70. <https://doi.org/10.1016/j.virol.2006.07.008>
- Katsuma, S., Shimada, T., Kobayashi, M., 2004. Characterization of the Baculovirus *Bombyx Mori* Nucleopolyhedrovirus Gene Homologous to the Mammalian FGF Gene Family. *Virus Genes* 29, 211–217. <https://doi.org/10.1023/B:VIRU.0000036381.11779.dd>
- Katsuma, S., Shimada, T., Kokusho, R., Sugano, S., Suzuki, Y., Koyano, Y., Kawamoto, M., 2015. *Bombyx mori* nucleopolyhedrovirus actin rearrangement-inducing factor 1 enhances systemic infection in *B. mori* larvae. *Journal of General Virology* 96, 1938–1946. <https://doi.org/10.1099/vir.0.000130>
- Kaverina, I., Stradal, T.E.B., Gimona, M., 2003. Podosome formation in cultured A7r5 vascular smooth muscle cells requires Arp2/3-dependent de-novo actin polymerization at discrete microdomains. *Journal of Cell Science* 116, 4915–4924. <https://doi.org/10.1242/jcs.00818>
- Keddie, B., Aponte, G., Volkman, L., 1989. The pathway of infection of *Autographa californica* nuclear polyhedrosis virus in an insect host. *Science* 243, 1728–1730. <https://doi.org/10.1126/science.2648574>
- Kuo, S.-L., Chen, C.-L., Pan, Y.-R., Chiu, W.-T., Chen, H.-C., 2018. Biogenesis of podosome rosettes through fission. *Sci Rep* 8, 524. <https://doi.org/10.1038/s41598-017-18861-2>
- Labernadie, A., Bouissou, A., Delobelle, P., Balor, S., Voituriez, R., Proag, A., Fourquaux, I., Thibault, C., Vieu, C., Poincloux, R., Charrière, G.M., Maridonneau-Parini, I., 2014. Protrusion force microscopy reveals oscillatory force generation and mechanosensing activity of human macrophage podosomes. *Nature Communications* 5, 5343. <https://doi.org/10.1038/ncomms6343>
- Lamason, R.L., Welch, M.D., 2017. Actin-based motility and cell-to-cell spread of bacterial pathogens. *Current Opinion in Microbiology* 35, 48–57. <https://doi.org/10.1016/j.mib.2016.11.007>
- Lehiy, C.J., Martinez, O., Passarelli, A.L., 2009. Virion-associated viral fibroblast growth factor stimulates cell motility. *Virology* 395, 152–160. <https://doi.org/10.1016/j.virol.2009.09.011>
- Leite, F., Way, M., 2015a. The role of signalling and the cytoskeleton during Vaccinia Virus egress. *Virus Research* 209, 87–99. <https://doi.org/10.1016/j.virusres.2015.01.024>
- Leite, F., Way, M., 2015b. The role of signalling and the cytoskeleton during Vaccinia Virus egress. *Virus Research* 209, 87–99. <https://doi.org/10.1016/j.virusres.2015.01.024>
- Li, C.M.-C., Chen, G., Dayton, T.L., Kim-Kiselak, C., Hoersch, S., Whittaker, C.A., Bronson, R.T., Beer, D.G., Winslow, M.M., Jacks, T., 2013. Differential Tks5 isoform expression

- contributes to metastatic invasion of lung adenocarcinoma. *Genes & Development* 27, 1557–1567. <https://doi.org/10.1101/gad.222745.113>
- Li, W., Fan, J., Woodley, D.T., 2001. Nck/Dock: an adapter between cell surface receptors and the actin cytoskeleton. *Oncogene* 20, 6403–6417. <https://doi.org/10.1038/sj.onc.1204782>
- Linder, S., 2007. The matrix corroded: podosomes and invadopodia in extracellular matrix degradation. *Trends in Cell Biology* 17, 107–117. <https://doi.org/10.1016/j.tcb.2007.01.002>
- Linder, S., Higgs, H., Hüfner, K., Schwarz, K., Pannicke, U., Aepfelbacher, M., 2000. The Polarization Defect of Wiskott-Aldrich Syndrome Macrophages Is Linked to Dislocalization of the Arp2/3 Complex. *J Immunol* 165, 221–225. <https://doi.org/10.4049/jimmunol.165.1.221>
- Linder, S., Nelson, D., Weiss, M., Aepfelbacher, M., 1999. Wiskott-Aldrich syndrome protein regulates podosomes in primary human macrophages. *Proceedings of the National Academy of Sciences* 96, 9648–9653. <https://doi.org/10.1073/pnas.96.17.9648>
- Lock, P., 1998. A new method for isolating tyrosine kinase substrates used to identify Fish, an SH3 and PX domain-containing protein, and Src substrate. *The EMBO Journal* 17, 4346–4357. <https://doi.org/10.1093/emboj/17.15.4346>
- Lu, H.-Y., Chen, Y.-H., Liu, H.-J., 2012. Baculovirus as a vaccine vector. *Bioengineered* 3, 271–274. <https://doi.org/10.4161/bioe.20679>
- Lu, R., Drubin, D.G., Sun, Y., 2016. Clathrin-mediated endocytosis in budding yeast at a glance. *J Cell Sci* 129, 1531–1536. <https://doi.org/10.1242/jcs.182303>
- Luxenburg, C., Geblinger, D., Klein, E., Anderson, K., Hanein, D., Geiger, B., Addadi, L., 2007. The Architecture of the Adhesive Apparatus of Cultured Osteoclasts: From Podosome Formation to Sealing Zone Assembly. *PLoS ONE* 2, e179. <https://doi.org/10.1371/journal.pone.0000179>
- Mader, C.C., Oser, M., Magalhaes, M.A.O., Bravo-Cordero, J.J., Condeelis, J., Koleske, A.J., Gil-Henn, H., 2011. An EGFR–Src–Arg–Cortactin Pathway Mediates Functional Maturation of Invadopodia and Breast Cancer Cell Invasion. *Cancer Res* 71, 1730–1741. <https://doi.org/10.1158/0008-5472.CAN-10-1432>
- Marchisio, P., 1987. Rous sarcoma virus-transformed fibroblasts and cells of monocytic origin display a peculiar dot-like organization of cytoskeletal proteins involved in microfilament-membrane interactions*1. *Experimental Cell Research* 169, 202–214. [https://doi.org/10.1016/0014-4827\(87\)90238-2](https://doi.org/10.1016/0014-4827(87)90238-2)
- Marchisio, P.C., Cirillo, D., Naldini, L., Primavera, M.V., Teti, A., Zamboni-Zallone, A., 1984. Cell-substratum interaction of cultured avian osteoclasts is mediated by specific adhesion structures. *Journal of Cell Biology* 99, 1696–1705. <https://doi.org/10.1083/jcb.99.5.1696>
- Mayer, B.J., Hamaguchi, M., Hanafusa, H., 1988. Characterization of p47gag-crk, a novel oncogene product with sequence similarity to a putative modulatory domain of protein-tyrosine kinases and phospholipase C. *Cold Spring Harb. Symp. Quant. Biol.* 53 Pt 2, 907–914. <https://doi.org/10.1101/sqb.1988.053.01.104>
- Means, J.C., Passarelli, A.L., 2010. Viral fibroblast growth factor, matrix metalloproteases, and caspases are associated with enhancing systemic infection by baculoviruses. *Proceedings of the National Academy of Sciences* 107, 9825–9830. <https://doi.org/10.1073/pnas.0913582107>
- Miyauchi, A., Hruska, K.A., Greenfield, E.M., Duncan, R., Alvarez, J., Barattolo, R., Colucci, S., Zamboni-Zallone, A., Teitelbaum, S.L., 1990. Osteoclast Cytosolic Calcium,

- Regulated by Voltage-gated Calcium Channels and Extracellular Calcium, Controls Podosome Assembly and Bone Resorption. *Journal of Cell Biology* 111, 10.
- Mizutani, K., Miki, H., He, H., Maruta, H., Takenawa, T., 2002. Essential Role of Neural Wiskott-Aldrich Syndrome Protein in Podosome Formation and Degradation of Extracellular Matrix in src-transformed Fibroblasts. *Cancer Res* 62, 669–674.
- Monsky, W.L., Lin, C.Y., Aoyama, A., Kelly, T., Akiyama, S.K., Mueller, S.C., Chen, W.T., 1994. A potential marker protease of invasiveness, seprase, is localized on invadopodia of human malignant melanoma cells. *Cancer Res.* 54, 5702–5710.
- Monsma, S.A., Oomens, A.G., Blissard, G.W., 1996. The GP64 envelope fusion protein is an essential baculovirus protein required for cell-to-cell transmission of infection. *Journal of Virology* 70, 4607–4616. <https://doi.org/10.1128/JVI.70.7.4607-4616.1996>
- Moreau, V., Frischknecht, F., Reckmann, I., Vincentelli, R., Rabut, G., Stewart, D., Way, M., 2000. A complex of N-WASP and WIP integrates signalling cascades that lead to actin polymerization. *Nat Cell Biol* 2, 441–448. <https://doi.org/10.1038/35017080>
- Moreau, V., Tatin, F., Varon, C., Génot, E., 2003. Actin Can Reorganize into Podosomes in Aortic Endothelial Cells, a Process Controlled by Cdc42 and RhoA. *MCB* 23, 6809–6822. <https://doi.org/10.1128/MCB.23.19.6809-6822.2003>
- Mueller, J., Pfanzelter, J., Winkler, C., Narita, A., Le Clainche, C., Nemethova, M., Carlier, M.-F., Maeda, Y., Welch, M.D., Ohkawa, T., Schmeiser, C., Resch, G.P., Small, J.V., 2014. Electron Tomography and Simulation of Baculovirus Actin Comet Tails Support a Tethered Filament Model of Pathogen Propulsion. *PLoS Biol* 12, e1001765. <https://doi.org/10.1371/journal.pbio.1001765>
- Mueller, S.C., Ghersi, G., Akiyama, S.K., Sang, Q.-X.A., Howard, L., Pineiro-Sanchez, M., Nakahara, H., Yeh, Y., Chen, W.-T., 1999. A Novel Protease-docking Function of Integrin at Invadopodia. *J. Biol. Chem.* 274, 24947–24952. <https://doi.org/10.1074/jbc.274.35.24947>
- Murphy, D.A., Courtneidge, S.A., 2011. The “ins” and “outs” of podosomes and invadopodia: characteristics, formation and function. *Nat Rev Mol Cell Biol* 12, 413–426. <https://doi.org/10.1038/nrm3141>
- Nakahara, H., Howard, L., Thompson, E.W., Sato, H., Seiki, M., Yeh, Y., Chen, W.-T., 1997. Transmembrane/cytoplasmic domain-mediated membrane type 1-matrix metalloprotease docking to invadopodia is required for cell invasion. *Proceedings of the National Academy of Sciences* 94, 7959–7964. <https://doi.org/10.1073/pnas.94.15.7959>
- Newsome, T., Scaplehorn, N., Way, M., 2004. Src Mediates a Switch from Microtubule- to Actin-Based Motility of Vaccinia Virus. *Science (New York, N.Y.)* 306, 124–9. <https://doi.org/10.1126/science.1101509>
- Newsome, T.P., Weisswange, I., Frischknecht, F., Way, M., 2006. Abl collaborates with Src family kinases to stimulate actin-based motility of vaccinia virus. *Cellular Microbiology* 8, 233–241. <https://doi.org/10.1111/j.1462-5822.2005.00613.x>
- Ohkawa, T., Rowe, A.R., Volkman, L.E., 2002. Identification of Six *Autographa californica* Multicapsid Nucleopolyhedrovirus Early Genes That Mediate Nuclear Localization of G-Actin. *J. Virol.* 76, 12281–12289. <https://doi.org/10.1128/JVI.76.23.12281-12289.2002>
- Ohkawa, T., Volkman, L.E., 1999. Nuclear F-Actin Is Required for AcMNPV Nucleocapsid Morphogenesis. *Virology* 264, 1–4. <https://doi.org/10.1006/viro.1999.0008>

- Ohkawa, T., Volkman, L.E., Welch, M.D., 2010. Actin-based motility drives baculovirus transit to the nucleus and cell surface. *Journal of Cell Biology* 190, 187–195. <https://doi.org/10.1083/jcb.201001162>
- Ohkawa, T., Washburn, J.O., Sitapara, R., Sid, E., Volkman, L.E., 2005. Specific Binding of *Autographa californica* Multiple Nucleopolyhedrovirus Occlusion-Derived Virus to Midgut Cells of *Heliothis virescens* Larvae Is Mediated by Products of pif Genes Ac119 and Ac022 but Not by Ac115. *JVI* 79, 15258–15264. <https://doi.org/10.1128/JVI.79.24.15258-15264.2005>
- Ohkawa, T., Welch, M.D., 2018. Baculovirus Actin-Based Motility Drives Nuclear Envelope Disruption and Nuclear Egress. *Current Biology* 28, 2153–2159.e4. <https://doi.org/10.1016/j.cub.2018.05.027>
- Oikawa, T., Itoh, T., Takenawa, T., 2008. Sequential signals toward podosome formation in NIH-src cells. *Journal of Cell Biology* 182, 157–169. <https://doi.org/10.1083/jcb.200801042>
- Ornitz, D.M., Itoh, N., 2015. The Fibroblast Growth Factor signaling pathway. *WIREs Dev Biol* 4, 215–266. <https://doi.org/10.1002/wdev.176>
- Oser, M., Yamaguchi, H., Mader, C.C., Bravo-Cordero, J.J., Arias, M., Chen, X., DesMarais, V., van Rheenen, J., Koleske, A.J., Condeelis, J., 2009. Cortactin regulates cofilin and N-WASp activities to control the stages of invadopodium assembly and maturation. *Journal of Cell Biology* 186, 571–587. <https://doi.org/10.1083/jcb.200812176>
- Passarelli, A.L., 2011. Barriers to success: How baculoviruses establish efficient systemic infections. *Virology* 411, 383–392. <https://doi.org/10.1016/j.virol.2011.01.009>
- Paterson, E.K., Courtneidge, S.A., 2018. Invadosomes are coming: new insights into function and disease relevance. *FEBS J* 285, 8–27. <https://doi.org/10.1111/febs.14123>
- Paz, H., Pathak, N., Yang, J., 2014. Invading one step at a time: the role of invadopodia in tumor metastasis. *Oncogene* 33, 4193–4202. <https://doi.org/10.1038/onc.2013.393>
- Pearson, M.N., Rohrmann, G.F., 2002. Transfer, Incorporation, and Substitution of Envelope Fusion Proteins among Members of the *Baculoviridae*, *Orthomyxoviridae*, and *Metaviridae* (Insect Retrovirus) Families. *JVI* 76, 5301–5304. <https://doi.org/10.1128/JVI.76.11.5301-5304.2002>
- Peng, K., van Oers, M.M., Hu, Z., van Lent, J.W.M., Vlak, J.M., 2010. Baculovirus Per Os Infectivity Factors Form a Complex on the Surface of Occlusion-Derived Virus. *JVI* 84, 9497–9504. <https://doi.org/10.1128/JVI.00812-10>
- Pfaff, M., Jurdic, P., 2001. Podosomes in osteoclast-like cells: structural analysis and cooperative roles of paxillin, proline-rich tyrosine kinase 2 (Pyk2) and integrin $\alpha V\beta 3$. *Journal of Cell Science* 114, 2775–2786.
- Pietrantonì, G., Ibarra-Karmy, R., Arriagada, G., 2020. Microtubule Retrograde Motors and Their Role in Retroviral Transport. *Viruses* 12. <https://doi.org/10.3390/v12040483>
- Poincloux, R., Lizárraga, F., Chavrier, P., 2009. Matrix invasion by tumour cells: a focus on MT1-MMP trafficking to invadopodia. *J Cell Sci* 122, 3015–3024. <https://doi.org/10.1242/jcs.034561>
- Pollard, T.D., 2016. Actin and Actin-Binding Proteins. *Cold Spring Harb Perspect Biol* 8, a018226. <https://doi.org/10.1101/cshperspect.a018226>
- Reddy, J.T., Locke, M., 1990. The size limited penetration of gold particles through insect basal laminae. *Journal of Insect Physiology* 36, 397–407. [https://doi.org/10.1016/0022-1910\(90\)90057-M](https://doi.org/10.1016/0022-1910(90)90057-M)

- Reichman-Fried, M., Dickson, B., Hafen, E., Shilo, B.Z., 1994. Elucidation of the role of breathless, a *Drosophila* FGF receptor homolog, in tracheal cell migration. *Genes Dev.* 8, 428–439. <https://doi.org/10.1101/gad.8.4.428>
- Ren, R., Mayer, B.J., Cicchetti, P., Baltimore, D., 1993. Identification of a ten-amino acid proline-rich SH3 binding site. *Science* 259, 1157–1161. <https://doi.org/10.1126/science.8438166>
- Rietdorf, J., Ploubidou, A., Reckmann, I., Holmström, A., Frischknecht, F., Zettl, M., Zimmermann, T., Way, M., 2001. Kinesin-dependent movement on microtubules precedes actin-based motility of vaccinia virus. *Nat. Cell Biol.* 3, 992–1000. <https://doi.org/10.1038/ncb1101-992>
- Rohrman, G.F., 2019. *Baculovirus Molecular Biology* 298.
- Romoser, W.S., Turell, M.J., Lerdthusnee, K., Neira, M., Dohm, D., Ludwig, G., Wasieloski, L., 2005. Pathogenesis of Rift Valley fever virus in mosquitoes — tracheal conduits & the basal lamina as an extra-cellular barrier, in: Peters, C.J., Calisher, C.H. (Eds.), *Infectious Diseases from Nature: Mechanisms of Viral Emergence and Persistence*. Springer-Verlag, Vienna, pp. 89–100. https://doi.org/10.1007/3-211-29981-5_8
- Romoser, W.S., Wasieloski, L.P., Pushko, P., Kondig, J.P., Lerdthusnee, K., Neira, M., Ludwig, G.V., 2004. Evidence for arbovirus dissemination conduits from the mosquito (*Diptera: Culicidae*) midgut. *J. Med. Entomol.* 41, 467–475. <https://doi.org/10.1603/0022-2585-41.3.467>
- Roncarati, R., Knebel-Mörsdorf, D., 1997. Identification of the Early Actin-Rearrangement-Inducing Factor Gene, arif-1, from *Autographa californica* Multicapsid Nuclear Polyhedrosis Virus. *J. Virol.* 71, 11.
- Rottiers, P., Saltel, F., Daubon, T., Chaigne-Delalande, B., Tridon, V., Billottet, C., Reuzeau, E., Genot, E., 2009. TGF- α -induced endothelial podosomes mediate basement membrane collagen degradation in arterial vessels. *Journal of Cell Science* 122, 4311–4318. <https://doi.org/10.1242/jcs.057448>
- Rottner, K., Faix, J., Bogdan, S., Linder, S., Kerkhoff, E., 2017. Actin assembly mechanisms at a glance. *J Cell Sci* 130, 3427–3435. <https://doi.org/10.1242/jcs.206433>
- Rous, P., 1910. A transmissible avian neoplasm. (Sarcoma of the common fowl.). *J Exp Med* 12, 696–705.
- Sadowski, I., Stone, J.C., Pawson, T., 1986. A noncatalytic domain conserved among cytoplasmic protein-tyrosine kinases modifies the kinase function and transforming activity of Fujinami sarcoma virus P130gag-fps. *Mol. Cell. Biol.* 6, 4396–4408. <https://doi.org/10.1128/MCB.6.12.4396>
- Sato, M., Kornberg, T.B., 2002. FGF is an essential mitogen and chemoattractant for the air sacs of the *Drosophila* tracheal system. *Dev. Cell* 3, 195–207. [https://doi.org/10.1016/s1534-5807\(02\)00202-2](https://doi.org/10.1016/s1534-5807(02)00202-2)
- Sato, T., Ovejero, M. del C., Hou, P., Heegaard, A.M., Kumegawa, M., Foged, N.T., Delaisse, J.M., 1997. Identification of the membrane-type matrix metalloproteinase MT1-MMP in osteoclasts. *Journal of Cell Science* 110, 589–596.
- Scaplehorn, N., Holmström, A., Moreau, V., Frischknecht, F., Reckmann, I., Way, M., 2002. Grb2 and Nck Act Cooperatively to Promote Actin-Based Motility of Vaccinia Virus. *Current Biology* 12, 740–745. [https://doi.org/10.1016/S0960-9822\(02\)00812-6](https://doi.org/10.1016/S0960-9822(02)00812-6)
- Schaks, M., Giannone, G., Rottner, K., 2019. Actin dynamics in cell migration. *Essays in Biochemistry* 63, 483–495. <https://doi.org/10.1042/EBC20190015>

- Schudt, G., Dolnik, O., Kolesnikova, L., Biedenkopf, N., Herwig, A., Becker, S., 2015. Transport of Ebolavirus Nucleocapsids Is Dependent on Actin Polymerization: Live-Cell Imaging Analysis of Ebolavirus-Infected Cells. *J Infect Dis.* 212, S160–S166. <https://doi.org/10.1093/infdis/jiv083>
- Seals, D.F., Azucena, E.F., Pass, I., Tesfay, L., Gordon, R., Woodrow, M., Resau, J.H., Courtneidge, S.A., 2005. The adaptor protein Tks5/Fish is required for podosome formation and function, and for the protease-driven invasion of cancer cells. *Cancer Cell* 7, 155–165. <https://doi.org/10.1016/j.ccr.2005.01.006>
- Seano, G., Chiaverina, G., Gagliardi, P.A., di Blasio, L., Puliafito, A., Bouvard, C., Sessa, R., Tarone, G., Sorokin, L., Helley, D., Jain, R.K., Serini, G., Bussolino, F., Primo, L., 2014. Endothelial podosome rosettes regulate vascular branching in tumour angiogenesis. *Nat Cell Biol* 16, 931–941. <https://doi.org/10.1038/ncb3036>
- Seiler, C., Davuluri, G., Abrams, J., Byfield, F.J., Janmey, P.A., Pack, M., 2012. Smooth Muscle Tension Induces Invasive Remodeling of the Zebrafish Intestine. *PLOS Biology* 10, e1001386. <https://doi.org/10.1371/journal.pbio.1001386>
- Sens, K.L., Zhang, S., Jin, P., Duan, R., Zhang, G., Luo, F., Parachini, L., Chen, E.H., 2010. An invasive podosome-like structure promotes fusion pore formation during myoblast fusion. *Journal of Cell Biology* 191, 1013–1027. <https://doi.org/10.1083/jcb.201006006>
- Shah, N.H., Amacher, J.F., Nocka, L.M., Kuriyan, J., 2018. The Src module: an ancient scaffold in the evolution of cytoplasmic tyrosine kinases. *Critical Reviews in Biochemistry and Molecular Biology* 53, 535–563. <https://doi.org/10.1080/10409238.2018.1495173>
- Shrestha, A., Bao, K., Chen, Y.-R., Chen, W., Wang, P., Fei, Z., Blissard, G.W., 2018. Global Analysis of Baculovirus *Autographa californica* Multiple Nucleopolyhedrovirus Gene Expression in the Midgut of the Lepidopteran Host *Trichoplusia ni*. *J Virol* 92, e01277-18, /jvi/92/23/e01277-18.atom. <https://doi.org/10.1128/JVI.01277-18>
- Simpson, C., Yamauchi, Y., 2020. Microtubules in Influenza Virus Entry and Egress. *Viruses* 12, 117. <https://doi.org/10.3390/v12010117>
- Smith, G.L., Vanderplassen, A., Law, M., 2002. The formation and function of extracellular enveloped vaccinia virus. *Journal of General Virology* 83, 2915–2931. <https://doi.org/10.1099/0022-1317-83-12-2915>
- Snapper, S.B., Takeshima, F., Antón, I., Liu, C.-H., Thomas, S.M., Nguyen, D., Dudley, D., Fraser, H., Purich, D., Lopez-Illasaca, M., Klein, C., Davidson, L., Bronson, R., Mulligan, R.C., Southwick, F., Geha, R., Goldberg, M.B., Rosen, F.S., Hartwig, J.H., Alt, F.W., 2001. N-WASP deficiency reveals distinct pathways for cell surface projections and microbial actin-based motility. *Nat Cell Biol* 3, 897–904. <https://doi.org/10.1038/ncb1001-897>
- Spuul, P., Daubon, T., Pitter, B., Alonso, F., Fremaux, I., Kramer, Ij., Montanez, E., Génot, E., 2016. VEGF-A/Notch-Induced Podosomes Proteolyse Basement Membrane Collagen-IV during Retinal Sprouting Angiogenesis. *Cell Reports* 17, 484–500. <https://doi.org/10.1016/j.celrep.2016.09.016>
- Stradal, T.E.B., Schelhaas, M., 2018. Actin dynamics in host–pathogen interaction. *FEBS Lett* 592, 3658–3669. <https://doi.org/10.1002/1873-3468.13173>
- Stylli, S.S., I, S.T.T., Verhagen, A.M., Xu, S.S., Pass, I., Courtneidge, S.A., Lock, P., 2009. Nck adaptor proteins link Tks5 to invadopodia actin regulation and ECM degradation. *Journal of Cell Science* 122, 2727–2740. <https://doi.org/10.1242/jcs.046680>

- Summers, M.D., Volkman, L.E., 1976. Comparison of biophysical and morphological properties of occluded and extracellular nonoccluded baculovirus from *in vivo* and *in vitro* host systems. *Journal of Virology* 17, 962–972. <https://doi.org/10.1128/JVI.17.3.962-972.1976>
- Sutherland, D., Samakovlis, C., Krasnow, M.A., 1996. branchless Encodes a *Drosophila* FGF Homolog That Controls Tracheal Cell Migration and the Pattern of Branching. *Cell* 87, 1091–1101. [https://doi.org/10.1016/S0092-8674\(00\)81803-6](https://doi.org/10.1016/S0092-8674(00)81803-6)
- Svitkina, T., 2018. The Actin Cytoskeleton and Actin-Based Motility. *Cold Spring Harb Perspect Biol* 10. <https://doi.org/10.1101/cshperspect.a018267>
- Swaine, T., Dittmar, M., 2015. CDC42 Use in Viral Cell Entry Processes by RNA Viruses. *Viruses* 7, 6526–6536. <https://doi.org/10.3390/v7122955>
- Taka, H., Ono, C., Sato, M., Asano, S., Bando, H., 2013. Complex genetic interactions among non-essential genes of BmNPV revealed by multiple gene knockout analysis. *Journal of Insect Biotechnology and Sericulture* 82, 25–32. https://doi.org/10.11416/jibs.82.1_025
- Tang, H., Li, H., Lei, S.M., Harrison, R.L., Bonning, B.C., 2007. Tissue specificity of a baculovirus-expressed, basement membrane-degrading protease in larvae of *Heliothis virescens*. *Tissue and Cell* 39, 431–443. <https://doi.org/10.1016/j.tice.2007.08.003>
- Tarone, G., Cirillo, D., Giancotti, F.G., Comoglio, P.M., Marchisio, P.C., 1985. Rous sarcoma virus-transformed fibroblasts adhere primarily at discrete protrusions of the ventral membrane called podosomes. *Experimental Cell Research* 159, 141–157. [https://doi.org/10.1016/S0014-4827\(85\)80044-6](https://doi.org/10.1016/S0014-4827(85)80044-6)
- Tsuboi, S., 2007. Requirement for a Complex of Wiskott-Aldrich Syndrome Protein (WASP) with WASP Interacting Protein in Podosome Formation in Macrophages. *Journal of Immunology* 178, 2987–2995. <https://doi.org/10.4049/jimmunol.178.5.2987>
- Tu, C., Ortega-Cava, C.F., Chen, G., Fernandes, N.D., Cavallo-Medved, D., Sloane, B.F., Band, V., Band, H., 2008. Lysosomal Cathepsin B Participates in the Podosome-Mediated Extracellular Matrix Degradation and Invasion via Secreted Lysosomes in v-Src Fibroblasts. *Cancer Research* 68, 9147–9156. <https://doi.org/10.1158/0008-5472.CAN-07-5127>
- Vainker, S.J., 2004. *Chinese Silk: A Cultural History*. British Museum Press.
- van Eijl, H., Hollinshead, M., Smith, G.L., 2000. The Vaccinia Virus A36R Protein Is a Type Ib Membrane Protein Present on Intracellular but Not Extracellular Enveloped Virus Particles. *Virology* 271, 26–36. <https://doi.org/10.1006/viro.2000.0260>
- van Oers, M.M., 2006. Vaccines for Viral and Parasitic Diseases Produced with Baculovirus Vectors, in: *Advances in Virus Research, Insect Viruses: Biotechnological Applications*. Academic Press, pp. 193–253. [https://doi.org/10.1016/S0065-3527\(06\)68006-8](https://doi.org/10.1016/S0065-3527(06)68006-8)
- Varon, C., Tatin, F., Moreau, V., Obberghen-Schilling, E.V., Fernandez-Sauze, S., Reuzeau, E., Kramer, I., Genot, E., 2006. Transforming Growth Factor β Induces Rosettes of Podosomes in Primary Aortic Endothelial Cells. *Mol. Cell Biol.* 26, 13.
- Volkman, L.E., 1988. *Autographa californica* MNPV nucleocapsid assembly: Inhibition by cytochalasin D. *Virology* 163, 547–553. [https://doi.org/10.1016/0042-6822\(88\)90295-4](https://doi.org/10.1016/0042-6822(88)90295-4)
- Volkman, L.E., Goldsmith, P.A., 1983. *In Vitro* Survey of *Autographa californica* Nuclear Polyhedrosis Virus Interaction with Nontarget Vertebrate Host Cells. *Applied and Environmental Microbiology* 45, 1085–1093. <https://doi.org/10.1128/AEM.45.3.1085-1093.1983>

- Volkman, L.E., Goldsmith, P.A., Hess, R.T., 1987. Evidence for microfilament involvement in budded *Autographa californica* nuclear polyhedrosis virus production. *Virology* 156, 32–39. [https://doi.org/10.1016/0042-6822\(87\)90433-8](https://doi.org/10.1016/0042-6822(87)90433-8)
- Volkman, L.E., Goldsmith, P.A., Hess, R.T., Faulkner, P., 1984. Neutralization of budded *Autographa californica* NPV by a monoclonal antibody: Identification of the target antigen. *Virology* 133, 354–362. [https://doi.org/10.1016/0042-6822\(84\)90401-X](https://doi.org/10.1016/0042-6822(84)90401-X)
- Volkman, L.E., Kasman, L.M., 2000. Filamentous actin is required for lepidopteran nucleopolyhedrovirus progeny production. *Journal of General Virology* 81, 1881–1888. <https://doi.org/10.1099/0022-1317-81-7-1881>
- Volkman, L., Talhouk, S., Oppenheimer, D., Charlton, C.A., 1992. Nuclear F-actin: A functional component of baculovirus-infected lepidopteran cells? *Journal of Cell Science* 103, 15–22.
- Volkman, L.E., Zaal, K.J.M., 1990. *Autographa californica* M nuclear polyhedrosis virus: Microtubules and replication. *Virology* 175, 292–302. [https://doi.org/10.1016/0042-6822\(90\)90211-9](https://doi.org/10.1016/0042-6822(90)90211-9)
- Walsh, D., Naghavi, M.H., 2019. Exploitation of cytoskeletal networks during early viral infection. *Trends Microbiol* 27, 39–50. <https://doi.org/10.1016/j.tim.2018.06.008>
- Ward, B.M., Moss, B., 2004. Vaccinia Virus A36R Membrane Protein Provides a Direct Link between Intracellular Enveloped Virions and the Microtubule Motor Kinesin. *JVI* 78, 2486–2493. <https://doi.org/10.1128/JVI.78.5.2486-2493.2004>
- Ward, B.M., Moss, B., 2001. Vaccinia virus intracellular movement is associated with microtubules and independent of actin tails. *J. Virol.* 75, 11651–11663. <https://doi.org/10.1128/JVI.75.23.11651-11663.2001>
- Washburn, J.O., Kirkpatrick, B.A., Volkman, L.E., 1995. Comparative pathogenesis of *Autographa californica* M nuclear polyhedrosis virus in larvae of *Trichoplusia ni* and *Heliothis virescens*. *Virology* 209, 561–568. <https://doi.org/10.1006/viro.1995.1288>
- Washburn, J.O., Lyons, E.H., Haas-Stapleton, E.J., Volkman, L.E., 1999. Multiple Nucleocapsid Packaging of *Autographa californica* Nucleopolyhedrovirus Accelerates the Onset of Systemic Infection in *Trichoplusia ni*. *J. Virol.* 73, 411–416. <https://doi.org/10.1128/JVI.73.1.411-416.1999>
- Weaver, S.C., Scott, T.W., Lorenz, L.H., Lerdthusnee, K., Romoser, W.S., 1988. Togavirus-associated pathologic changes in the midgut of a natural mosquito vector. *J Virol* 62, 2083–2090.
- Webb, B.A., Eves, R., Crawley, S.W., Zhou, S., Côté, G.P., Mak, A.S., 2005. PAK1 induces podosome formation in A7r5 vascular smooth muscle cells in a PAK-interacting exchange factor-dependent manner. *Am. J. Physiol., Cell Physiol.* 289, C898-907. <https://doi.org/10.1152/ajpcell.00095.2005>
- Weisswange, I., Newsome, T.P., Schleich, S., Way, M., 2009. The rate of N-WASP exchange limits the extent of ARP2/3-complex-dependent actin-based motility. *Nature* 458, 87–91. <https://doi.org/10.1038/nature07773>
- Williams, K.C., Cepeda, M.A., Javed, S., Searle, K., Parkins, K.M., Makela, A.V., Hamilton, A.M., Soukhtezari, S., Kim, Y., Tuck, A.B., Ronald, J.A., Foster, P.J., Chambers, A.F., Leong, H.S., 2019. Invadopodia are chemosensing protrusions that guide cancer cell extravasation to promote brain tropism in metastasis. *Oncogene* 38, 3598–3615. <https://doi.org/10.1038/s41388-018-0667-4>

- Wood, H.A., Granados, R.R., 1991. Genetically Engineered Baculoviruses as Agents for Pest Control. *Annual Review of Microbiology* 45, 69–87.
<https://doi.org/10.1146/annurev.mi.45.100191.000441>
- Xeros, N., 1952. Cytoplasmic Polyhedral Virus Diseases. *Nature* 170, 1073–1073.
<https://doi.org/10.1038/1701073a0>
- Xu, Y.-P., Gu, L.-Z., Lou, Y.-H., Cheng, R.-L., Xu, H.-J., Wang, W.-B., Zhang, C.-X., 2012. A baculovirus isolated from wild silkworm encompasses the host ranges of *Bombyx mori* nucleopolyhedrosis virus and *Autographa californica* multiple nucleopolyhedrovirus in cultured cells. *Journal of General Virology*, 93, 2480–2489.
<https://doi.org/10.1099/vir.0.043836-0>
- Xu, Y.-P., Ye, Z.-P., Niu, C.-Y., Bao, Y.-Y., Wang, W.-B., Shen, W.-D., Zhang, C.-X., 2010. Comparative analysis of the genomes of *Bombyx mandarina* and *Bombyx mori* nucleopolyhedroviruses. *J Microbiol.* 48, 102–110. <https://doi.org/10.1007/s12275-009-0197-4>
- Yamaguchi, H., 2012. Pathological roles of invadopodia in cancer invasion and metastasis. *European Journal of Cell Biology, Podosomes, Invadopodia and Focal Adhesions in Physiology and Pathology* 91, 902–907. <https://doi.org/10.1016/j.ejcb.2012.04.005>
- Yamaguchi, H., Lorenz, M., Kempiak, S., Sarmiento, C., Coniglio, S., Symons, M., Segall, J., Eddy, R., Miki, H., Takenawa, T., Condeelis, J., 2005. Molecular mechanisms of invadopodium formation. *Journal of Cell Biology* 168, 441–452.
<https://doi.org/10.1083/jcb.200407076>
- Zambonin-Zallone, A., Teti, A., Carano, A., Marchisio, P.C., 2009. The distribution of podosomes in osteoclasts cultured on bone laminae: Effect of retinol. *J Bone Miner Res* 3, 517–523. <https://doi.org/10.1002/jbmr.5650030507>
- Zettl, M., Way, M., 2002. The WH1 and EVH1 domains of WASP and Ena/VASP family members bind distinct sequence motifs. *Curr. Biol.* 12, 1617–1622.
[https://doi.org/10.1016/s0960-9822\(02\)01112-0](https://doi.org/10.1016/s0960-9822(02)01112-0)
- Zhou, S., Webb, B.A., Eves, R., Mak, A.S., 2006. Effects of tyrosine phosphorylation of cortactin on podosome formation in A7r5 vascular smooth muscle cells. *Am. J. Physiol., Cell Physiol.* 290, C463-471. <https://doi.org/10.1152/ajpcell.00350.2005>

Appendix

Video S1: Dynamic invadosome-like structures form in AcMNPV infected Sf21 cells. Confocal timelapse imaging of Sf21 cells expressing GFP-actin and infected AcMNPV. Cells were imaged every 2 min starting at 140 min post infection. Scale bar is 5 μ m. Time post AcMNPV infection is shown.

Video S2: Stationary invadosome-like structures form clusters. Confocal timelapse imaging of Sf21 cells expressing GFP-actin and infected with AcMNPV. Cells were imaged every 2 min starting at 218 min post infection. Red circles indicate individual invadosome-like structures which disappear, modulating the shape of the larger cluster. Yellow circles indicate individual invadosome-like structures that are maintained. Scale bar is 5 μ m. Time post AcMNPV infection is shown.

Video S3: ARIF-1 expression is sufficient for formation of dynamic invadosome-like structures. Confocal timelapse imaging of Sf21 cells expressing GFP-actin and ARIF-1. Cells were imaged 2 days post transfection. Scale bar is 5 μ m. Time elapsed during imaging is shown.

Video S4: Plasma membrane targeted ARIF-1 C-terminal cytoplasmic region is sufficient for formation of dynamic clusters of invadosome-like structures. Confocal timelapse imaging of Sf21 cells expressing GFP-actin and gp64::ARIF-1(219-417). Cells were imaged 2 days post transfection. Scale bar is 5 μ m. Time elapsed during imaging is shown.

Video S5: Invadosome-like structures are uniformly distributed along the basal PM in Sf21 cells expressing ARIF-1(Y332F). Confocal timelapse imaging of Sf21 cells expressing GFP-actin and ARIF-1(Y332F). Cells were imaged 2 days post transfection. Scale bar is 5 μ m. Time elapsed during imaging is shown.

Video S6: Invadosome-like structures are uniformly distributed along the basal PM in Sf21 cells expressing ARIF-1(P335A). Confocal timelapse imaging of Sf21 cells expressing GFP-actin and ARIF-1(P335A). Cells were imaged 2 days post transfection. Scale bar is 5 μ m. Time elapsed during imaging is shown.

Video S7: Latrunculin A induces rapid dissolution of clusters of invadosome-like structures. Confocal timelapse imaging of Sf21 cells expressing GFP-actin and infected with AcMNPV. At 4 hpi, 4 μ M Latrunculin A was added to cell medium. Scale bar is 5 μ m. Time elapsed after viral infection and Latrunculin A addition is shown.

Video S8: Arp2/3 complex inhibitor CK666 induces dissolution of clusters of invadosome-like structures. Confocal timelapse imaging of Sf21 cells expressing GFP-actin and infected with AcMNPV. At 4 hpi, 100 μ M of CK666 was added to cell medium. Scale bar is 5 μ m. Time elapsed after viral infection and CK666 addition is shown.

Video S9: Inactive control Arp2/3 inhibitor CK869 has no effect on clusters of invadosome-like structures. Confocal timelapse imaging of Sf21 cells expressing GFP-actin and infected with AcMNPV. At 4 hpi, 100 μ M of CK869 was added to cell medium. Scale bar is 5 μ m. Time elapsed after viral infection and CK666 addition is shown.